The role of the *mir-310s* in Hedgehog signaling regulation under dietary stress in *Drosophila* ovary

Doctoral Thesis

Dissertation for the award of the degree
"Doctor rerum naturalium (Dr. rer. nat.)" in
the GGNB program: "Molecular Biology" of
the Georg August University Göttingen
Faculty of Biology

submitted by

Ibrahim Ömer Çiçek

born in Istanbul, Turkey

Göttingen, 2015

Members of the Thesis Committee

Thesis Committee Members

PD Halyna Shcherbata, PhD
Max Planck Research Group for Gene Expression and Signaling
Max Planck Institute for Biophysical Chemistry
Am Fassberg 11 37077 Göttingen Germany

Dr. Roland Dosch
Department of Developmental Biochemistry
University Medical Center Göttingen
Justus-von-Liebig-Weg 11 37077 Göttingen Germany

Prof. Dr. Andreas Wodarz
Microscopic Anatomy and Molecular Cell Biology
University of Cologne
Joseph-Stelzmann-Str.9 50931 Köln Germany

Extended Thesis Committee Members

Prof. Dr. Reinhard Schuh
Department of Molecular Developmental Biology
Max Planck Institute for Biophysical Chemistry
Am Fassberg 11 37077 Göttingen Germany

Prof. Dr. Michael Kessel
Department of Developmental Biology
Max Planck Institute for Biophysical Chemistry
Am Fassberg 11 37077 Göttingen Germany

Dr. Henrik Bringmann
Max Planck Research Group Sleep and Waking
Max Planck Institute for Biophysical Chemistry
Am Fassberg 11 37077 Göttingen Germany

Date of Oral Examination: 22.05.2015

Table of Contents

Table of Contents

Table of Contents

Table of Contents

Table of Contents

Summary

Perturbations in nutrition and energy homeostasis can have deleterious effects on human health. Therefore, mechanisms controlling metabolic balance and initiating fast response to changing dietary conditions are essential. Such fast and robust responses at the cellular level can be achieved by microRNA (miRNA) mediated control of gene expression.

In this study, the *mir-310s* are shown as important controllers of metabolic status of *Drosophila*. The *mir-310s* mutants have numerous starvation-sensitive genes deregulated at the protein and mRNA levels and exhibit diet-sensitive physiological phenotypes, such as low fecundity and high body fat accumulation.

Moreover, the *mir-310s* regulate Hedgehog (Hh) signaling by targeting three Hh pathway-associated genes (*Rab23, DHR96,* and *ttk*), linking the egg production with the dietary status. In the ovary, this regulation is essential to tune the Hh signaling strength, which has to be kept at low levels under nutritional restriction. Here, *Drosophila Rab23* is identified as a novel positive regulatory element of Hh signaling. Rab23 is shown to act cell-autonomously, regulating Hh ligand release by facilitating its intracellular mobility.

These findings shed light on miRNA-based control of the Hh pathway in a nutrition-sensitive context. From flies to humans, the conservation of *mir-310s* seed sequences, Rab23, and Hh signaling raises the possibility that this control mechanism is existing in humans as well. Therefore, these findings are important for the better understanding of metabolic diseases and development of miRNA related therapeutics.

1 Introduction

Keeping proper metabolic balance is crucial for the fitness of every organism. Food intake has to be matched to energy output in order to survive, experience a healthy development, and generate a viable offspring. Energy homeostasis of an animal is maintained via its feeding behavior and nutrient consumption, which have to be calibrated according to the availability of the food in terms of quantity and quality.

1.1 Nutrition

Nutrition in general encompasses classes of basic non-interchangeable components. Different animals in various faunas depend on their specific sets of basal nutrients in accordance with the supplies from their surroundings. While the fundamental energy production can be sustained through few basic resources like sugars, fats, and proteins; species-specific essential substances, which cannot be synthesized by the organism, need to be taken directly by feeding. For instance, certain types of fatty acids (linoleic acid and α-linolenic acid), amino acids (e.g. lysine, tryptophan), and vitamins (e.g. biotin, riboflavin) are essential for humans to receive from dietary sources (Eagle, 1955; Holman, 1971; Young, 1994). In comparison, cholesterol, some amino acids, and folic acid are examples of the necessary dietary constituents for a fruit fly (Begg and Robertson, 1948; Piper et al., 2014; Sang, 1956; Sang and King, 1961; Tatum, 1939). In addition to basic components, protein uptake was shown to be important for development. For example, adequate level of protein consumption during childhood is essential for proper brain development, influencing neural composition, motor and cognitive function (Laus et al., 2011). In fruit flies, nutrient restriction at larval stages interferes with the developmental timing and has gross morphological consequences, most strikingly reducing the body size of the adult fly (Conlon and Raff, 1999; Stern, 2001). Similar to malnourished women experiencing weight loss (e.g. people with anorexia nervosa and bulimia nervosa), who experience infertility and miscarriage (Group, 2006), female fruit flies deprived from protein source lose their reproductive capacity and stop producing and laying eggs (Ashburner, 1989).

1.1.1 Nutritional stress

Critical deviations from the optimal window of food intake are harmful to the organism. More than 35% of the human population, majorly in developed countries, suffers from being overweight with

consequences like type 2 diabetes, cardiovascular disease, and shorter life expectancy (Haslam and James, 2005; Ng et al., 2014). On the other side, more than 28% of the population suffers from malnutrition in terms of essential micronutrients and more than 12.5% of humans are not consuming enough calories to sustain a healthy life. These populations are located predominantly in developing countries and have to face undesirable outcomes like impairments in brain development and cognitive function, and (particularly in children) mortality (Laus et al., 2011; McGuire, 2013). Such aberrations of the normal nutritional homeostasis translate themselves into physiological stress to the organism as a whole. The non-healthy condition of the organs and their response are direct readouts of the altered molecular network defining cellular stress. The nutritional stress at the cellular level can show itself in various ways via perturbation of important metabolic and signaling pathways.

1.1.2 Response to nutritional stress at the molecular level

To adapt the organism to such stress conditions, fine-tuning of metabolic and regenerative pathways is essential for organismal fitness, survival, and generation of progeny. There are numerous feedforward, feedback mechanisms ensuring effective and quick response at the cellular level (Wu et al., 2009). These include process manipulations done by adjusting gene expression on multiple levels ranging from the transcriptional control of the genomic loci up to translation. One important element of gene expression control is through microRNAs (miRNA). These regulatory RNAs have the function of fine-tuning and balancing gene expression and adapting the cell, subsequently the organism, to changing environmental conditions like altered nutritional status (Schneeberger et al., 2015). miRNAs have been shown to regulate gene expression in various types of stress conditions in order to overcome the undesirable results of the stress-perturbed homeostasis. miRNA-dependent responses to DNA-damage, osmotic stress, temperature fluctuations, and starvation were shown previously (Leung and Sharp, 2010).

1.2 miRNAs

miRNAs are short non-coding RNA molecules, which regulate gene expression post-transcriptionally (Ding et al., 2009). miRNA control over gene expression occurs in various processes ranging from cellular metabolism to organismal homeostasis (Barrio et al., 2014; Teleman et al., 2006; Xu et al., 2003).

It has been just over two decades since the first members of the miRNA family have been discovered (Lee et al., 1993; Wightman et al., 1993). This unconventional mRNA stability regulation mechanism was first observed in studies of developmental timing in *Caenorhabditis elegans*. The discovery was possible by the identification of the reciprocal mutant phenotypes in the *lin-4* and *lin-14* genes. The protein coding gene, *lin-14*, was found to be negatively regulated by the short (22 nucleotide) RNA product (miRNA) of the non-coding *lin-4* via seven *lin-4* RNA binding sites in its 3'UTR (Lee et al., 1993; Wightman et al., 1993). Few years later, the molecular details of this interaction were unraveled by the Nobel Prize-winning discovery of the RNAi, the mechanisms of double stranded RNA induced gene silencing (Fire et al., 1998). Up to date, 2588 *H. sapiens* and 466 *D. melanogaster* mature miRNA sequences are identified (Enright et al., 2003; Griffiths-Jones et al., 2008).

1.2.1 miRNA biogenesis

The synthesis of miRNAs starts with transcription by RNA polymerase II (Pol II), which gives rise to single stranded RNA molecules with a stem-loop structure and in variable sizes (pri-miRNA). Subsequently, the pri-miRNA is modified by 5' capping and 3' polyadenylation similar to the mRNAs transcribed by the same Pol II enzyme (Bracht et al., 2004; Cai et al., 2004; Lee et al., 2004).

Next, the pri-miRNAs undergo structural modifications by the "Microprocessor" protein complex, which involves Drosha (RNase III enzyme) and Pasha (or DGCR8, the double stranded RNA-binding domain protein (dsRBD)) (Denli et al., 2004; Gregory et al., 2004; Han et al., 2004; Landthaler et al., 2004; Lee et al., 2003). This complex acts as a molecular ruler for the hairpin junction and cleaves the pri-miRNA generating the next intermediate, the ~70 nt long hairpin precursor-microRNA (pre-miRNA). For further processing, the pre-miRNA is transported to the cytoplasm through the nuclear pores. This transport relies on Exportin-5, which recognizes the 2 nucleotides long 3' overhang of the pre-miRNA (Bohnsack et al., 2004; Lund et al., 2004; Yi et al., 2003). In the cytoplasm, the RNase III enzyme, Dicer, and dsRBD Loquacious act on the pre-miRNA and performs the last cleavage on the hairpin loop, thereby producing the mature ~22 nt miRNA-miRNA-complementary duplex (Chendrimada et al., 2005; Forstemann et al., 2005; Hutvagner et al., 2001; Jiang et al., 2005; Ketting et al., 2001; Saito et al., 2005). Next, an Argonaute protein, Ago2, is recruited by Loquacious and together with Dicer, they facilitate the

formation of the RNA-induced silencing complex (RISC), which includes the single stranded miRNA and other factors (Gregory et al., 2005; Maniataki and Mourelatos, 2005). The choice of the miRNA and miRNA-complementary strand is based on their 5' base pairing stability; and after the miRNA is bound by the RISC, the miRNA-complementary strand undergoes degradation (Du and Zamore, 2005; Schwarz et al., 2003) (Figure 1).

1.2.2 miRNA mode of action

The driving force of the RISC and the target mRNA interaction is the miRNA-mRNA complementarity (Hutvagner and Zamore, 2002; Martinez and Tuschl, 2004). miRNAs mostly rely on non-perfect match to exert their regulatory function. There are rare cases, where full complementarity results in mRNA cleavage in siRNA-like manner (Yekta et al., 2004). Upon binding by RISC, which includes the miRNA, the mRNA experiences stalling at the translation initiation or elongation steps (Humphreys et al., 2005; Maroney et al., 2006; Nottrott et al., 2006; Petersen et al., 2006; Pillai et al., 2005). In addition, this interaction can result in destabilization of the mRNA via deadenylation or decapping (Behm-Ansmant et al., 2006; Giraldez et al., 2006; Wu et al., 2006). Note that the RISC targeted mRNAs are not destined for degradation necessarily. In this case, the Argonaute proteins bound to mRNAs can accumulate in processing bodies (P-bodies), which are distinct cytoplasmic RNA degradation sites devoid of ribosomes (Liu et al., 2005; Pillai et al., 2005; Sen and Blau, 2005). The translation repression of these mRNAs and their localization to the P-bodies are shown to be transient; so, the temporary storage mechanism of translationally inactive mRNAs can feed them back to the cytoplasm for ribosome recruitment and subsequent translation (Bhattacharyya et al., 2006).

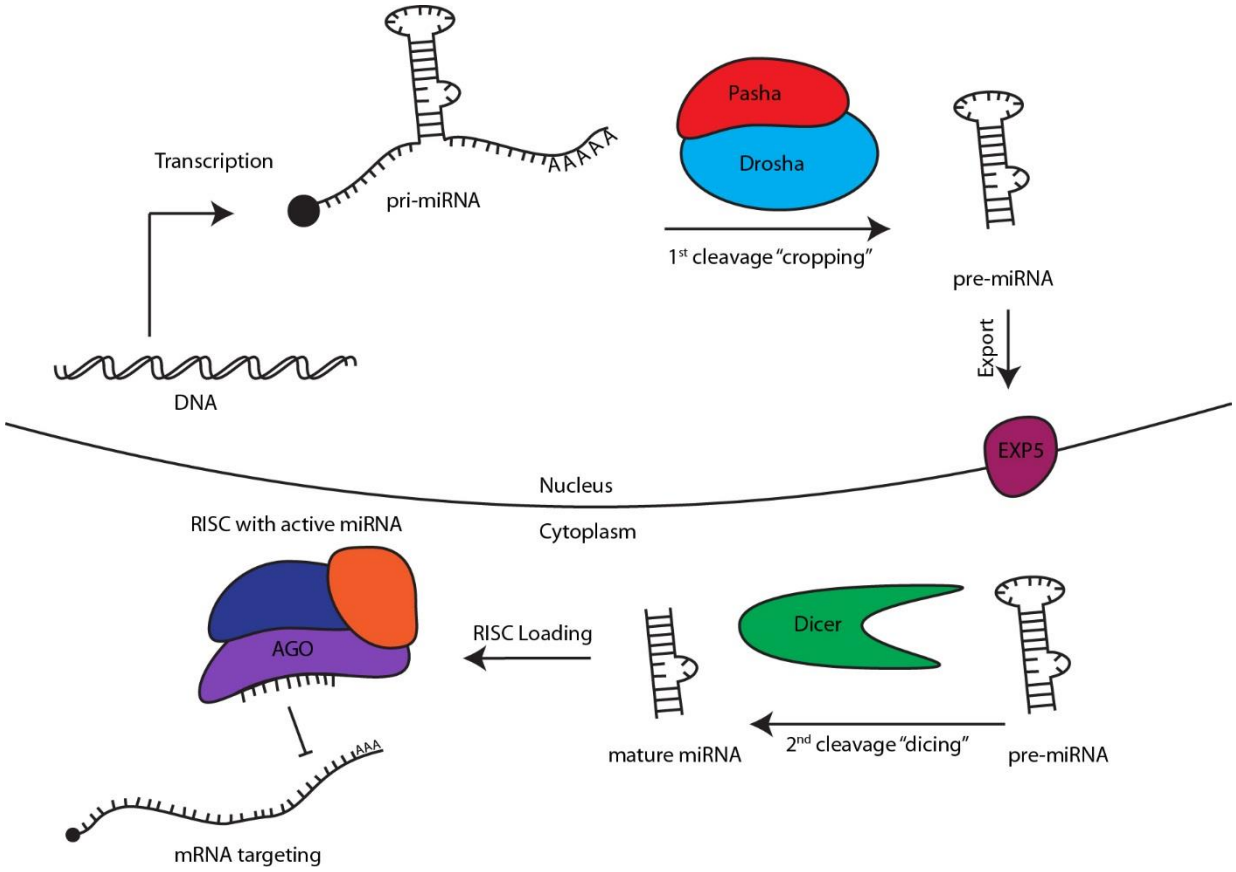

Figure 1. The miRNA biogenesis pathway (Ding et al., 2009)

1.2.3 miRNA target identification, seed sequence and database algorithms

Few miRNA-mRNA interactions were found to be as robust as the first discovered ones and phenotypically reciprocal (*lin-4* miRNA and its target *lin-14*). Further research based on miRNA binding sites mutation and miRNA overexpression assays revealed that the nature of miRNA action works via non-perfect sequence complementarity in target recognition (Brennecke et al., 2005; Doench and Sharp, 2004; Kiriakidou et al., 2004; Kloosterman et al., 2004; Lewis et al., 2003). Studies have shown that 7-8nt long 5' seed region of miRNAs has a determining role in target mRNA binding, which is further facilitated by pairing through the miRNA 3' region. The importance of the seed region in mRNA target recognition is supported by direct interaction experiments and bioinformatical analyses, which also demonstrate that these regions are evolutionary conserved and reveal their relevance in target recognition (Brennecke et al., 2005;

Grun et al., 2005; Krek et al., 2005; Lewis et al., 2005; Xie et al., 2005). The discovery of seed sequence made it possible to develop target prediction algorithms generating databases of predicted target mRNAs for a given miRNA, and of predicted regulatory miRNAs for a given mRNA (Betel et al., 2008; Enright et al., 2003; Kheradpour et al., 2007).

1.2.4 miRNAs in gene regulation

In order to cope with stochastic gene expression, miRNAs make up one important regulatory network, where they can fine-tune or buffer their target mRNA levels through different modes of feedforward and feedback loops (Wu et al., 2009). The fine-tuning ensures the precise amounts of target gene expression, which cannot be achieved only by transcriptional control. This can be achieved (1) by simple direct targeting (Li et al., 2006), (2) by a third element positively regulating the miRNA and negatively regulating its target (the coherent feedforward loop) collectively downregulating the target gene (Hornstein et al., 2005), or (3) by miRNA downregulation by its target, thus forming a feedback loop resulting in robust expression of the miRNA or the target mRNA exclusively (Rybak et al., 2008). These modes would fine-tune the expression output levels of the target gene establishing exact amounts required for the biological process. On the other hand, expression buffering networks are important in cases of aberrant target mRNA or miRNA expression. This stabilization can be accomplished (1) by an incoherent feedforward loop, where the miRNA is upregulated by the target's activator, thus stabilizing the target expression levels against activator level fluctuations (O'Donnell et al., 2005). Another such mode of buffering acts through (2) activation of miRNA expression by its target in a negative feedback loop, which readjusts both the miRNA and target mRNA levels in case one or the other is misexpressed (Martinez et al., 2008). Lastly, (3) the expression of a gene can be kept under control by an activator and a repressor, both of which are miRNA targets. This incoherent feedforward loop will ensure stable expression in case of aberrant miRNA activity (Choi et al., 2007; Wu et al., 2009). Strikingly, these important fine-tuning and buffering roles of miRNAs make them appear dispensable in well-controlled laboratory environments, where stochastic external stimuli are minimized. As a result, numerous individual miRNA mutants show no or very mild phenotypes (Miska et al., 2007). However, the fact that many miRNAs are highly evolutionary conserved (on the level of seed sequences) and their functional potency and combinatorial versatility demonstrates miRNAs'

unconventional role in sustaining homeostasis at the cellular level upon environmental or internal changes caused by various stress conditions (Leung and Sharp, 2010; Wu et al., 2009).

1.2.5 miRNA related diseases

Perturbed miRNA expression has been linked to many human diseases. For instance, the *mir-17-92* locus has been found to be amplified in B cell lymphoma (He et al., 2005). In the same study the authors report that the overexpression of these miRNAs caused increase in tumorigenesis and reduction in apoptosis rates. The *mir-17-92* were shown to be downstream of an important oncogene, *c-Myc*, and upstream of their target proapoptotic (E2F1) and anti-angiogenic genes (Dews et al., 2006; He et al., 2005; O'Donnell et al., 2005). Reports support altered miRNA expression profiles, in primary tumors (Calin et al., 2004; Lu et al., 2005). Like cancer, other diseases are also associated with perturbed miRNA profiles making them potential biomarkers for diagnostic purposes and targets for therapeutics (Calin and Croce, 2006).

The *Drosophila mir-310s* cluster contains four recently evolved miRNAs (*mir-310, mir-311, mir-312,* and *mir-313*) (Lu et al., 2008) with orthologous seed sequences to human *mir-17-92* family. The *mir-310s* have few confirmed target genes, *Khc-73, armadillo,* and *Dystroglycan*, which are associated with synaptic strength, cell differentiation, and lissencephaly type II-like brain phenotypes, respectively (Pancratov et al., 2013; Tsurudome et al., 2010; Yatsenko et al., 2014). They are also known to be responsive to external stress conditions (Marrone et al., 2012).

Importantly, there have been further discoveries of miRNA involvement in human diseases and metabolic disorders like starvation induced physiological conditions, obesity, diabetes, and carcinogenesis, which is highly energy demanding (Bhattacharyya et al., 2006; Leung and Sharp, 2010; Ross and Davis, 2011). It has been shown that the changes in the dietary input exerts changes in the expression of stress response genes (Mendell and Olson, 2012); however, the exact molecular networks of miRNAs and their targets, which govern the dietary response and adapt the animal to the changing conditions, is yet incomplete. *In vivo* studies offer relevant research opportunities to better understand the relationship between nutrition and miRNA-controlled gene expression. The requirement for basic nutritional elements appears to be well conserved, which makes the use of model organisms well suited to uncover the details of dietary stress response.

1.3 *Drosophila* as model organism

Currently, *Drosophila melanogaster* (fruit fly) is one of the most popular model organisms in basic research, which takes its roots from the pioneering studies performed more than a hundred years ago (Castle et al., 1906). Many have chosen fruit fly as an experimental animal model because of the ease and relatively low costs of its cultivation in laboratories. It is possible to cultivate large numbers of flies using simple yeast based food in short time compensating for the small amount of starting material for biochemical assays. Another reason of choice for *Drosophila* is its short life cycle involving four distinct developmental stages: egg, larva, pupa, and adult, all of which can be cultured in the same medium and sustained together without taking special measures for maintenance other than humidity and temperature (Figure 2). Development of the fertilized egg occurs into an adult animal in ~9 days (Ashburner, 1989). This short-lasting fast development compared to other model organisms makes *Drosophila* a very attractive model in many fields of basic and translational research. More importantly, the accumulated knowledge about *Drosophila* genetics together with developed and freely shared genetic tools transformed the fruit fly into a sophisticated, rich, fast, and low-cost toolbox for many research spheres.

1.3.1 Significant part of human and fruit fly biology is conserved

Importantly, in last decades, comparative genomic and molecular approaches together with the whole genome sequence analyses have revealed evolutionarily conserved nature of many fundamental genetic elements and molecular processes between fruit flies and human (Adams et al., 2000; Venter et al., 2001). The use of fruit fly as a model organism is of extreme relevance helping to understand the physiological and molecular dynamics of these orthologous systems. For instance, the systems of nutrient uptake, storage, and mobilization within the body are packed with analogous structures and elements shared by fruit flies and humans. For instance, the *Drosophila* midgut is the analogous organ for the human stomach and intestines, as both are responsible for food digestion and absorption. The fat tissue (fat body) in the fly is not only an equivalent of human adipose tissue, it also assumes the duties of the liver with regard to lipid processing (Canavoso et al., 2001). Another example of functionally conserved sub-organ structures is represented by β-cells in the human pancreas. These insulin hormone secreting cells have *Drosophila* analogs located in the brain, where a small group of neurosecretory cells are responsible for the production and release of the *Drosophila* insulin orthologues (Brogiolo et al., 2001). In terms of the metabolite

similarities, *Drosophila* uses glycogen as its main sugar storage and triaclyglycerols as the main lipid storage form in the fat body similar to humans (Scott et al., 2004; Wigglesworth, 1949). At the molecular level, a receptive system for these metabolites, the TOR (target of rapamycin) pathway, is conserved in both animals sensing cellular amino acid concentrations regulating growth and translation in the context of nutritional favorability (Baker and Thummel, 2007; Russell et al., 2011).

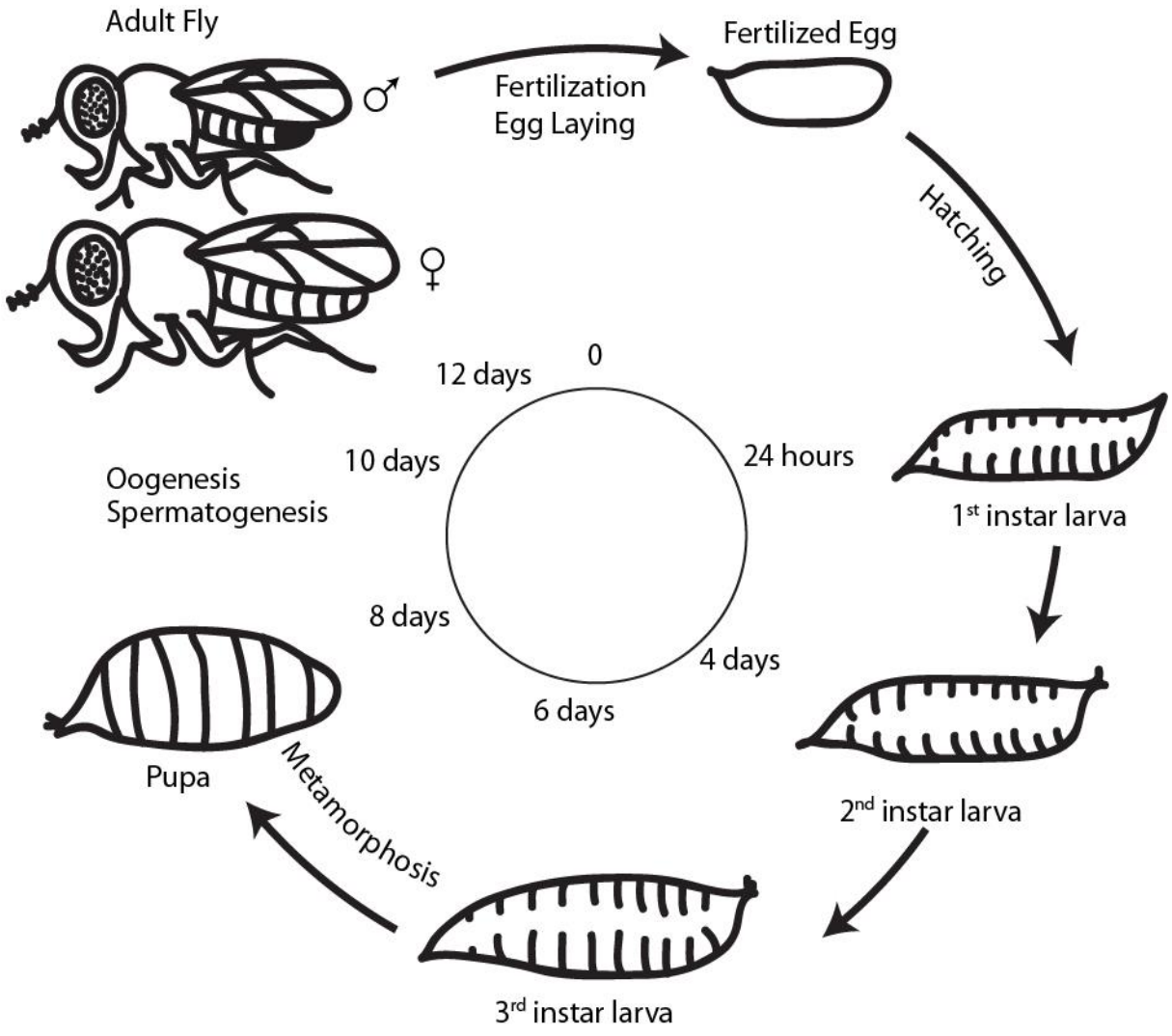

Figure 2. Life Cycle of *Drosophila melanogaster* (Wolpert et al., 1998)

1.3.2 The Ovary as a model system

Among different organ systems *Drosophila* ovary is one of the best suited for studying the dietary responses of the organism upon changes in the environmental conditions, where the food availability and its composition are strict determinants of the ovary functionality and output rate. The eggs are produced in, fertilized at and laid by the female reproductive system, which consists of two ovaries, connected ducts, sperm-holding organs, and accessory glands. After maturation, the egg is positioned from the ovaries through the oviducts into the genital chamber for fertilization. The ovaries lie in the abdomen of the fly between 3rd and 5th segments bilaterally blanketed by the adipose tissue. Ovaries are juxtaposed by the midgut and the crop, a sac like organ connected to the gastrointestinal system, anterior to the gut, which can dislocate the ovaries upon changes in size according to the nutritional status. It can store food in liquid form, which can be reutilized upon food and/or water starvation. The nurture of the fly has a dramatic effect on the ovary size directly causing it to shrink or expand under nutritional poor and rich conditions, respectively. This results in great changes of the abdomen size. One ovary consists of 16-18 ovarioles, egg production units, which are set up as parallel assembly lines for the inception, development, and maturation of the egg (Miller, 1950; Thomas-Orillard, 1984) (Figure 3).

Each ovariole is covered by an individual epithelial sheath that separates them from each other. All the ovarioles are held together by the peritoneal sheath up until they meet at the oviduct. Ovarioles are made of progressively developing egg chambers, the premature egg units, which consist of the follicular epithelium monolayer enwrapping 16 germline cells, the nurse cells and the oocyte. Neighboring egg chambers are connected to each other by a stalk of cells during maturation and progression towards posterior (Miller, 1950) (Figure 4).

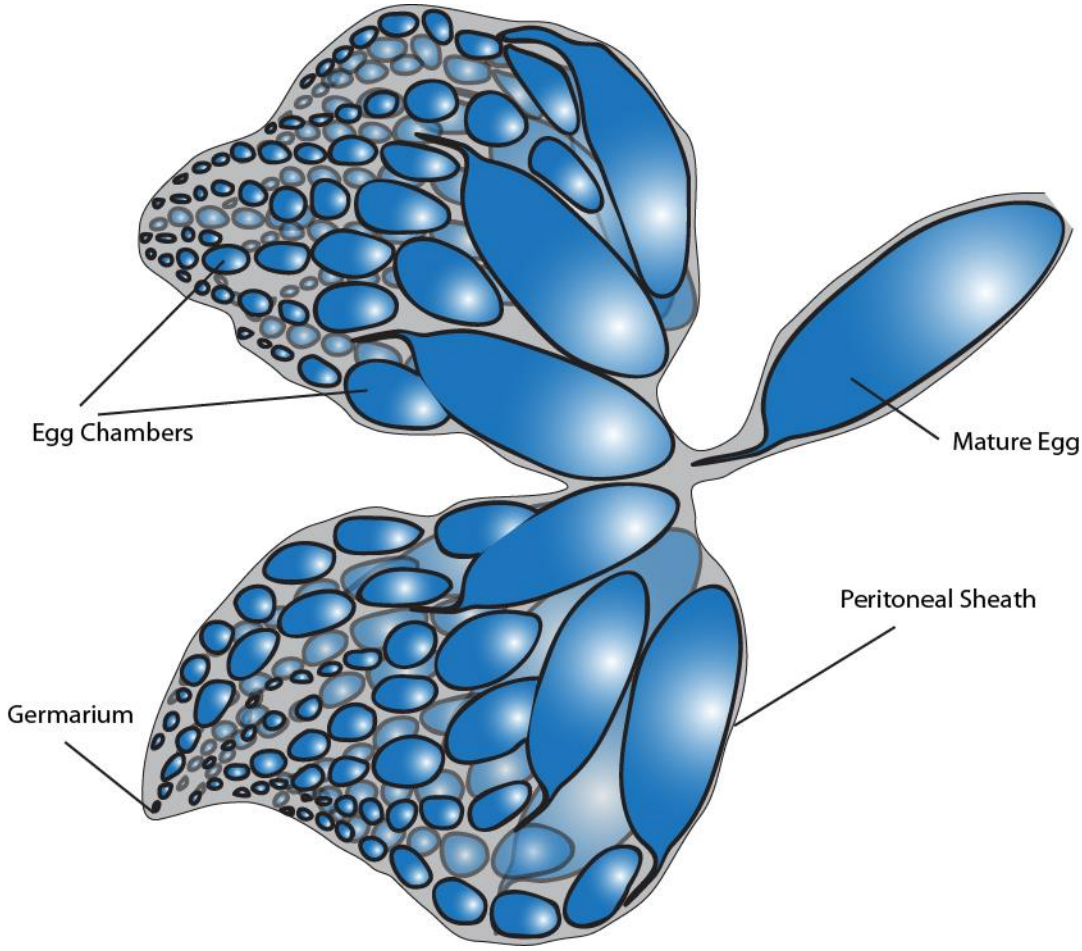

Figure 3. Schematic of *Drosophila* ovaries

1.3.2.1 Oogenesis

The developmental stages of an egg chamber are associated with the progressively enlarging nuclei of the nurse cells, which undergo 10-12 rounds of endoreplication during maturation (Hammond and Laird, 1985). At the end of the egg maturation nurse cells shrink in size in expense of the yolk accumulating in the oocyte and their remains including nuclei stay at the very anterior of the mature egg (Miller, 1950). Similarly, the follicle cells (FCs) divide until stage 6, then switch to endocycling for three rounds, and eventually initiate the amplification cycle replicating only the egg maturation specific genes (i.e. chorion genes) (Hammond and Laird, 1985; Royzman and Orr-Weaver, 1998). Through the course of egg maturation, the FCs change their morphology significantly. They start as cuboidal cells in early egg chambers, where they form homogenous

follicular epithelium. Later, the anterior part of the epithelium, which is covering the nurse cells, assumes a squamous form, while FCs at the posterior part of the epithelium, which are covering the oocyte become more tightly packed and columnar shaped. In later stages, they assume a squamous form, producing the chorion and giving rise to the dorsal appendages (Miller, 1950; Spradling, 1993) (Figure 4).

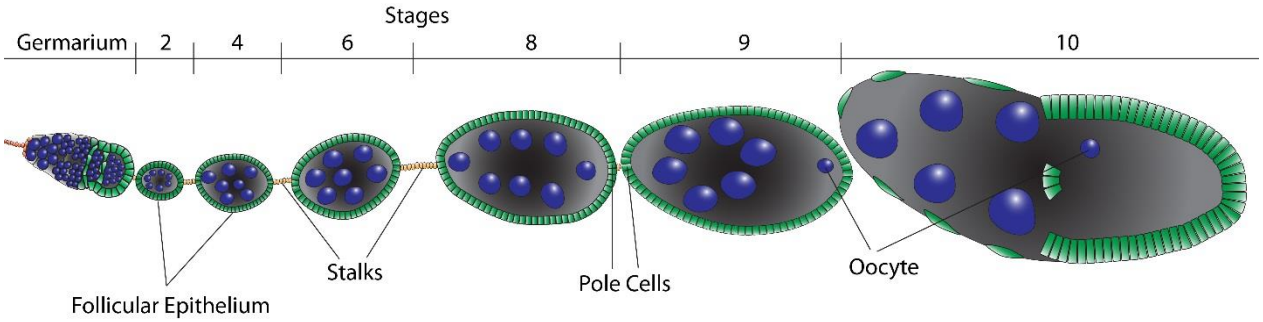

Figure 4. Schematic of ovariole with progressively developing egg chambers

1.3.2.2 Germarium

The oogenesis starts at the very anterior tip of the ovariole, at the specialized structure called the germarium, which harbors the two stem cell sources for the whole cell population of the developing egg: the germline stem cells (GSCs) and the somatic follicular stem cells (FSCs) (Margolis and Spradling, 1995; Nystul and Spradling, 2007). At the start of germline progression, one of the 2-3 GSCs divides and gives rise to dividing cystoblast while renewing itself. Next, the cystoblast undergoes four rounds of mitosis with incomplete cytokinesis giving rise to the 16-cell cyst, which in turn exits mitosis. Nurse cells start endocycling and the oocyte initiates meiosis. With the guidance and control of the surrounding and enwrapping somatic escort cells (ECs) the cyst moves towards the posterior (Decotto and Spradling, 2005; Morris and Spradling, 2011). At the junction of the germarial regions 2A and 2B, the two FSCs divide at a similar rate (Nystul and Spradling, 2010) and give rise to the pre-follicular cells, which move towards the interior and toward the posterior of the germarium separating single germline cyst (now free of ECs) by encapsulation (Margolis and Spradling, 1995; Nystul and Spradling, 2007). Then, the cyst and the follicular epithelium bud off from the germarium forming an egg chamber that develops while moving

towards the posterior. During this process, the FSC progeny gives rise to the FCs, polar cells, and stalk cells, the whole somatic cell population of the egg chambers (Margolis and Spradling, 1995) (Figure 5).

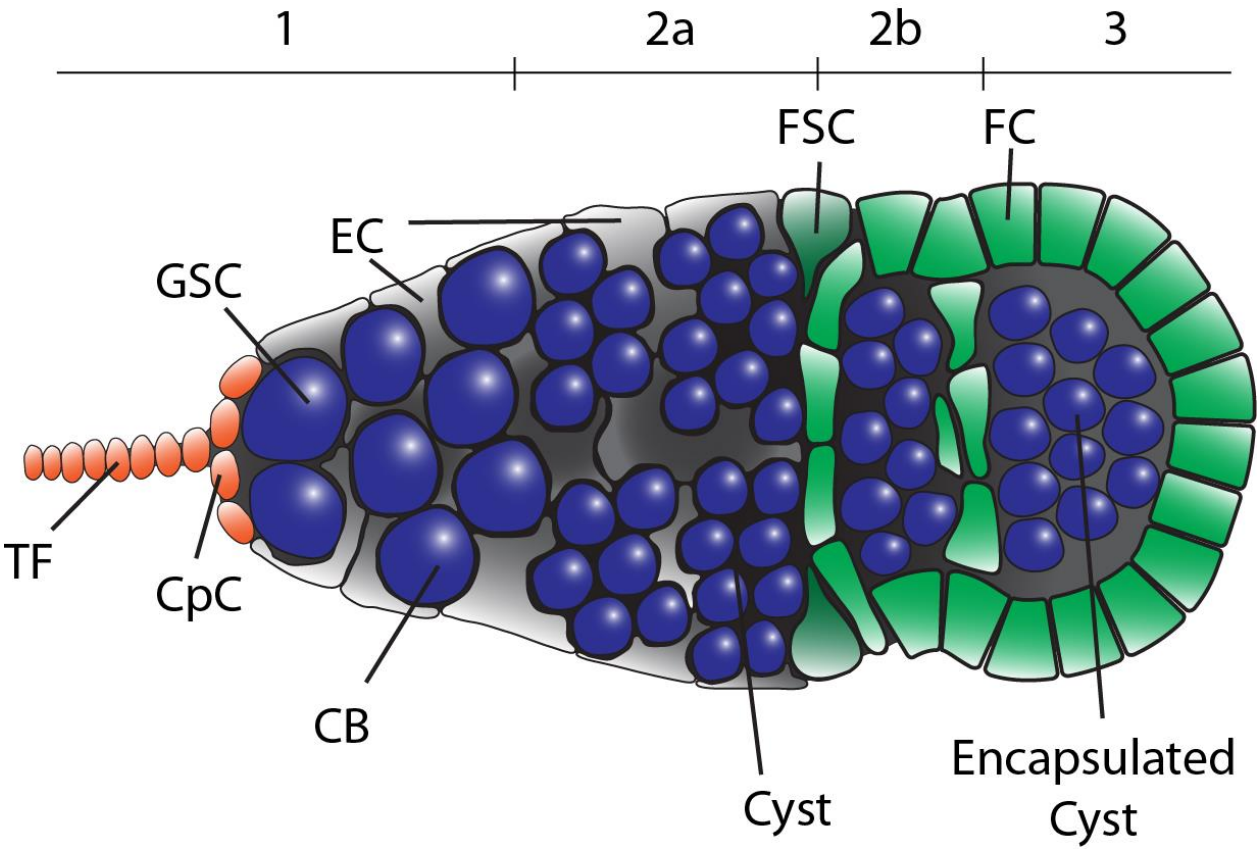

Figure 5. Schematic of the germarium

1.3.2.3 Ovarian stem cells

There are two known stem cell types (GSC and FSC), which are maintained and controlled by different niches. The GSCs depend on the stationary niche at the very anterior of the germarium consisting of terminal filament cells (TF) and the cap cells (CpCs), whereas the FSCs are maintained by dynamic cell to matrix interactions (Morrison and Spradling, 2008; Nystul and Spradling, 2007; Song and Xie, 2002). FSCs are maintained through cell-cell attachments with the ECs through adherens junctions. The lack of junction components, *armadillo* and *shotgun*, causes

rapid loss of FSCs (Song and Xie, 2002). Similarly, cell-matrix interactions between the FSCs and the basement membrane via integrins and LamininA are essential for FSC maintenance (O'Reilly et al., 2008). Proper FSCs division and self-renewal depend on several evolutionary conserved signaling pathways (Sahai-Hernandez et al., 2012). For instance, the Wingless (Wg) pathway controls FSC proliferation, and lack of positive regulators (*disheveled, armadillo*) of this pathway leads to division and proliferation perturbations. In contrast, the loss of Wg negative regulators (*axin, shaggy*) results in overproliferation (Song and Xie, 2003). Bone Morphogenic Pathway (BMP) signaling has also been shown to play a role in FSC fitness, where decrease or increase in signaling activity causes shorter and longer FSC lifespan, respectively (Kirilly et al., 2005). In addition, FSCs division and differentiation is controlled through long range Hh (Hedgehog) signaling by the GSC niche (O'Reilly et al., 2008; Rojas-Rios et al., 2012).

1.3.2.4 Nutrition and stem cells in the germarium

The fact that the germline (nurse cells and the oocyte) and the somatic components (FCs, stalk cells, and polar cells) of the developing egg chambers originate from two distinct stem cell populations makes the synchronization of their division and differentiation rate crucial, which is achieved by distinct systemic and cellular cues (Chang et al., 2013; Gilboa and Lehmann, 2006; Konig and Shcherbata, 2015). For instance, hormonal signaling (e. g. insulin, steroid hormones, insulin-like growth factor (IGF)) and the interconnected TOR and AMPK pathways exemplify systemic control of metabolism and cell proliferation across tissues. The cell cycle progression of GSCs (but not of FSCs) and the establishment of the right proliferation rate is regulated by insulin pathways cell-autonomously (Drummond-Barbosa and Spradling, 2001). In context of dietary status, GSCs are known to divide at a higher rate under yeast-rich and at a slower rate under yeast-free conditions (Drummond-Barbosa and Spradling, 2001). Hh signaling originating from the GSC niche governs the rate of FSCs proliferation.

1.4 The evolutionary conserved Hedgehog Pathway in *Drosophila*

The *hedgehog* (*hh*) gene was discovered in the pioneering *Drosophila* genetic screen by Nüsslein-Volhard and Wieschaus (Nusslein-Volhard and Wieschaus, 1980). The gene was named after the continuous array of cuticular denticles in the larva caused by the loss-of-function of the *hh* locus. In addition to the initial discovery of *hh* as a segment-polarity gene, it was later found to be involved

in development of various tissues and organs, patterning of larval imaginal discs as well as in maintenance of adult homeostasis.

1.4.1 Model of the ligand

The *Drosophila hh* codes for a 52kDa protein with N-terminal Hedge and C-terminal Hog domains (Ingham et al., 2011). The Hog domain acts in its own cleavage (an intein-like process) and facilitates covalent addition of a cholesterol moiety (Eaton, 2008; Porter et al., 1996a; Porter et al., 1996b) resulting in a 19kDa peptide (Figure 6). This cholesterol linked peptide is palmitoylated at its N-terminus by the *skinny hedgehog* gene product (Chamoun et al., 2001). These lipid modifications are utmost important for membrane association and mobility of the ligand.

1.4.2 Modes of signaling

Hh can act on short range through one cell diameter distance during embryonic development. The signal activates *wg* expression in the anterior neighboring cells and *Ser* expression in the posterior neighboring cells. In turn, loss of *hh* causes loss of positional identity of the neighboring segments, which depend on this morphogenic effect of Hh (Alexandre et al., 1999). This activation ensures proper downstream signaling activity and therefore cell fate determination for embryonic patterning through the established effect of short range Hh control (Ingham and McMahon, 2001).

On the other hand, in larval morphogenesis of the wing disc Hh ligand exerts a long range effect, where it acts over distance of several cell diameters to regulate its downstream Decapentaplegic (Dpp) pathway (Ingham and Fietz, 1995; Tabata and Kornberg, 1994; Zecca et al., 1995). This long range systemic transfer of the Hh signal is facilitated by the ligand cholesterol moiety, its interaction with apo-lipoprotein and lipophorin, and packaging into lipoprotein particles (Eugster et al., 2007; Panakova et al., 2005).

Regulation of Hh signaling can be exerted by its coreceptors Interference Hedgehog (Ihog) and Brother of Ihog (Boi) that facilitate binding of the Hh-receptor, Ptc, to the Hh ligand during the first step of downstream signal transduction (Ingham et al., 2011; Lum et al., 2003; Yao et al., 2006). Boi is also involved in the diet-sensitive regulation of Hh signal sending (i.e. controlled sequestration and release of the ligand) via cholesterol receptor DHR96 (Hartman et al., 2010) (Figure 6).

1.4.3 Signal reception

On the signal-receiving cell, in the absence of the ligand, the downstream pathway is negatively regulated by the receptor Patched (Ptc) via blockage of Smoothened activity (Richards and Degnan, 2009) by a yet unknown mechanism. However, research suggests that Ptc controls phosphatidylinositol-4-phosphate (PI4P) levels required for Smo activation by inhibiting PI4P associated kinase (Chen et al., 2002). Binding of the Hh ligand to Ptc results in their internalization and subsequent degradation (Briscoe and Therond, 2013). In this case, the Ptc-unconstrained Smo relays the signal to the Hh Signaling Complex by phosphorylating some of its components and establishing intra-complex interactions. The complex consists of cAMP-dependent protein kinase 1 (PKA), Shaggy (GSK3), and Casein kinase Iα (CKI), which are recruited together by Costal 2 (Cos2) (Robbins et al., 1997; Stegman et al., 2000; Zhang et al., 2005). Importantly, this complex is responsible for controlling the most downstream effector, the transcription factor Cubitus Interruptus (Ci) (Alexandre et al., 1996; Forbes et al., 1993) (Figure 6).

Ci has dual roles on transcription. If the Hh ligand is present and the pathway is active, the full length (155kDa) protein, Ci-155 accumulates and moves to the nucleus, where after further processing it acts as a transcriptional activator. If Hh ligand is absent, Ci-155 cleavage is facilitated by the Hedgehog Signaling Complex and the cleavage product Ci-75 acts as a transcriptional repressor in the nucleus (Briscoe and Therond, 2013; Ingham and McMahon, 2001) (Figure 6).

Few canonical *hh* targets, such as *ptc*, *wg*, and *dpp* are well studied and have been shown to be transcriptionally activated through Ci directly (Alexandre et al., 1996; Forbes et al., 1993; Ingham, 1993). Until now, great efforts have been spent to identify Ci targeted genes by genome wide chromatin immunoprecipitation experiments (Vokes et al., 2008).

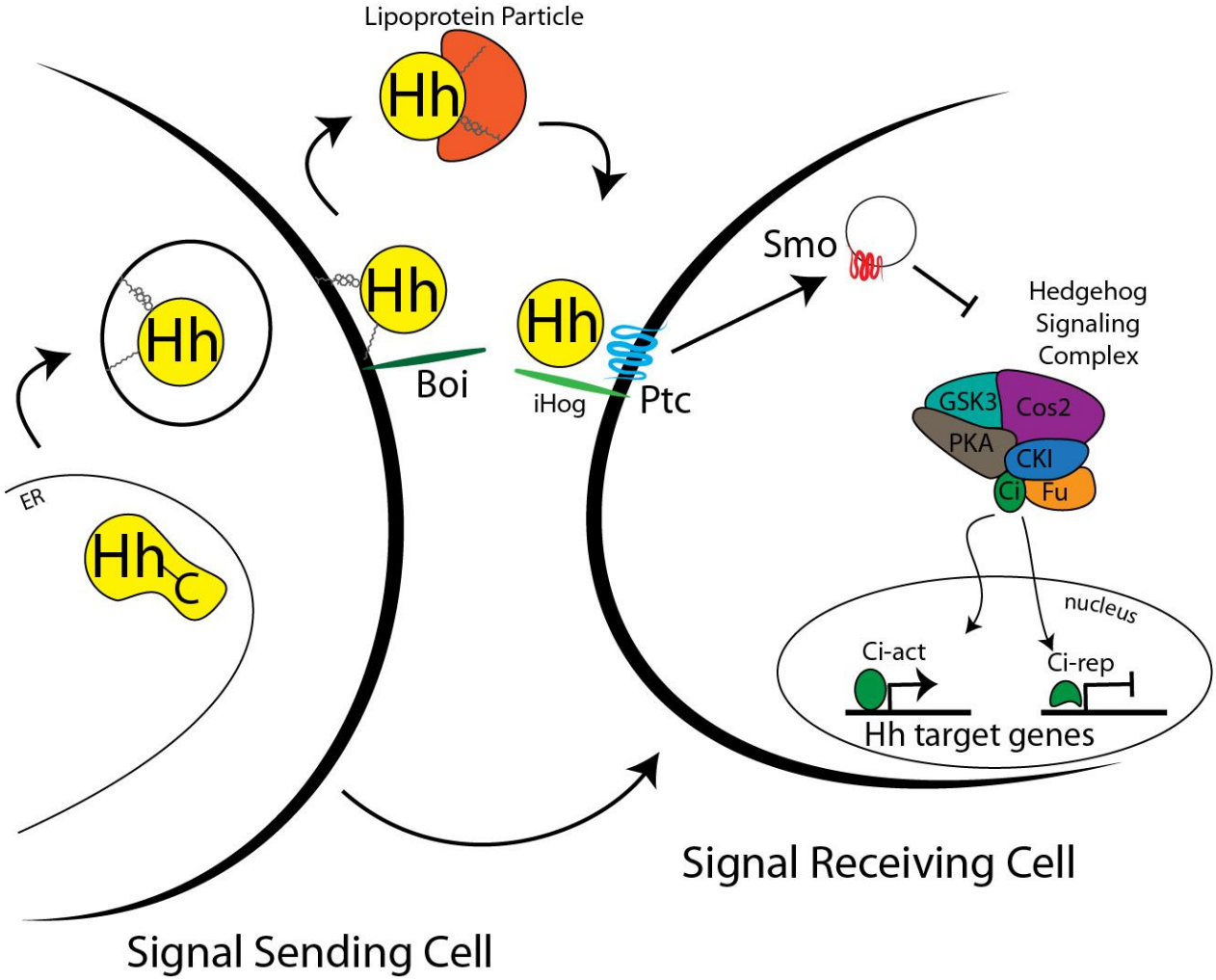

Figure 6. The Hedgehog signaling pathway (Ingham et al., 2011)

1.4.4 Signaling in the germarium

In *Drosophila* germarium, *hh* is expressed in the germline stem cell (GSC) niche, including terminal filament (TF) and cap cells (CpC), and to some extend in the escort cells (EC) (Forbes et al., 1996a). The downstream components of the Hh signaling, such as *ptc, PKA, and ci* are also expressed in the germarial soma (Sun and Deng, 2007). The Hh ligand acts long range in the

germarium, where it is released from the GSC niche and travels to the follicle stem cells (FSC) and pre-follicular cells promoting their division by activating downstream signaling (Forbes et al., 1996a; Zhang and Kalderon, 2001). It is known that the Hh ligand can be mobilized on membrane protrusions, cytonemes, of CpCs; however it is not known if this type of logistics has a relevance to FSCs (Rojas-Rios et al., 2012). Later in the oogenesis, the specification of stalk and polar cells is known to be Hh dependent. Perturbation in the Hh signal strength affects the stalk cell number and interferes with their fate choice, which results in differentiation defects (Tworoger et al., 1999). In egg chambers after stage 6, the FCs depend on the transcription factor *tramtrack (ttk)* for the cessation of Hh signaling in order to switch their cell cycle state from mitosis to endocycle (Sun and Deng, 2007). The strength of the signal depends on the ligand modification with a cholesterol moiety, which enables the long range signaling in the germarium (Eaton, 2008; Eugster et al., 2007; Panakova et al., 2005). Furthermore, the release of the active ligand and the activation of the downstream signaling requires dietary cholesterol, where the absence or presence of cholesterol in the food is necessary in order to stop and reinitiate Hh release or subsequent launch of the FSC division and differentiation program (Hartman et al., 2013). In summary, the Hh pathway was suggested to be essential for FSC progression and proper synchronization of their division rate with GSCs (Forbes et al., 1996a; Forbes et al., 1996b; Hartman et al., 2013; Zhang and Kalderon, 2000, 2001).

1.5 Aim of the study

This study aims to find the biological significance of the stress responsive *mir-310s* in *Drosophila*. The initial focus was set on the changes in proteome globally and on gross morphological and physiological aspects to decipher the *mir-310s* function. Since the *mir-310s* deficiency resulted in metabolism related phenotypes, further analyses were done in the starvation-sensitive ovary model in order to find direct target genes and cellular processes the *mir-310s* are involved in. Finally, the nature and specificity of *mir-310s'* involvement was characterized in the Hh pathway in oogenesis and nutritional stress response through three target genes including a novel Hh pathway component, *Rab23*.

2 Materials and Methods

2.1. *Drosophila melanogaster* handling and usage

2.1.1 Stock maintenance

D. melanogaster stocks were maintained on standard solid food prepared in water with:

6.25g/l agar (Serva)

18g/l dry yeast (Saf-Instant)

80g/l corn flour (Zieler & Co)

22g/l beet syrup (Ferdinand Kreutzer Sabamühle GmbH)

80g/l malt (Ulmer Spatz)

0.625% propionic acid (Merck)

and 1.5g/l methylparaben (Sigma)

Flies were kept in environment-controlled isolated rooms with constant humidity, temperature of 25°C, and 12 -12 hours daily light-dark cycle. The crosses were set up under these conditions unless stated otherwise in the experimental setup.

2.1.2 Nutritional restriction

For nutritional restriction solid cultivation medium was prepared using 2% agar-agar (Serva), 25% apple juice, and 2.5% sugar (Nordzucker AG). This medium was used to deprive flies from yeast-derived nutritional sources, which is referred as starved. On the other hand, well-fed flies were given additional fresh yeast paste prepared from dry yeast and 5% propionic acid. In both cases, food plates/vials were replaced with fresh ones every two days throughout the experiments.

2.1.3 *Drosophila* genetics

2.1.3.1 *mir-310s* mutants

For loss-of-function experiments homozygous viable *mir-310s* mutants were used, which have an 1159bp deletion on chromosome 2R previously generated by remobilization of a P element *(P(GSW1)GSd033)* (Tsurudome et al., 2010). As *wild type* controls, parental w^{1118} flies were used, which have the closest genetic background to the mutants.

2.1.3.2 Analysis of the *mir-310s* expression pattern

To obtain the expression pattern of the *mir-310s*, *mir-310s-Gal4* line (P(GawB)NP4255 line from Kyoto DGRC) bearing a Gal4 expressing P element downstream of the *mir-310s* locus (Yatsenko et al., 2014) was crossed to *UAS-mCD8-GFP, UAS-nLacZ* line (gift from Frank Hirth). The spatiotemporal specific activity of the reporter locus was revealed by the membrane GFP and nuclear LacZ expression visualized by immunohistochemistry.

2.1.3.3 Overexpression experiments

To overexpress *Rab23*, and *hh* specifically in the germarial niche cells, the *UAS-Rab23* (see section 2.1.7) and *UAS-hh* (gift from Christian Bökel) lines were crossed to the *w; +; bab1-Gal4/TM6* (#6803 BDSC) and *w; tubGal80^{ts}; bab1-Gal4, UAS-Flp/TM6* lines, respectively.

2.1.3.4 Clonal overexpression experiments

Clonal overexpression experiments were conducted by crossing *hsFlp; Stau-GFP; act>FRT-CD2-FRT>Gal4, UAS-GFP* (gift from Wu-Min Deng) flip out line to *UAS-mir-310s* line. Adult progeny was heat shocked for one hour in a 37ºC water bath for two consecutive days. After 3-4 days, ovaries were dissected and analyzed subsequently by immunohistochemistry.

2.1.3.5 Rescue experiments

The rescue experiments were conducted using *yw; +; act-Gal4/TM6b* (#3954 BDSC) and *w; +; bab1-Gal4/TM6* (#6803 BDSC) lines as soma and GSC niche specific Gal4 drivers. For specific downregulation, *UAS-Rab23 RNAi* (#28025 BDSC) and *UAS-hh RNAi* (Sahai-Hernandez and Nystul, 2013) lines were used. Both of these transgenes are positioned in the 3rd chromosome and the *mir-310s* locus is in the 2nd chromosome. This genetic setup enabled the generation of flies bearing the driver and the UAS transgenes on the *mir-310s* mutant background.

2.1.3.6 Generation of Rab23 overexpression *Drosophila* line

2.1.3.6.1 Cloning of the UAS-Rab23 vector

The *Rab23* UAS overexpression vector was generated using standard cloning techniques (Sambrook et al., 2001) by digesting the *Rab23* cDNA vector (RH23273 clone was acquired from Drosophila Genomics Resource Center) and the *UASt* vector (Figure 7) (Gunesdogan et al., 2010) using EcoRI and KpnI restriction enzymes (New England Biolabs® Inc.). Subsequently, the vector-insert ligation was performed using Quick Ligation™ Kit (New England Biolabs® Inc.);

and DH5α *E.Coli* cells were transformed by electroporation in 0.1mm cuvettes (Bio-Rad) at 1.8kV with a single pulse for the recovery of the plasmids. For all mentioned cloning steps, instructions of the respective manufacturers were followed.

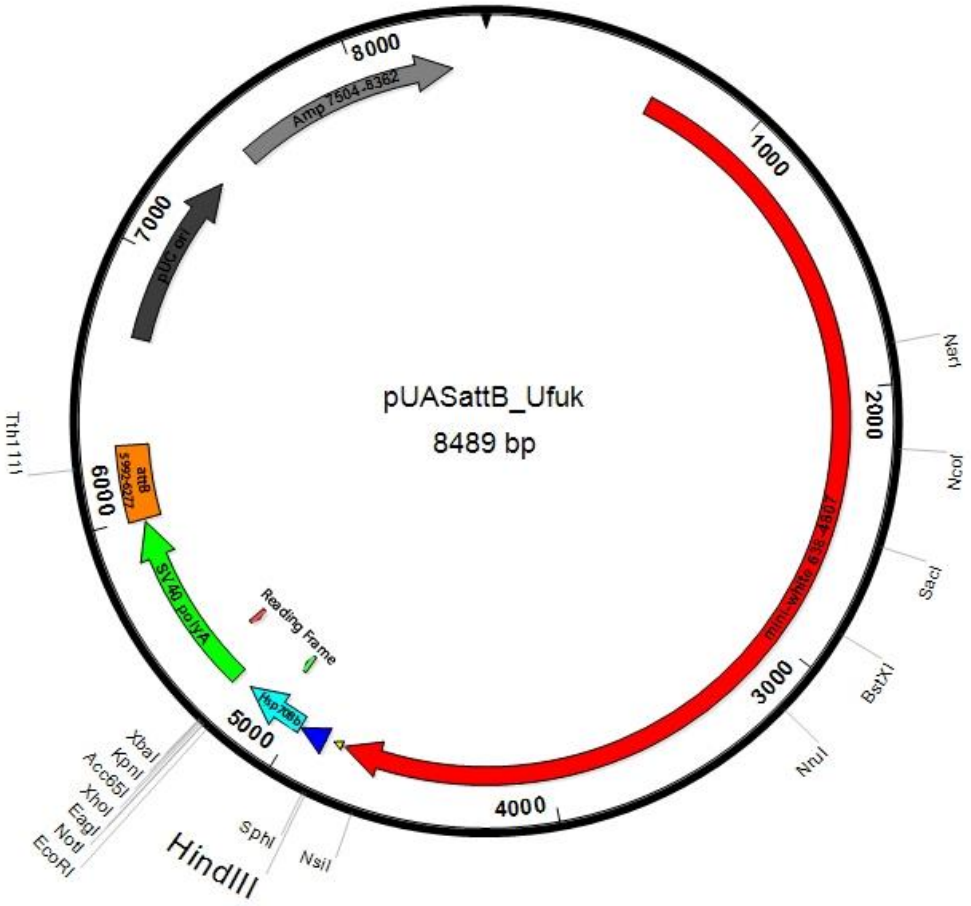

Figure 7: Vector map of the UASt vector indicating the restriction enzyme recognition sites, *att* sites for site specific integration mini-white gene for transformant selection

2.1.3.6.2 Site specific integration and transformant selection

Next, the *UASt-Rab23* plasmid was injected to *Drosophila* embryos and transformants were selected for red eye color rescue by the mini-white gene in the plasmid. The site-specific integration

on the 3rd chromosome (76A2 site) was achieved by the *att* sites in the *UASt-Rab23* plasmid and *PhiC31* into the *PBac[yellow[+]-attP-9A]VK00013* strain (Bestgene Inc.) (Çiçek et al., 2016).

2.1.3.7 Generation of the tagged *Rab23-YFP-4xmyc* line

Rab23-YFP-4xmyc line (also referred as *Rab23-YFP*) was generated by Marko Brankatschk and Suzanne Eaton in Max Planck Institute of Molecular Cell Biology and Genetics, Dresden. The line was created by ends-in homologous recombination; and the primary genomic duplication was resolved by the I-Cre system (Maggert et al., 2008; Rong and Golic, 2000). Homologous sequences with sizes of 4045bp and 3601bp were used upstream of the YFP start codon and myc tag, respectively (see Dunst et al., submitted). Donor sequence was confirmed by sequencing. The recombinations were confirmed by PCR. In the experimental setups, homozygous flies were used, which carry both *Rab23* loci endogenously tagged.

2.2. Proteome analysis by SILAC

2.2.1 Cultivation of heavy (Lysine-8) labeled *Saccharomyces cerevisiae*

To culture heavy amino acid (Lys-8, Lys-13C615N2) labeled yeast and *Drosophila*, an already established SILAC (stable isotope labeling by amino acids in cell culture) protocol was used (Sury et al., 2010). Lysine auxotrophic *S. cerevisiae* strain SUB62 (gift from Matthias Selbach) was recovered, maintained, cultured, and stored in YPD Broth (Sigma).

Defined labeling medium for *S. cerevisiae* was prepared with the below mentioned ingredients with either Lys-0 (Lys-12C614N2) (for “light” labeling) or Lys-8 (for “heavy” labeling) in water and sterilized by filtering through 0.22µm pore sized bottle top filters (Corning®) (Sury et al., 2010).

Defined labeling yeast culture medium:

1.7g/l yeast nitrogen base (without amino acids, without ammonium sulfate) (Sigma)

20g/l D-glucose (Sigma)

5g/l ammonium sulfate (Sigma)

200mg/l adenine hemisulfate (Sigma)

20mg/l Uracil (Sigma)

100mg/l Tyr (Sigma)

10mg/l His (Sigma)

60mg/l Leu (Sigma)

10mg/l Met (Sigma)

60mg/l Phe (Sigma)

40mg/l Trp (Sigma)

100mg/l Arg (Sigma)

30mg/l Lys-12C614N2 (Lys-0) (Sigma)

30mg/l Lys-13C615N2 (Lys-8) (Cambridge Isotope Laboratories, Inc.)

The SUB62 strain was initially recovered from YPD agar plates by inoculation into YPD medium first in 5ml and then in 200ml (with OD_{600} 0.2) volumes overnight at 30ºC. Defined labeling media (Lys-0 and Lys-8) of 50ml were inoculated by the YPD culture with a dilution of 1:1000. Next, this labeling preculture was used to inoculate 400ml of labeling media in 1:100 dilution rate. After this last cultivation for 24 hours at 30ºC, yeast cells were pelleted by centrifugation at 6000g for 15 minutes at 4ºC, which was used for the *Drosophila* labeling food preparation.

Prior to feeding of *Drosophila*, yeast Lys-8 incorporation efficiency was measured by mass spectrometry. Aliquots of yeast pellets were boiled in a buffer containing 50mM Tris (pH 7.5, Merck), 5% SDS (Carl Roth), 5% glycerol (Sigma), 50mM dithiothreitol (Sigma), and protein inhibitor cocktail 2X (Thermo) for 10 min. After centrifugation at 12000g for 5 minutes, the supernatants were analyzed by mass spectrometry for the measurement of Lys-8 incorporation efficiency. >95% efficiency was enough to continue with labeling of the flies (Figure 8).

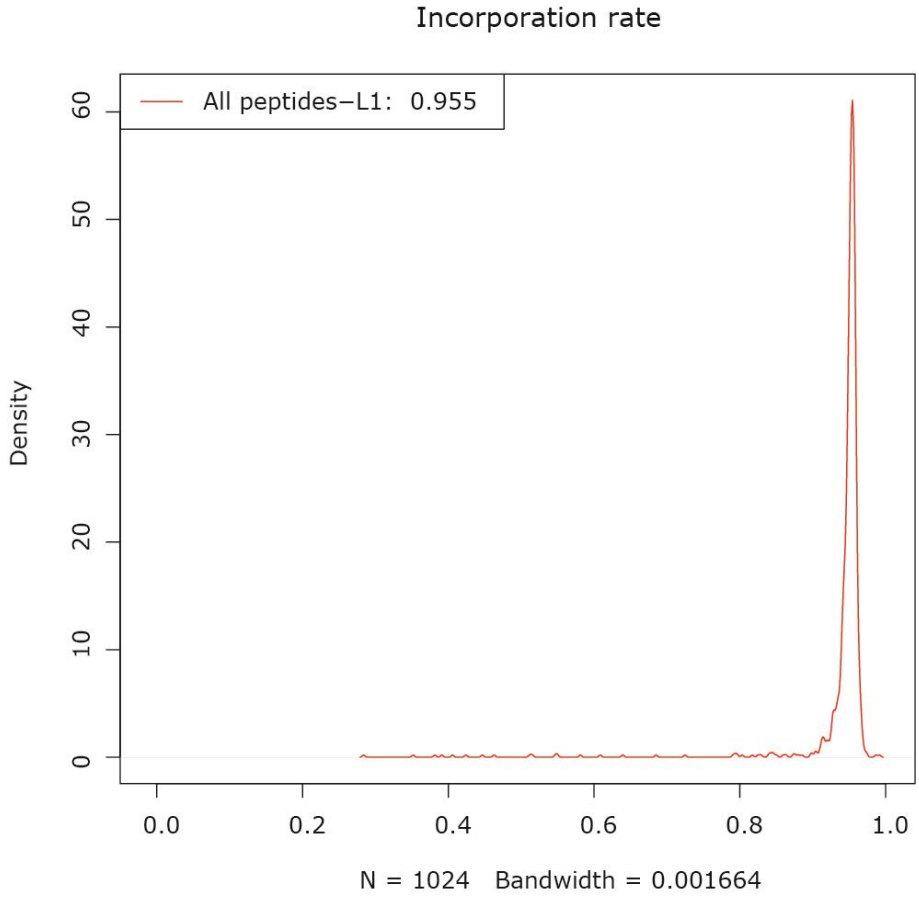

Figure 8. Lys-8 incorporation efficiency of the yeast used for *Drosophila* labeling (Çiçek et al., 2016)

2.2.2 Cultivation of heavy (Lysine-8) labeled *D. melanogaster*

Labeling culture medium

Lys-0 (light) labeled medium was used to cultivate *control* and Lys-8 (heavy) labeled medium was used to cultivate *mir-310s* mutant flies. The labeled yeast was used in a buffer with the following constituents (Sury et al., 2010).

60% (w/v) labeled S. cerevisiae (wet mass)

320mM sucrose (Sigma)

0.3mM ampicillin (Sigma)

6 mM methylparaben (Sigma)

0.5‰ propionic acid (Merck)

2.5‰ phosphoric acid (Merck)

In parallel, a reverse labeling was performed, where *control* flies were grown on Lys-8 and *mir-310s* mutant flies were grown on Lys-0 labeling media serving as a replicate experiment. Prior to harvesting, adult flies were fed on respective media supplemented with labeled yeast pellets.

2.2.3 Whole protein extract preparation

For the whole extract sample preparation, 10 female flies were harvested by freezing in liquid nitrogen and subsequent homogenization using an automated pestle (in a 1.5ml test tube) in 100µl RIPA buffer containing 50mM Tris HCl (pH 7.4, Carl Roth), 150mM NaCl (Merck), 1% NP-40 (Sigma), 0.25% Nadeoxycholate (Sigma), 1mM EDTA (Carl Roth), 0.1% SDS (Carl Roth) and 1x protease inhibitor cocktail complete (Thermo).

The protein concentrations of the lysates were measured using Bradford Reagent (Sigma). Next, lysate samples from respective genotype-label set with a total protein content of 25µg were used for subsequent mass spectrometry analysis.

2.2.4 Mass spectrometry analysis

The analyses of the samples and the spectra were done by Samir Karaca and Henning Urlaub in the Bioanalytical Mass Spectrometry Group in Max Planck Institute for Biophysical Chemistry, Göttingen.

2.2.4.1 Gel electrophoresis and protein digestion

Proteins were separated using one-dimensional SDS-PAGE (4%–12% NuPAGE Bis-Tris Gel, Invitrogen) and gels were stained using Coomassie Blue G-250 (Fluka). Gel lanes were cut into 23 slices and used in the in-gel digestion of proteins (Shevchenko et al., 2006) via Lys-C (Roche Applied Science) in an overnight reaction. 10 mM DTT was used for 50 min at 50°C for reducing, followed by alkylation using 55 mM iodoacetamide for 20 min at 26 °C. As the next step, extracted peptides were applied onto the in-house packed C18 trap column (ReproSil-Pur 120 C18-AQ, 5µm, Dr. Maisch GmbH; 20 x 0.100 mm) at 5 µl/min flow rate using loading buffer with the composition 2% acetonitrile, 0.1% formic acid.

2.2.4.2 Column chromatography and ESI-TOF-TOF mass spectrometry

The separation of the peptides were performed on the analytical column (ReproSil-Pur 120 C18-AQ, 3µm, Dr. Maisch GmbH; 200 x 0.050 mm), which was packed in-house into a PF360-75-15-N picofrit capillary (New Objective) using linear gradient from 5% to 40% acetonitrile containing 0.1% formic acid at 300nl/min flow rate for 90 minutes using nanoflow liquid chromatography system (EASY n-LC 1000 Thermo Scientific). The chromatography was coupled to hybrid quadrupole-Orbitrap (Q Exactive, Thermo Scientific). Regarding data acquisition, the mass spectrometer was used in data-dependent mode via survey scans attained from m/z 350-1600 in the Orbitrap at 70,000 FWHM resolution settings, 200 m/z, and 1E+06 target value. A maximum number of 15 most abundant ≥2+ charge stated precursor ions were consecutively isolated and fragmented using higher collision-induced dissociation (HCD) with 28 normalized collision energy. In order to avoid repeated peptide sequencing, dynamic exclusion was set to 18s.

2.2.4.3 Analysis of the spectra

To analyze the mass spectrometry data the MaxQuant software was used (version 1.3.0.5, via Andromeda search engine) (Cox and Mann, 2008) against UniProtKB *D. melanogaster* and Flybase databases with 18826 entries (acquired online in April 2013) complemented with common contaminants with reverse sequences. The Andromeda search constraints were fixed as following: Lys-C specificity with the restriction of no prolines and up to two missed cleavages; as a variable modification, N-terminal acetylation and oxidation of methionine; and as a fixed modification, carbamidomethylation of cysteines. For the MS survey scan mass tolerance 7ppm, and for the MS/MS 20 ppm was set.

As the requirement for protein identification a minimum of five amino acids per peptide and one peptide for protein were set. 1% of false discovery rate at peptide and protein level was fixed. “Re-quantify” was enabled and “keep low scoring versions of identified peptides” disabled.

2.3 Gene expression analyses

2.3.1 Primer design

The design of the qPCR primers were done using Lasergene software (Table 1) (Çiçek et al., 2016). The amplicons were designed in 100-200bp length and intron spanning if applicable. In cases,

where the gene model did not allow intron spanning amplicons, RNA samples were treated with DNAse (Ambion); and no reverse transcriptase controls were included in the experiments.

Table 1: Primers used for qPCR

Experiment	Gene Name	Orientation	Sequence
qRT-PCR of targets	*Rab23*	Forward	AGCTGGCCATTAAAGTGGTCATT
	Rab23	Reverse	GATCTCGATCTGTCGCTCTAGGA
	DHR96	Forward	CCTCAGCGCCCTGATGATGG
	DHR96	Reverse	CAGCTGCAATAGCTTTGGGTTGTG
	ttk	Forward	CGAAACGATCAAAGAACTCCAAGG
	ttk	Reverse	CGCCTGCTCGTTGAGGTGACTAC
	Rpl32	Forward	AAGATGACCATCCGCCCAGC
	Rpl32	Reverse	GTCGATACCCTTGGGCTTGC
SILAC hits/ starvation sensitive gene expression confirmation	*Act88F*	Forward	GCGCCACCCGAGAGGAAGTA
	Act88F	Reverse	TGGAAGGTGGACAGCGAGGC
	ade2	Forward	TTCCGTCGGTTTGCCTACATCA
	ade2	Reverse	TCCGCGACGAGAAGCTCATTAG
	ade3	Forward	GCCCAAACCCAAAGCCAAGG
	ade3	Reverse	CATCCAGCTGGTGGAGAAGTGC
	Arr1	Forward	CAGTCAGGATGCGAGGGATGC
	Arr1	Reverse	CCCAGGGCTCCCAAGAAAAG
	CG3699	Forward	TCTGCCTGCGTGCCCTTCA
	CG3699	Reverse	CCGCCATCGCCCAAGTTCT
	CG3902	Forward	CACGGTGGCGATCTGATGCT

CG3902	Reverse	GCGCAAGCAGTTCGGTGATG
CG3999	Forward	CCATCGACAATGGGCGTGTTC
CG3999	Reverse	CTGGGCATTCATGTTGGCTCC
CG9914	Forward	GGGACCCAGGAAGGCGTAGC
CG9914	Reverse	GCCGGCATCCTGAATGTCAAG
CG11089	Forward	CCCGCAGGATCCACCAATGA
CG11089	Reverse	GGGCCATGATGATACCGTGCTC
CG15369	Forward	CGGTGCACCAAAAGTCCTCG
CG15369	Reverse	GTCCTTCGCCAGCAGCCAAT
CG16884	Forward	GCGATCGCGGGACCACTGT
CG16884	Reverse	GGCCACGGAAGCTACGGACAT
CG30360	Forward	CGATCAGCGGAGAGTGGGTAGT
CG30360	Reverse	ACGCCGGGCAGGAACATCT
CG31233	Forward	CCAGCACGCAGACCAACATAGC
CG31233	Reverse	GCCACCAGATCACCAAACCACA
Cpr62Bc	Forward	CGTCTCCGGTGTGAGAGTCAGC
Cpr62Bc	Reverse	GGTCACCACGACGAGGGAATC
Cpr72Ec	Forward	CGCATCCTCATCGGTCAGACTC
Cpr72Ec	Reverse	GCGTGAGGAGGCGGACAGA
Cpr100A	Forward	TCCAGCCAGCACTATCACCAGG
Cpr100A	Reverse	AGCTCCGAACTTTCCATCTCCG
Gal	Forward	CCAGACGCTTAGCGGGATTCA
Gal	Reverse	CCGGTGGCGTCACCACTAAGTA

Gasp	Forward	CTCGCCGTTCCAGCAGTTCC
Gasp	Reverse	CTCGCCTGTACGGCATCTTCC
GstD4	Forward	TCCCCAGCACACCATTCCC
GstD4	Reverse	CCTTGCCGTACTTTTCCACCAG
Lsp1beta	Forward	CCCGCCCACGAGCAGTTCT
Lsp1beta	Reverse	CGCACGGTCGAAGGGATAGC
Lsp2	Forward	TGCCCAACCGAATGATGCTG
Lsp2	Reverse	CGGGCTGGTGGTACGGGTAG
LvpH	Forward	CGACTTGAATATGGGCGACAGC
LvpH	Reverse	ACGGCATTGGCGACCTGAAC
Mgstl	Forward	GATGTCCCCCAAGCTGAAGGTC
Mgstl	Reverse	GGCGAAGAAGGGCAGGATGTT
mus209	Forward	ACATCGACAGCTGCACTTGGGT
mus209	Reverse	GCCGGTGACGCTGACATTTG
Obp44a	Forward	TGCTCGCTCGGAGGAAACTGT
Obp44a	Reverse	TGCGACATACCCACATTGAGCG
Obp56a	Forward	CGCCTCCAAGTTGTACGATTGC
Obp56a	Reverse	CCGAATCACAATTTGCCAAGCA
Obp56e	Forward	CCGCCCTTGCAGCTCTATCTTT
Obp56e	Reverse	TTGCCTCAGCCTTTTGGGAATC
Obp99b	Forward	CTCCTCGCTGGCGTGAACCT
Obp99b	Reverse	TCACCATCACCATCACCACGAC
obst-A	Forward	CATCCCACCGACTGCCAGAAG

obst-A	Reverse	ATCGTTGTAGACCTCGCCCAGC
pro-PO-A1	Forward	GGCGGTCCACGTCCCTCAG
pro-PO-A1	Reverse	CCAGCACGAATAACCGCACCTA
Sucb	Forward	TTGGCTGATCTGCGGTGGTAAC
Sucb	Reverse	CGGCGATTTTCGGTTGTGTTT

2.3.2 Whole RNA extraction and cDNA synthesis

The females from *control* and *mir-310s* genotype were kept on starvation and well-feeding conditions for 10 days before harvesting for RNA isolation. Total RNA was extracted from three biological replicates of 10 females for each genotype-feeding condition by homogenization in 200µl Trizol (Ambion) by automatic pestles in 1.5ml test tubes; and the following isolation was done by Direct-Zol RNA Miniprep (Zymo Research). Total cDNA was reverse transcribed using random primers with High Capacity Reverse Transcriptase (Applied Biosystems) with 1.5µg of total RNA template in 20µl reaction.

2.3.3 Quantitative PCR

2.3.3.1 qPCR conditions

The qPCR was performed using Fast SYBR Green reagents in Step One Plus Real Time PCR System (Applied Biosystems) according to the manufacturer's instructions. Each reaction was set up with 300nM of forward and reverse primer concentrations and 20ng cDNA as template in 20µl volume.

2.3.3.2 C_T value analysis and relative gene expression calculation

The analysis of the acquired C_T values were done by StepOne Software (Applied Biosystems) and Excel (Microsoft). The technical replicate average C_T values of the respective genes were normalized to the values of housekeeping gene, *Rpl32*, by subtraction (ΔC_T). Next, these ΔC_T values were put through another round of normalization by subtraction, this time to the ΔC_T values of the *control* well-fed samples ($\Delta\Delta C_T$). Finally, the $\Delta\Delta C_T$ values were used to calculate the relative gene expression levels using the formula: $2^{-\Delta\Delta C_T}$. Refer to the Table 5, 8, and 10 for the C_T, ΔC_T, $\Delta\Delta C_T$, and relative expression values. Non-paired two-tailed Student's t-test was used for the calculation of p values for statistics.

2.3.4 Quantitative miRNA expression analysis

To measure relative *mir-310*, *mir-311*, *mir-312*, and *mir-313* expression levels, TaqMan® microRNA Assays (Applied Biosystems) were used according to the manufacturer's instructions. The technique involves reverse transcribing the specific mature miRNAs in a reaction and subsequently detecting the quantity via PCR coupled with labeled oligonucleotide probes. In the assays, 10ng of total RNA was used for each 20µl reverse transcription reaction and 1.33µl of this reaction as the template for the subsequent qPCR. The 2S rRNA assay was used to standardize the experiment and normalize the data. The calculation of the relative miRNA expression levels and statistics were done using the respective C_T values as described above.

2.4 Immunohistochemistry

2.4.1 Ovary dissection

The dissection procedure was performed in cold 1X Phosphate buffered saline (PBS) (Applichem) on soft plastic plates. In case of well-fed flies, to access the ovaries, the posterior-most cuticle was removed from the abdomen with the help of two forceps. Then, the abdomen was squeezed gently in an anterior to posterior direction to push the ovaries out from the cuticle opening. In case of dissecting starved ovaries, approximately one fifth of the abdominal posterior-most cuticle was ripped off, which is attached to the very small ovary pair. The ovaries from starved females were kept connected to the remaining neighboring tissues throughout the staining procedure for easier replacement of the solutions and to avoid losing the specimens. Next, ovaries were fixed in 4% paraformaldehyde (PFA) (Polysciences Inc.) (in 1X PBS) for 15 minutes and then washed with PBT (0.2% Triton™ X-100 (Sigma) in PBS) 3 times for 10 minutes at room temperature (RT) on a nutator (Polymax 1040, Heidolph).

2.4.3 Antibody staining and mounting

The subsequent staining procedure was performed as described (Konig and Shcherbata, 2013). Fixed tissues were blocked with PBTB (2g/l Bovine Serum Albumin (BSA) (AppliChem), 5% Normal Goat Serum (NGS) (Abcam), 0.5g/l sodium azide (Sigma)) for one hour at RT and then added primary antibody solutions (Table 2) and incubated overnight at 4ºC on a nutator. The following day, the specimens were washed with PBT 3 times for 10 minutes at RT. Next, a secondary blocking of the tissues followed again with PBTB for one hour at RT; and then

secondary antibody solutions were added and 2-3 hours of incubation followed at RT on a nutator. After this, the samples were again washed with PBT 3 times for 10 minutes at RT. Then, 10mg/l DAPI (Sigma) in PBT was added for 10 minutes and then the samples were washed for the final two times with PBT. In the end, the solution was aspirated completely and the mounting medium (70% glycerol (Sigma), 3% n-propyl gallate (Sigma) in 1X PBS) was added on the samples and left at 4ºC overnight. For mounting, ovaries from well-fed females were separated into their individual ovarioles with help of syringe needles. On the other hand, ovaries from starved females were just freed from extra tissues and cuticle and were kept as a whole on the slides (76 x 26mm, Thermo Scientific).

Antibodies were used with the following dilutions:

Table 2. Dilutions and sources of antibodies used for immunohistochemistry

Type	Specificity	Dilution	Source
mouse monoclonal	anti-Adducin	1:50	DSHB
mouse monoclonal	anti-LaminC	1:20	DSHB
mouse monoclonal	anti-Fasciclin III	1:50	DSHB
mouse monoclonal	anti-β-Gal	1:25	DSHB
rat monoclonal	anti-DE-Cadherin	1:25	DSHB
chicken polyclonal	anti-GFP	1:5000	Abcam
guinea pig polyclonal	anti-Hh	1:100	Acaimo González-Reyes
rabbit polyclonal	anti-PH3	1:5000	Upstate Biotechnology
Secondary, goat	Alexa 568 anti-mouse	1:500	Invitrogen
Secondary, goat	Alexa 488 anti-rat	1:500	Invitrogen

Secondary, goat	Alexa 488 anti-rabbit	1:500	Invitrogen
Secondary, goat	Alexa 488 anti-chicken	1:500	Invitrogen
Secondary, goat	Alexa 568 anti-guinea pig	1:500	Invitrogen

2.4.4 Imaging

A confocal laser-scanning microscope (Zeiss LSM 700) was used for taking of fluorescence images, which were processed with Zeiss ZEN microscope, Adobe Photoshop and Adobe Illustrator software for figure design.

2.5 Luciferase assay

An *in vitro Drosophila* S2 cell culture based reporter assay was used, which involves generation of three different reporter constructs and transfection based delivery of the reporter plasmids to the cells. The readout is based on the enzymatic activity of the reporter luciferase genes.

2.5.1 Cloning of the sensor constructs

The 3'UTR segments containing *mir-310s* binding sites from the genes *Rab23, DHR96,* and *ttk* were cloned downstream of a luciferase (*Renilla*) reporter gene using standard cloning techniques (Sambrook et al., 2001). The respective 3'UTR segments were amplified by PCR using primers (Table 3) (Çiçek et al., 2016) in 0.5µM concentration on 2µg genomic DNA template with HotStarTaq Master Mix (Qiagen) at an annealing temperature of 59ºC in a total of 50µl reaction according to the manufacturer's instructions. The primers were designed using Lasergene software and were manually added restriction enzyme recognition sites (with additional four base pairs at the 5'). The PCR products and the target reporter vector (psiCHECK^{TM} -2, Figure 9 and 10) were digested with NotI-HF and XhoI enzymes (New England Biolabs® Inc.). The subsequent steps of ligation and transformation was done as described in section 2.1.3.6.1.

Table 3. Primers used for cloning

Rab23 NotI	Forward	GCAAGCGGCCGCTTTTTGCATAGAATGCGAGCAGC
Rab23 XhoI	Reverse	GCAACTCGAGCCAAGCCCAGATCACAGGTCC
ttk XhoI	Forward	GCAACTCGAGAAGCGCAATCAAATAATAAACAAG
ttk NotI	Reverse	GCAAGCGGCCGCGCGAGAAAATTGCTGAAGGTT
DHR96 XhoI	Forward	GCAACTCGAGTGTCTGTTTTATCTTGTCGCTTGT
DHR96 NotI	Reverse	GCAAGCGGCCGCTCCTTTTTGCACAGAACCCAC

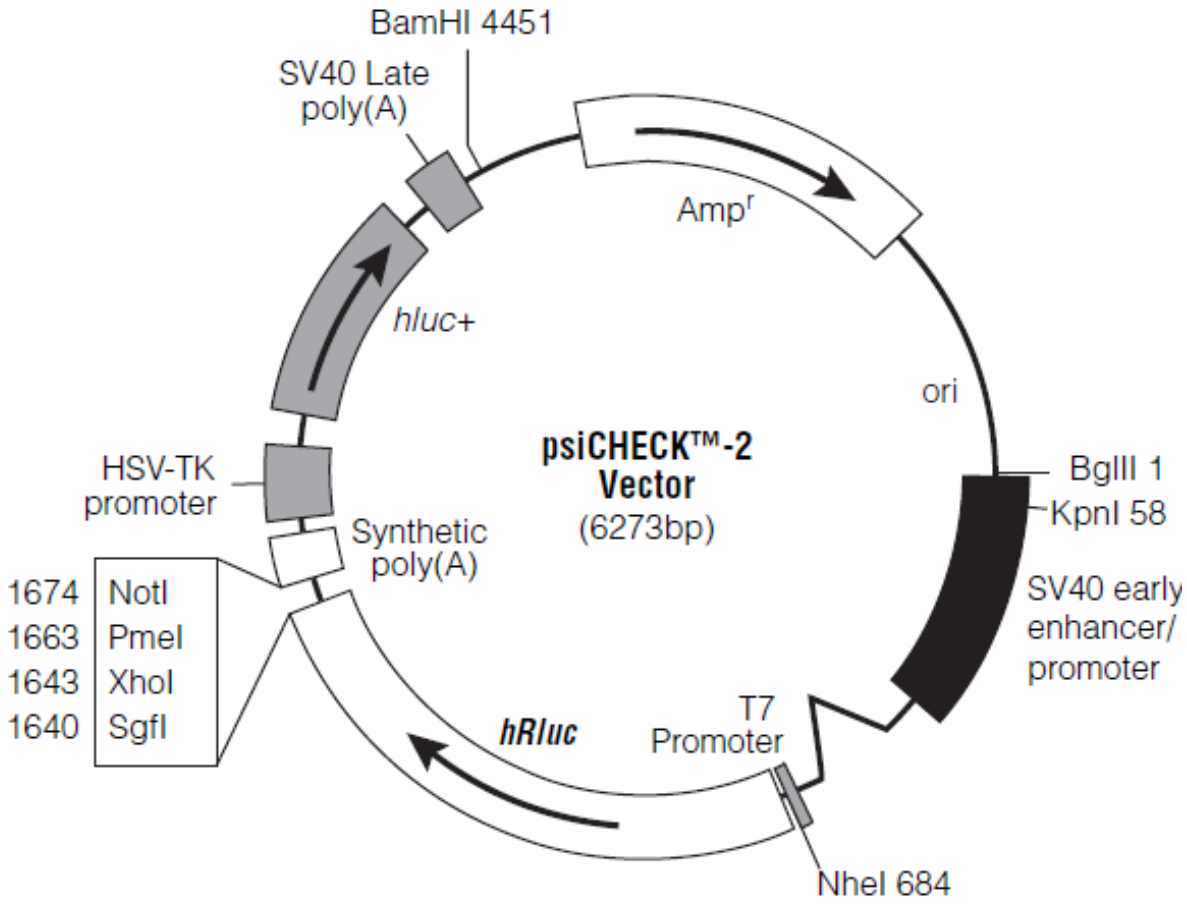

Figure 9. psiCHECK™ -2 vector (Promega, 2009) used for cloning of the 3'UTR fragments of *Rab23*, *DHR96*, and *ttk* genes for luciferase assay

Note that the psiCHECK^{TM} -2 vector also contains the *Firefly* luciferase gene, which serves as an internal transfection control and therefore was left unmodified.

Cloned 3'UTR fragments with *mir-310s* binding sites

Rab23

[CCAAGCCCAGATCACAGGTCCATGTGAAATCCCTTTGCCAATTCGCGTTGGCCAAATGTGCAATTAAA
CATTCAGCTTTTATAATTATTAACTAATTGCAAGTCATGCCAGAGCGCAATTTGACGCGATTCATGTAG
ACCAGTGCTGCTCGCATTC]

DHR96

[TGTCTGTTTTATCTTGTCGCTTGTAATGTTAGATTTTAATCGAATGTGATTGTTAGATTTGCATATACTG
CATAGATTTTATATTTCTACATCAAAGAGAGCATATTTAGGATACCAAGTGCAAAGCAACACAATCTAT
ATGTAATGTACACCGTTTACCTAGTTTCAAATAAACTAGACGATAATGCAATAACTAACTTGGAAGCGT
GGGTTCTGTGCAAAAAGGA]

ttk

[AAGCGCAATCAAATAATAAACAAGCTGCGTACGCTAACTTATTAAATAATTTTGTTTTTAATTCTTTAT
TTAGTGGTAGCTAGTGCAATTTAGTTAGTAAGCCGCCGTCTCCCAAACACCGACTAACCAATATCGCAA
ATATATATTTCCACCCAATCGAACCAATCTTCCAAACATCTCTTTTGGCGTTAATTTTAAACAATCAATC
AAACAGGTCATGCATATTTATTTGTATGTGTTTGTTTGTACTATATTTTACTTTATTTTTAGTCTACTTTT
TTATATGAATACATTTACATATATTTTTGCATTCAACAACTATAAACCTTCAGCAATTTTCTCGC]

Figure 10. The cloned *Rab23, DHR96,* and *ttk* 3'UTR fragments with annotated *mir-310s* seed sequence complementary sites

2.5.2 Maintenance and transfection of the Drosophila S2 cells

Drosophila S2 cells were cultivated in Schneider's *Drosophila* medium (Gibco®) complemented with 10% heat inactivated fetal bovine serum (GE healthcare), 100 units/ml penicillin, and 100 µg/ml streptomycin (Gibco®) in 25cm^2 culture flasks in 6ml medium at 25ºC in an incubator. Prior to transfection, S2 cells were split 1:6 and seeded into 96-well plates (Thermo Scientific™ Nunc™) and incubated overnight. Transfection mixes were prepared using Effectene® Transfection

Reagent (Qiagen) using manufacturer's instructions. Each well was transfected with 5ng *actin Gal4*, 20ng *UAS-mir-310s*, (gift from Eric Lai), and 10ng luciferase reporter plasmids. For the experiment, *Rab23, DHR96*, and *ttk* 3'UTR reporters were used in addition to the unmodified psiCHECK™ -2 plasmid, which served as control. All transfections were performed in two biological replicates.

2.5.3 Luciferase reporter activity measurement

The transfected cells were incubated for 72 hours before measuring the Firefly and Renilla luciferase activities using the Dual-Glo® Luciferase Assay System (Promega) and a Wallac 1420 luminometer (PerkinElmer). To measure the Firefly luminescence the wells were added 75µl of Dual-Glo® Luciferase Reagent. After 10 minutes of incubation at RT, the luminescence was recorded. Next, to measure the Renilla luciferase activity 75µl of Dual-Glo® Stop & Glo® Reagent was added on the cells. Again, after 10 minutes at RT, the luminescence was recorded.

2.5.4 Analysis of the luciferase signals

To calculate the relative downregulation of the reporter luciferase signals by the *mir-310s*, first, the raw readouts of the Renilla luciferase signal was divided by the Firefly luciferase signal for internal normalization to compensate for the variation of the transfected cell numbers in each well. Next, the respective Renilla/Firefly ratios were normalized to the unmodified psiCHECK™ -2 transfection by division. For statistics, non-paired two-tailed Student's t-test was used.

2.6 Quantitative protein measurement of Rab23

2.6.1 Sample preparation

In order to assess the effect of *mir-310s* loss on Rab23 protein content under different nutritional stress, two lines with the *Rab23-YFP* locus and *control* or *mir-310s* mutant background were used, where each genotype (*w^{1118} ; Rab23-YFP-4xmyc* and *mir-310s ; Rab23-YFP-4xmyc*) was set under well-fed and starvation conditions for 10 days.

The homogenization of the 100-200mg of fly samples were performed in 2ml lysis buffer containing 20mM Tris (pH 7.4, Merck), 150mM NaCl (Merck), 5% glycerol (Sigma), 5mM EDTA (Merck), 1% Triton™ X-100 (Sigma), and 2X protease inhibitor cocktail (Roche) with the help of a mortar, pestle, and periodically addition of liquid nitrogen. Next, the lysates were thawed on ice. The clearance of the lysates from the cuticular and cellular debris was achieved by centrifugation

once for 5 minutes and twice for 15 minutes at 21000g at 4ºC and by carrying over the supernatants. To measure the total protein contents of the clear lysates, Bradford Reagent (Sigma) was used according to manufacturer's instructions using BSA serial dilutions and calculated standard curve.

2.6.2 SDS-PAGE and western blotting

Samples with 40µg total protein content were run on 12% polyacrylamide (Bio-Rad) gels at 100, 200, and 250V, for 90, 60, and 30 minutes respectively at maximum 0.03A until the prestained 50 and 70kDA band (Nippon Genetics) had the best separation (Laemmli, 1970). For western blot analysis (Towbin et al., 1979) pre-packed transfer sets with PVDF membranes (Bio-Rad) were used. For semi-dry transfer (Kyhse-Andersen, 1984), the gel-membrane packs were subjected to 25V maximum 3A for 15 minutes in a Trans-Blot Turbo System (Bio-Rad). Next, the membranes were washed with 1X PBS and blocked by nutating in 1X Blocking Buffer (Sigma) for one hour at RT. Then, primary antibodies were applied overnight with the following dilutions in the blocking buffer. Next day, the membranes were washed 3 times in 0.1% Triton™ X-100 (Sigma) in 1X PBS for 10 minutes and secondary antibody dilutions were added for 1 hour incubation at RT. Rab23-YFP and β-tubulin were detected using primary polyclonal chicken anti-GFP (1:10000, Abcam) and monoclonal mouse anti-β-tubulin (1:1000, Developmental Studies Hybridoma Bank), and secondary anti-chicken-HRP and anti-mouse-HRP (1:5000, Jackson Laboratories) antibodies, respectively. The generation of the HRP signals was achieved using WesternBright ECL HRP substrate (Advansta).

2.6.3 Analysis of the HRP signals

Three biological replicates were analyzed via SDS-PAGE and western blotting followed by HRP signal measurement by a luminescent image analyzer (LAS-1000plus, Fujifilm). The respective Rab23-YFP and β-tubulin signals were quantified by Adobe Photoshop software. The total pixel intensities of respective bands were calculated and Rab23 signals were normalized to the β-tubulin signals of respective sample (Table 9).

2.7 Total body fat content measurement

An established enzymatic coupled colorimetric assay (CCA) (Hildebrandt et al., 2011) was used to measure the total body fat content of *control* and *mir-310s* mutant flies, which were well-fed (3 days) or starved (10 days).

2.7.1 Sample preparation

The harvested female flies (5 flies per genotype/condition, in biological triplicates) were homogenized in 1000µl 0.05% TWEEN® 20 (Sigma) using automated homogenizer (Precellys 24, Bertin Technologies) for 10 seconds at 5000 rpm in 2ml tubes with 6.8mm ceramic beads. The lysates were then incubated at 70°C for 5 minutes and cleared using centrifugation at 3000g for 3 minutes. The resulting supernatant was made use as substrate for the subsequent assays. Samples with volumes of 50µl for the well-fed and 75µl for the starved fly harvests were used for the triglyceride (TAG) equivalent measurements.

2.7.2 Coupled colorimetric assay (CCA)

In addition, to calculate a standard curve and absolute TAG equivalent amounts, serial dilutions of Thermo Trace Triglyceride standard (Thermo Scientific™) were included in the assay. The fly samples and the standards were added 200µl of prewarmed (37°C) Triglycerides Reagent (Thermo Scientific™) and incubated at 37°C for 30 minutes. Next, the absorbance values at 540nm were measured. In parallel, total protein content of the lysates were measured using BCA Protein Assay Reagent (Thermo Scientific Pierce). From each lysate 50µl samples were assayed in addition to serial dilutions of BSA standard for calculation of a standard curve and absolute protein content of the lysates. These samples were then added 200µl BCA mix and incubated for 30 minutes at 37°C. Next, the absorbance values were recorded at 570nm. All reactions were performed in 96-well microtest plates (Sarstedt) and absorbance values were measured using Benchmark Microplate Reader (Bio-Rad).

2.8 Rab23 co-immunoprecipitation

2.8.1 Sample preparation

Prior to lysate preparation, ~1 week old flies with *control* and *Rab23-YFP-4xmyc* genotypes were given fresh yeast paste for 2-3 days. Three biological replicates were done and flies were harvested by freezing in liquid nitrogen. 750mg fly harvests were homogenized in 2ml buffer containing 20mM Tris (pH 7.4, Merck), 150mM NaCl (Merck), 5% glycerol (Sigma), 5mM EDTA (Merck), 0.1% Triton™ X-100 (Sigma), and 2X protease inhibitor cocktail (Roche) with the help of a mortar, pestle, and repeated addition of liquid nitrogen. Next, the crude lysates were cleared by centrifugation once at 15000g and twice at 21000g for 10 minutes at 4°C.

2.8.2 Binding and elution

Next, the final lysates from *control* and *Rab23-YFP-4xmyc* flies were taken into 15ml tubes and were completed to 5ml volume using the same buffer. For binding Rab23-YFP-4xmyc, agarose beads coupled to anti-myc antibodies were used (Sigma). 50µl slurry of these beads are added to the 5ml clear lysate samples and incubated at 4°C for 100 minutes rotating. The bound beads were collected via centrifugation at 100g for 2 minutes at 4°C, where they were transferred to spin columns (Sigma) for washes and elution. Next, the beads were washed using 700µl of the same buffer for 10 times by centrifuging at 100g for 30 seconds and at 4°C. Finally, the elution of the bound proteins were achieved by addition of 50µl pre-warmed 2X sample buffer (NuPAGE® LDS Sample Buffer, Novex®) onto the beads and centrifugation at 100g for 1 minute.

2.8.3 Mass spectrometry analysis

The eluates from the anti-myc antibody coupled agarose beads were analyzed by mass spectrometry as described in section 2.2.4 with the only difference that Trypsin (Roche) instead of Lys-C (Roche Applied Science) was used for in-gel digestion of the proteins.

3 Results

3.1 The *mir-310s* have nutrition and energy metabolism-associated function

3.1.1 *mir-310s* loss-of-function mutants have perturbed expression of genes involved in nutritional homeostasis and energy metabolism

miRNAs regulate gene expression and are required to maintain healthy physiological state globally (Rottiers and Naar, 2012). They are post-transcriptional regulators of gene expression, where the amount and availability of a target mRNA is regulated to achieve optimal levels of protein expression. Therefore, omics approaches for miRNA function can be based on transcriptome or on proteome giving different hints about the level, specificity, and mode of regulation by the miRNAs. Here, functions of the *mir-310s* in *Drosophila* were investigated in terms of global changes in protein expression caused by *mir-310s* deficiency.

3.1.1.1 Stable isotope labeling of *Drosophila* reveals genes with altered protein expression as a cause of *mir-310s* deficiency

To obtain information about the regulated mechanisms by the *mir-310s* in terms of the global changes in protein expression, quantitative proteomics data of miRNA mutant flies was produced with the help of an established technique based on mass spectrometry of heavy isotope labeled *Drosophila* (Sury et al., 2010). The labeling of the flies was achieved by feeding them with heavy labeled yeast starting from larval stage. The heavy labeled yeast was cultivated using a lysine auxotrophic strain (SUB62) by heavy lysine (Lys8) ([$^{13}C_6$, $^{15}N_2$] Lys) for several generations. As reported (Sury et al., 2010), almost complete incorporation efficiency of the heavy lysine to the fly proteins (>95%) allowed the preparation of total lysates and the analysis of the relative protein abundance ratios between *control* and *mir-310s* mutants via mass spectrometry. The analysis of the spectra and database searches resulted in a large list of proteins, of which expression was changed due to *mir-310s* loss. The fact that miRNAs commonly fine-tune the expression of their target genes and thereby the activity of the associated pathways, proteins with a modest (≥30%) relative increase or decrease with p value 0.1 were taken into consideration as significant (see Table 4 and supplementary spreadsheets in the digital appendix). 190 genes were found to be up- and 163 genes were found to be significantly downregulated because of *mir-310s* deficiency.

3.1.1.2 Affected protein groups point to malfunctioning energy homeostasis

To establish a contextual overview and discover functional involvements of the *mir-310s* these hits were manually grouped by their physiological and functional involvements according to the associated gene ontology terms from UniProt database (UniProt, 2014). Next, the up- and downregulated genes (Table 4) were put in the interaction networks (Figure 11) (Franceschini et al., 2013). Analysis of these genes via database searches gave rise to several discrete yet interacting functional clusters, which contain genes directly related to energy and lipid metabolism, protein homeostasis, mitochondria, nucleotide synthesis, highly energy dependent muscle and neural development and function, and also cuticle formation. Furthermore, 20% of these gene hits were already reported to be linked to lipid droplets (Kuhnlein, 2011). Intriguingly, these clusters of genes with altered expression levels as a result of *mir-310s* deficiency came down to the term "energy metabolism and nutrient storage homeostasis" as their common denominator. Thus, this analysis demonstrated the role of *mir-310s* on metabolism and energy homeostasis via control of gene expression, as a result of direct miRNA-target interactions, as well as through downstream partners of *mir-310s* targets.

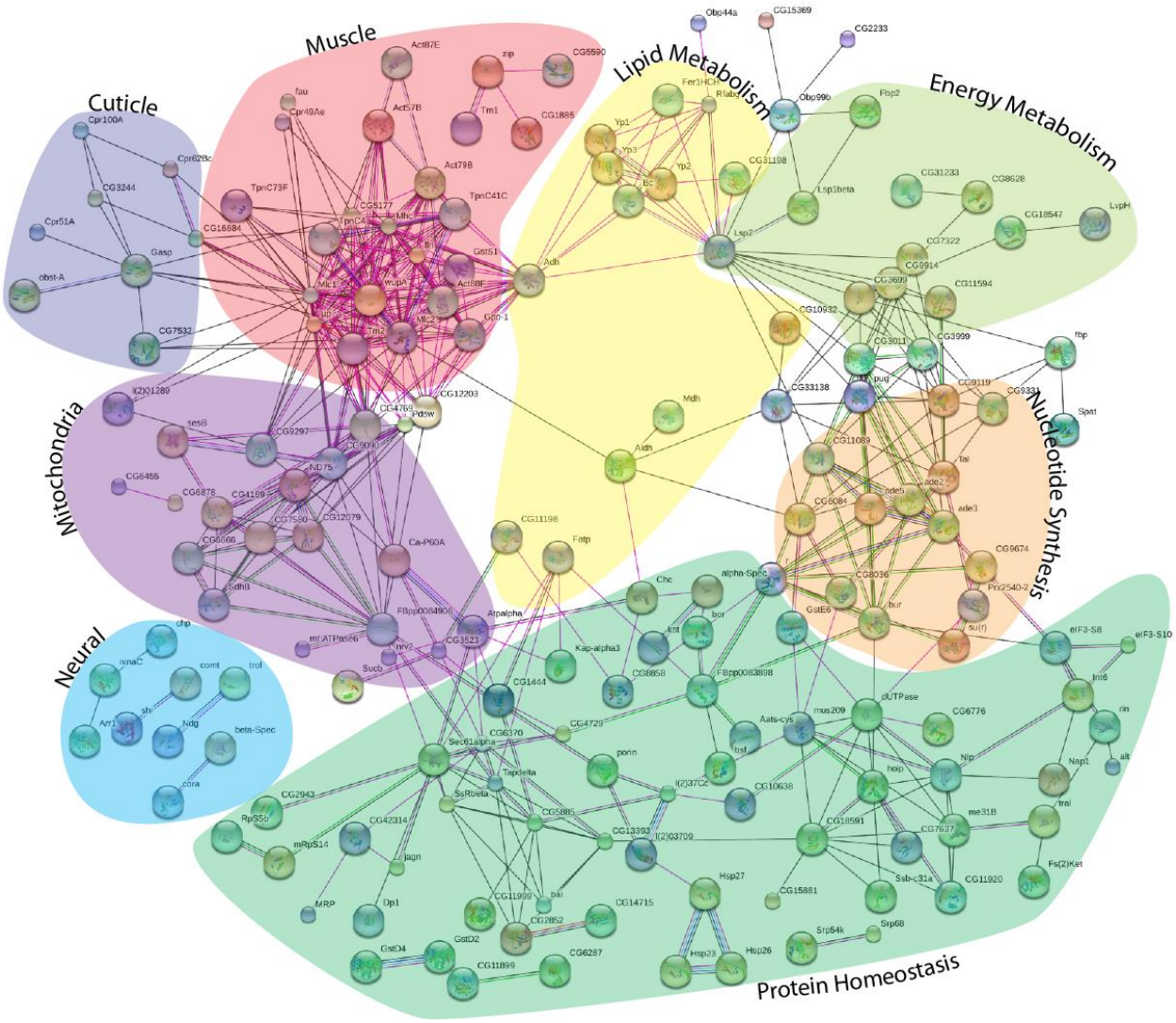

Figure 11. The genes with altered expression because of *mir-310s* loss indicate to an energy metabolism associated deficiency.

Proteomics data acquired via SILAC experiment and mass spectrometry are analyzed by generating functional interaction networks (Franceschini et al., 2013) of the *mir-310s* deficiency affected genes. The up- and downregulated genes are associated into distinct context groups, using the associated GO terms gathered from proteomics database (UniProt, 2014). Grouping resulted in eight interacting clusters: cuticle related, muscle development and function, lipid metabolism, energy homeostasis, mitochondrial, nucleotide synthesis, neural development and function, and protein hemostasis. (Table 4) (Çiçek et al., 2016).

3.1.1.3 Starvation sensitive genes are also affected at the mRNA level

In order to confirm the proteomics data pointing to the role of the *mir-310s* in nutrition response and to further narrow down the gene list, the genes were put into focus, which were previously reported to have expressions sensitive to changing nutritional conditions. Therefore, comparison was made with a published transcriptome study that identified starvation-responsive genes in *Drosophila* (Farhadian et al., 2012). 31 genes were affected by *mir-310s* deficiency (in this study) and sensitive to starvation (Farhadian et al., 2012); subsequently, these genes have been classified in the same eight distinct functional groups according to their function (see color coding in Figure 11). In order to confirm the deregulation of the mRNA expression of these 31 genes in *control* and *mir-310s* mutants in well-fed and starved conditions, expression analysis via qRT-PCR was performed. Plotting of the relative expression levels demonstrated the deregulation of the mRNA levels as a cause of *mir-310s* loss (Figure 12, Table 5). As an example on the *mir-310s* regulated starvation-sensitive genes, the mRNA of the gene *Larval serum protein 1 β* (*Lsp1beta*), with its nutrient reservoir function, were detected in tenfold higher levels in *mir-310s* mutants under well-fed conditions when compared to *controls*. Furthermore, in *control* flies, starvation from the yeast source resulted in a strong response, where the *Lsp1beta* transcript levels were downregulated above 30 fold. On the other hand, the *mir-310s* mutants showed a minor response with a 30% decrease in mRNA levels. The mRNA levels of an additional gene with similar function, *Larval serum protein 2* (*Lsp2*), were found at close to zero levels in *controls* upon protein starvation; whereas, the *mir-310s* deficiency inhibited this response and let *Lsp2* levels to be downregulated only mildly. Thus, in starved conditions, the ratio of the *Lsp2* transcript levels in *mir-310s* mutants to the *controls* was measured to be ~40 fold (Figure 12, Table 5).

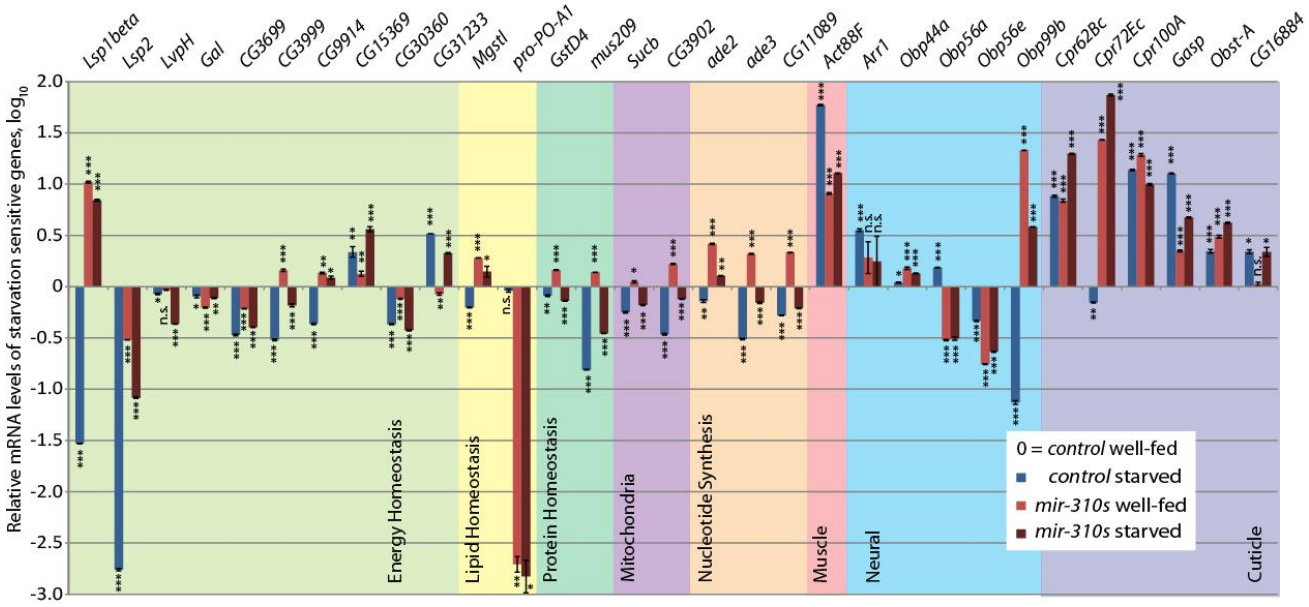

Figure 12. Energy metabolism related genes are also affected at the mRNA level as a result of *mir-310s* deficiency

qRT-PCR analysis confirms that genes sensitive to nutritional stress (Farhadian et al., 2012) have perturbed expression levels in well-fed and starved *mir-310s* mutant females (Table 5) (Functional clusters are color coded like in Figure 11) (Çiçek et al., 2016).

The bar graph indicates (AVE±SEM). p values were calculated using two-tailed Student's t-test. (*p<0.05, **p<0.005, ***p<0.0005)

Together with other genes confirmed in both studies, analysis of the relative mRNA expression revealed an uncharacteristic response of *mir-310s* mutants, where sets of genes being expressed at higher and lower levels compared to *controls* under well-fed and starvation conditions (Figure 12). In summary, the protein and mRNA based expression analyses revealed the *mir-310s* involvement in response to changing nutritional conditions.

3.1.2 *mir-310s* loss causes nutrition-dependent phenotypes

Parallel to the perturbed expression of the genes associated with energy and lipid metabolism, the analysis of *mir-310s* deficient flies exhibited four main physiological and morphological phenotypes, which are connected to the nutritional conditions of the environment. For the examination of the *mir-310s* necessity in dietary homeostasis and response to changes in the

environmental nutritional status two diets were set up. The well-fed diet contained simple sugars supplemented with fresh yeast paste, whereas the nutritional-restrictive diet contained only sugars. The pioneering studies and recent research on nutritional requirements of *Drosophila* have revealed the yeast source necessary for proper development and adult life (Piper et al., 2014; Tatum, 1939).

3.1.2.1 *mir-310s* deficiency has sex-specific and nutrition-dependent effect on lifespan

Firstly, *mir-310s* deficiency affected the longevity of the adult flies. Longevity assays showed a significantly shorter mean lifespan for *mir-310s* mutant flies compared to *controls* in case of well-fed nutritional conditions. However, an unexpected sex-specific effect of *mir-310s* loss was observed on the longevity under nutrient-restrictive conditions. Interestingly, *mir-310s* mutant females resisted nutritional restriction better than *control* females. Under starvation conditions, the *mir-310s* female median lifespan was significantly longer than that of *controls* (20 and 15 days, respectively; Figure 13A). On the other hand, not unexpectedly, the male lifespan was affected in favor of the *controls*, where upon nutritional restriction, the lifespan of *control* and *mir-310s* mutant males were shorter than their well-fed counterparts and *mir-310s* males still living shorter than *controls* (supplementary Figure 34). These findings showed that *mir-310s* deficient female flies coped with the nutritional stress better; and this adaptation resulted in longer lifespan.

3.1.2.2 *mir-310s* mutants have increased crop size

Secondly, the crops of the *mir-310s* deficient females were observed to be larger in size under normal food conditions, at all times. Crop is the food storage organ and part of the gastrointestinal system; and it is known to increase in size in females in case of post-starvation feeding (Al-Anzi et al., 2010; Edgecomb et al., 1994). Under normal laboratory conditions, the steady state size of *mir-310s* mutant female crops were measured to be 30% larger (Figure 13B'', Table 6). In addition, in case of nutritional restriction, the *mir-310s* and *control* crops assumed very similar sizes demonstrating that the size difference at normal conditions is a result of malfunctioning possible behavioral and physiological responses perturbed by *mir-310s* loss. In other words, *mir-310s* mutant females increase the size of their crops as if they were starved without being under any restriction.

3.1.2.3 *mir-310s* mutants lay fewer eggs

Thirdly, the egg laying performance of the *mir-310s* mutants was analyzed. It is known that egg laying is a very energy and nutrient demanding process hence depending on the nutritional status

of the environment and that it is stopped in case of nutritional shortage (Drummond-Barbosa and Spradling, 2001). *mir-310s* mutants are observed to lay 2.5 fold fewer eggs than the *control* under non-restrictive normal laboratory conditions (Figure 13C, Table 6). The crop size and egg laying phenotypes suggest that *mir-310s* mutant females exhibit post-starvational response even without being starved. In addition, these results pointed to the perturbed nutrient storage and energy homeostasis initially found by the proteomic analysis.

3.1.2.4 *mir-310s* mutants accumulate more body fat

In accordance with this interpretation, fourthly, the fat storage features of *mir-310s* deficient female flies were assessed by an established colorimetric assay (Hildebrandt et al., 2011). Under nutrient-rich feeding conditions, the total body fat content of *mir-310s* mutant females was moderately lower compared to *controls*. In *control* females, the restrictive diet for 10 days caused slight increase in fat content. However, when they were restricted from yeast source, the total body fat content of *mir-310s* mutants were measured to be significantly higher (2.5 fold to starved and 4 fold to well-fed *controls*) (Figure 13D, Table 6). This result pointed to the malfunction in lipid metabolism in *mir-310s* mutant females that have dramatically increased lipid amounts upon protein-restriction.

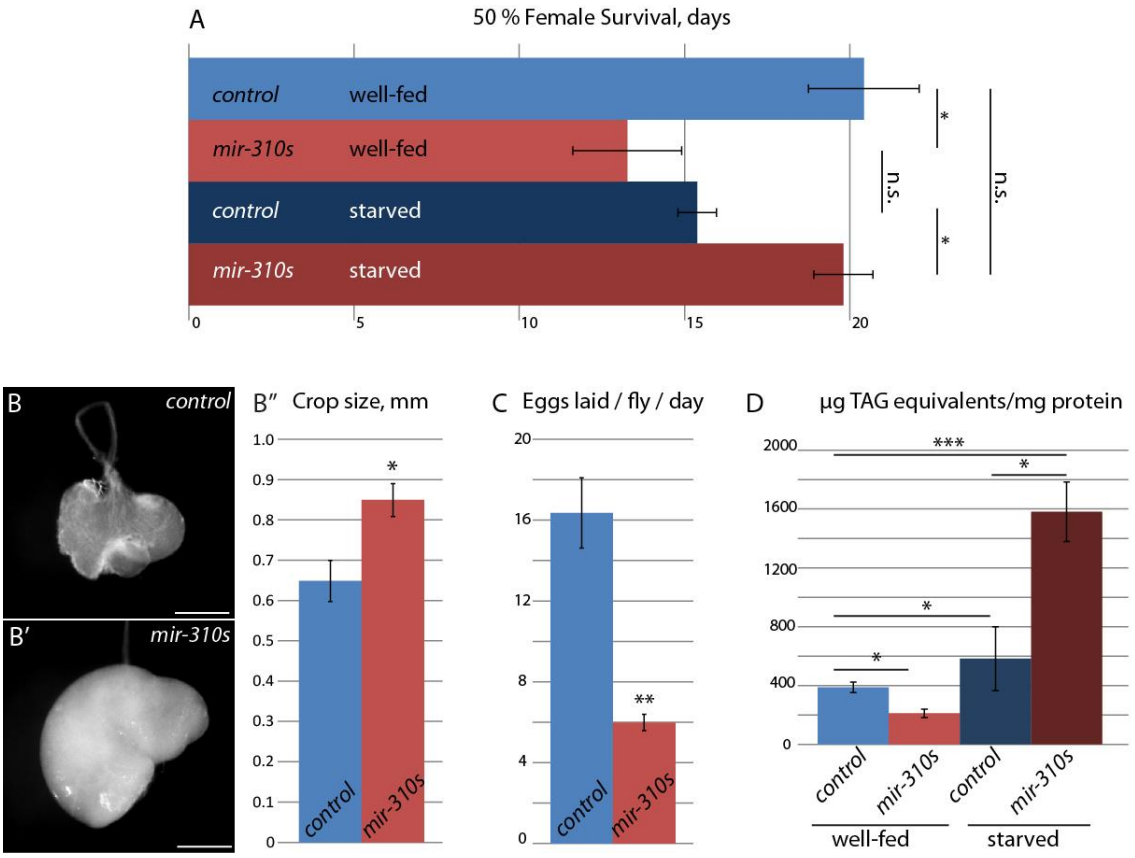

Figure 13. *mir-310s* deficient females show energy metabolism-associated defects.

(A) The *mir-310s* loss-of-function causes the female lifespan to decrease under well-fed and to increase under nutrient-restrictive conditions.

(B) *mir-310s* deficient females have larger crops (B) than *controls* (B') under normal feeding conditions (B'').

(C) The deficiency of *mir-310s* results in lower fecundity, i.e. lower numbers of laid eggs per female.

(D) Under nutrient-rich conditions, *mir-310s* deficient females have lower (50%) total lipid amounts than *controls*. The relative ratio changes in favor of the *mir-310s* mutants in nutrient restrictive conditions, where the total lipid amounts are increased to ~230% of the *controls* (Çiçek et al., 2016).

In (A), (B''), (C), and (D) bar graphs indicate (AVE±SEM). p values were calculated using two-tailed Student's t-test. (*p<0.05, **p<0.005, ***p<0.0005) In (B) and (B') scale bars represent 250µm.

All in all, the phenotypic analyses of *mir-310s* deficient females and the protein and mRNA expression assays proposed that the *mir-310s* are involved in the regulation of nutritional homeostasis through complex genetic, cellular, and physiological networks.

3.1.3 *mir-310s* mutants exhibit starvation sensitive phenotypes in the ovaries

To define the *mir-310s* mutant phenotypes and their function on the nutritional stress response at the cellular level more precisely, identification their direct target genes was necessary. Thus, oogenesis was chosen as the model system, which is well-studied and shown to respond to nutritional stress (Drummond-Barbosa and Spradling, 2001).

The examination of *mir-310s* mutant ovarioles in nutrient-rich food conditions revealed several soma-related phenotypes that were classified into three categories. First, the extra stalk cells were observed to cluster between neighboring egg chambers (Figure 14C). In *control* ovarioles, a maximum number of 8 stalk cells reside between the egg chambers in an orderly fashion forming a single layered epithelium (Figure 14A), while in *mir-310s* loss-of-function ovarioles, extra numbers of stalk cells were found to cluster together and/or form multilayered stalk epithelia connecting adjacent egg chambers (Figure 14C). Second, the FCs were observed to be misshapen with aberrations in cell polarity and developing into multilayered epithelium in patches with randomized positions and sizes (indented arrowheads in Figure 14D). Third, *mir-310s* mutant ovarioles were found to contain fused egg chambers. They are recognizable by the supernumerary nurse cells belonging to different stage egg chambers (empty arrowheads in Figure 14D). Nurse cells with different stage egg chamber origins are identified by their unequal nucleus size as a readout of different polyploidity stages (Figure 14D, red encircled in 14D'). In general, these epithelial defects were quantified, where each phenotype could be scored at least once in nearly all *mir-310s* deficient ovarioles (Figure 14E, Table 6).

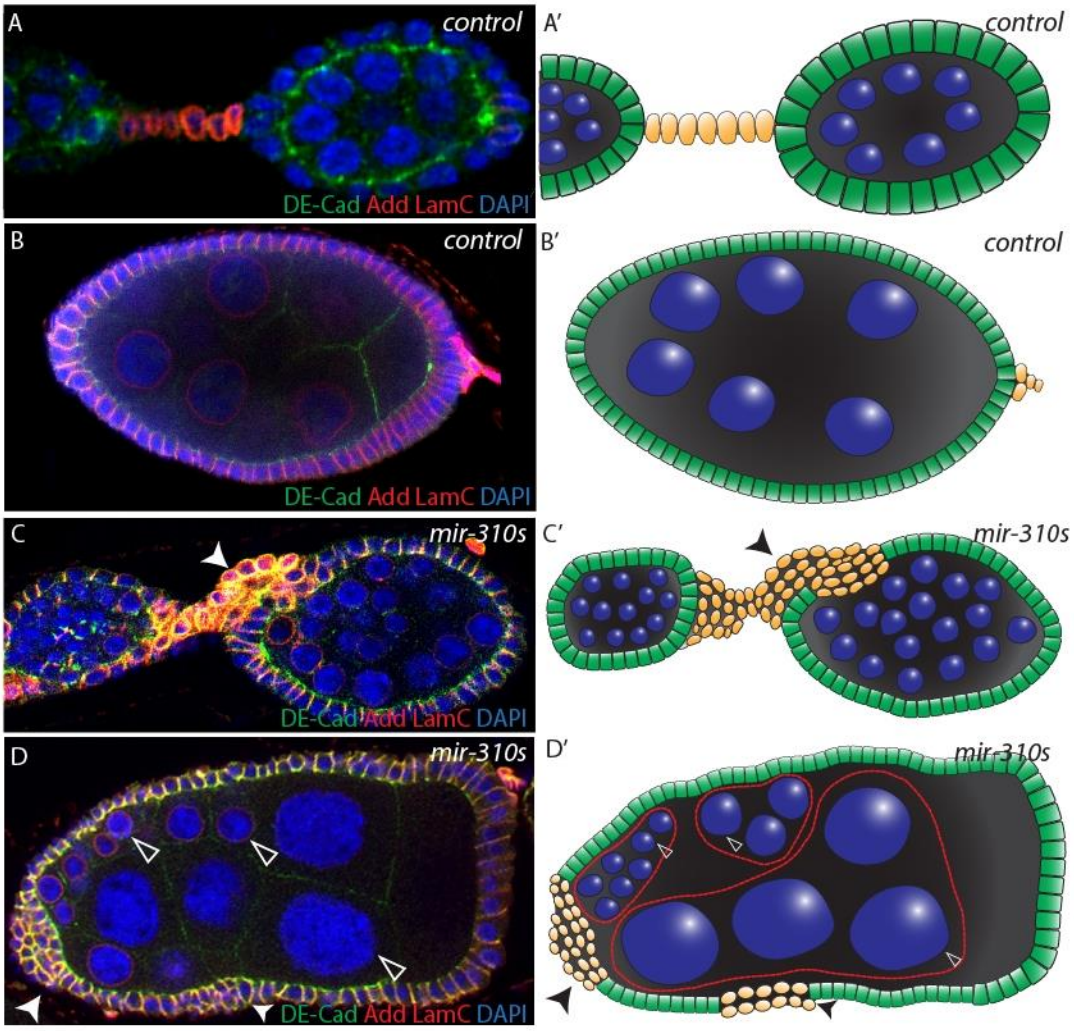
A
control
DE-Cad Add LamC DAPI
A'
control
B
control
DE-Cad Add LamC DAPI
B'
control
C
mir-310s
DE-Cad Add LamC DAPI
C'
mir-310s
D
mir-310s
DE-Cad Add LamC DAPI
D'
mir-310s

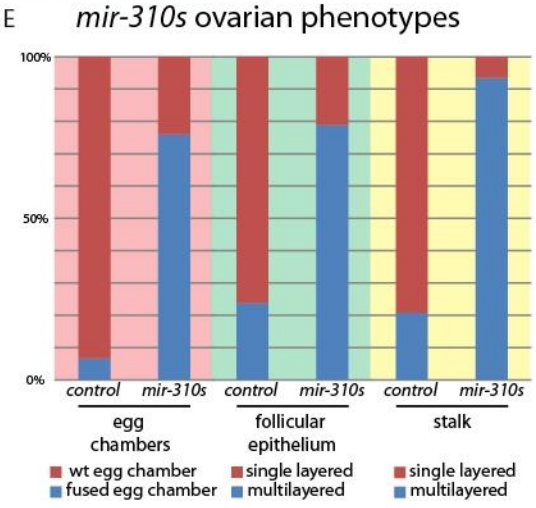
E
mir-310s ovarian phenotypes
100%
50%
0%
control
mir-310s
control
mir-310s
control
mir-310s
egg chambers
follicular epithelium
stalk
wt egg chamber
fused egg chamber
single layered
multilayered
single layered
multilayered

Figure 14. The *mir-310s* deficit causes Hh pathway related epithelial phenotypes in the ovary.

(A) The two early *control* egg chambers with the follicular epithelium marked by DE-Cadherin (DE-Cad) (in green) are connected by stalk cells marked by LamC (in red) (Schematic drawing A').

(B) The *control* late stage egg chamber consists of the single layered and columnar follicular epithelium and nurse cells of the same stage (Schematic drawing B').

(C) In case of *mir-310s* deficiency, there is excess number of cells in clusters where normally the stalk and polar cells reside (arrowhead). The clusters appear as a distorted epithelium with multilayer characteristics (Schematic drawing C').

(D) The *mir-310s* loss results in the appearance of fused egg chambers in the ovarioles. Two or more egg chambers of different stages (identified with nurse cells with different size nuclei, i.e. polyploidity stage, empty arrowheads in D and D') are found to be encapsulated in the same follicular epithelium of this perturbed compound egg chamber structure. The nurse cells originating from distinct stages are encircled in red in D'. In addition, *mir-310s* deficiency causes irregularities in the cellular polarity of the follicular epithelium (see DE-Cad, apical membrane marker, in D) and random patches, where the epithelium appears multilayered (indented arrowheads in D and D').

(E) The occurrence of each phenotype per ovariole was scored. In *control* and *mir-310s* deficient ovarioles the incidences were: for fused egg chambers 5% and 70%, for defective follicular epithelium 25% and 80%, and for misshapen stalk with extra numerous cells 25% and 95%, respectively (Çiçek et al., 2016).

In (A-D) anterior is to the left and single optical sections are represented.

With the fact that *mir-310s* mutants show phenotypes affected significantly by nutritional stress, same specific ovarian phenotypes were analyzed under nutritional restriction. Under sugar-only conditions, *control* females reacted to the nutritional stress as known (Drummond-Barbosa and Spradling, 2001), where they ceased producing eggs and contained only egg chambers up to stage 8 with normal appearance. On the other hand, nutrient-poor conditions caused *mir-310s* mutant ovaries to contain numerous late stage egg chambers and resulted in the higher penetrance of the *mir-310s* phenotypes, where the severity of the mutant phenotypes did not allow to perform a similar specific quantification of the phenotypes, endorsing the *mir-310s* role in nutritional stress response (Figure 15).

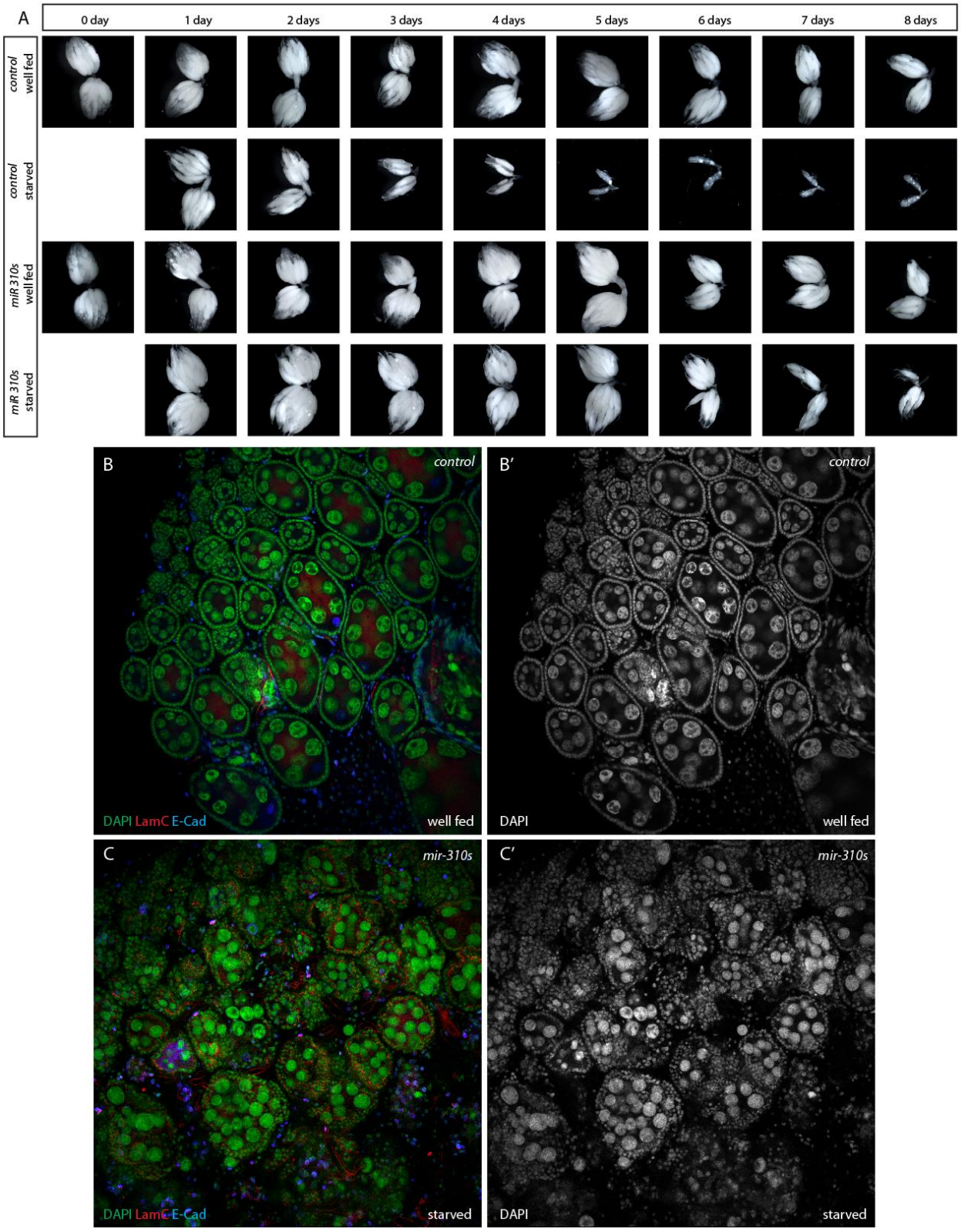
A
0 day
1 day
2 days
3 days
4 days
5 days
6 days
7 days
8 days
control well fed
control starved
miR 310s well fed
miR 310s starved
B
control
DAPI LamC E-Cad
well fed
B′
control
DAPI
well fed
C
mir-310s
DAPI LamC E-Cad
starved
C′
mir-310s
DAPI
starved

Figure 15. The *mir-310s* deficiency perturbs the response to nutritional restriction in the ovaries.

(A) *Control* females cease to produce eggs in sugar-only diet after 4-5 days. As a result of this reaction, the ovaries contain only early egg chambers. Instead, the *mir-310s* deficient ovaries persist to contain late stage egg chambers even after 7-8 days of restrictive diet.

(B) After a week of protein starvation, *control* ovaries are made of almost only stage 8 or earlier egg chambers.

(C) The nutrient restriction worsens the *mir-310s* deficiency phenotypes in the ovary; defective vitellogenesis and follicular epithelia, and increased numbers of fused egg chambers are observable. The overall morphology of the egg chambers are too disturbed to quantify specific epithelial defects (Çiçek et al., 2016).

3.2 The *mir-310s* are involved in the regulation of Hh signaling in the ovary

3.2.1 *mir-310s* regulate the Hh signaling through three target genes in the pathway

The search for the signaling pathways that control egg production and involves the *mir-310s* revealed the highly evolutionary conserved Hh pathway with similar phenotypes characterized for *mir-310s* deficit. In addition, the well-conserved seed sequence of the *mir-310s* highlighted the potential involvement of them in the evolutionary conserved signaling pathway. The overactive Hh signaling has been reported to cause cell accumulation between adjacent egg chambers (Figure 16A) and fused egg chambers (Figure 16B) (Forbes et al., 1996a; Forbes et al., 1996b; Zhang and Kalderon, 2001). Taking the similar phenotypes of the *mir-310s* and Hh pathway and the conserved seed sequence of the *mir-310s* (Figure 17), it was hypothesized that one or more elements and/or regulators of the Hh pathway can be targeted by the *mir-310s* actively during oogenesis.

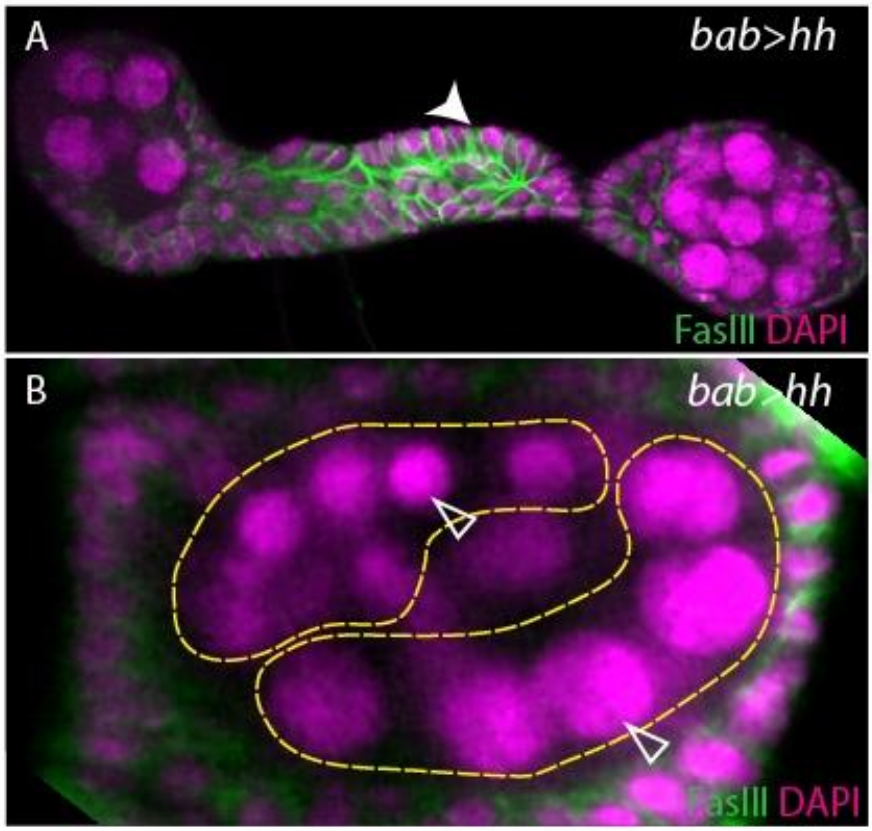

Figure 16. Interfering with the Hh Signaling results in epithelial phenotypes

(A-B) The *hh* overexpression specifically in the GSC niche (TF and CpCs) in the adult female (*bab1 Gal4; UAS hh, tub>Gal80^{ts}* flies at restrictive temperature, 29°C, for 4 days) causes extra numerous and multilayered stalk and polar cell clusters (A, indented arrowhead), and fused egg chambers (yellow encircled in B) as reported before (Forbes et al., 1996a). These appearances bear a resemblance to the *mir-310s* deficiency phenotypes in Figure 14C and 14D, respectively (Çiçek et al., 2016).

Anterior is to the left and maximum intensity projections of confocal Z-stacks are represented.

Thus, the search for prospective direct *mir-310s* targets was concentrated on the Hh pathway components and/or the genes they interact with. Several miRNA target search databases (Betel et

al., 2008; Enright et al., 2003; Kheradpour et al., 2007) were used to generate *in silico* putative target lists. Comprehensive search and following *in vitro* validations uncovered three candidates (*Rab23*, *tramtrack* (*ttk*), and *Hormone receptor-like in 96* (*DHR96*)), which are possibly targeted actively by the *mir-310s* in the ovary to regulate Hh signaling.

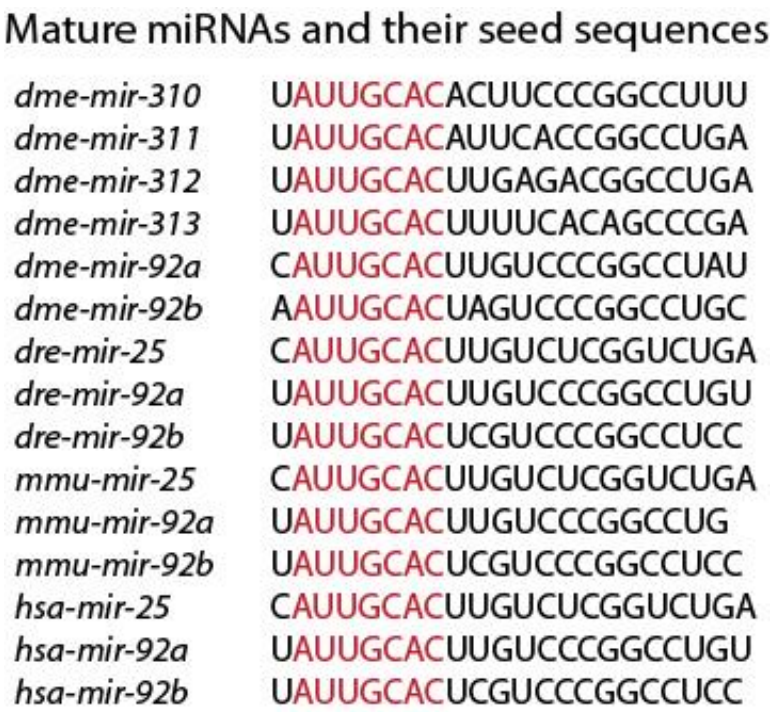

Figure 17. The *mir-310s* have conserved seed sequences

The analysis of the recently evolved *mir-310s* and their *Drosophila* ancestral miRNAs, the *mir-92a* and *92b* together with their zebrafish, mouse, and human orthologues demonstrates the conservation of the seed sequence among different animal species (Çiçek et al., 2016).

3.2.1.1 Hh pathway elements are targeted by the *mir-310s in vitro*

In order to validate the candidate genes (*Rab23*, *DHR96*, and *ttk*) a *Drosophila* S2 cell-based luciferase reporter assay was performed to test the targeting efficiency of their 3'UTRs by the *mir-310s*. The assay is built on the readout of the light signal exerted by the luciferase products of the constructed plasmids, which were selectively tested for *mir-310s* mediated downregulation.

The plotted relative signal intensity values show the significant downregulation by the *mir-310s* in case of all three candidates. This result clearly confirmed that *Rab23, DHR96,* and *ttk* 3'UTRs can be targeted by the *mir-310s in vitro* (Figure 18 and Table 7).

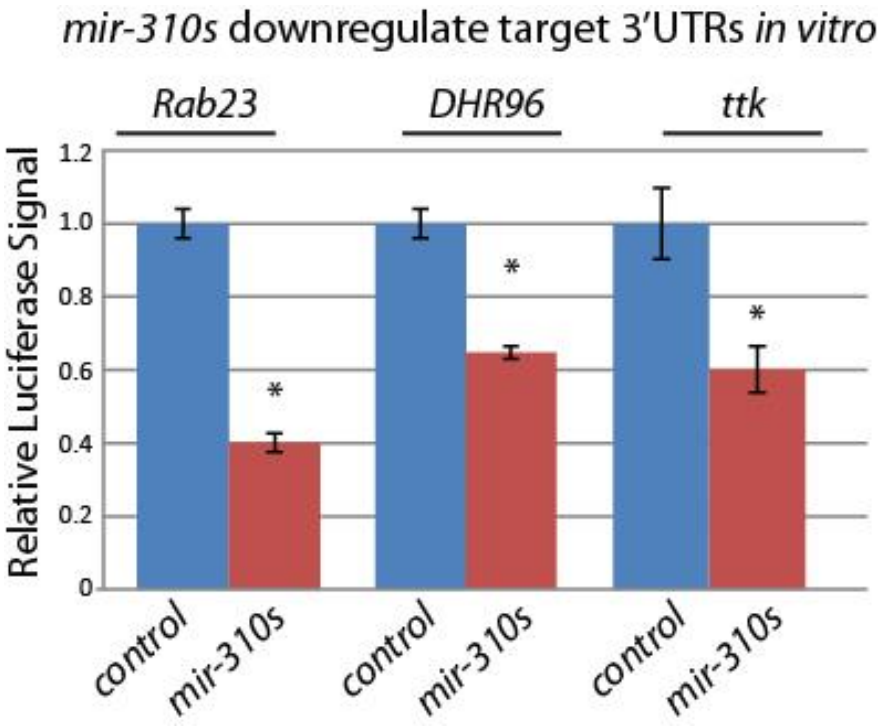

Figure 18. Luciferase assay confirms *mir-310s* targets *in vitro*

The *in vitro* Luciferase assay confirms that the 3'UTRs of the candidate genes (*Rab23, DHR96,* and *ttk*) can be targeted by the *mir-310s* in S2 cells (Çiçek et al., 2016).

Bar graph indicates AVE±SEM. p values were calculated using two-tailed Student's t-test. (*p<0.05, **p<0.005, ***p<0.0005)

3.2.1.2 Hh pathway elements are *in vivo* targets of the *mir-310s*

Next, the response of these predicted target genes were tested *in vivo* according to *mir-310s* absence and the nutritional favorability of the environment (Figure 19, Table 8).

3.2.1.2.1 *Rab23* is targeted *in vivo*

Firstly, *Rab23* was tested, which is one of the Rab family members having conserved roles in trafficking and membrane organization (Chan et al., 2011; Zerial and McBride, 2001) and has been shown to act in the Hh signaling in vertebrates, but not in *Drosophila* (Eggenschwiler et al., 2001; Pataki et al., 2010). Under well-fed conditions, *Rab23* mRNA levels were significantly, more than 1.5 fold, higher in *mir-310s* loss-of-function mutants. On the other hand, in *control* flies, nutritional stress caused a sharp (more than 10 fold) decrease of endogenous *Rab23* levels. However, in the *mir-310s* mutants *Rab23* mRNA expression was not suppressed as effectively as in *controls* under nutritional restriction resulting in a fourfold overexpression. These evaluations of the relative *Rab23* mRNA levels evidenced the negative regulatory role of the *mir-310s* controlling mRNA levels of *Rab23* in nutrient-rich and nutrient-poor conditions (Figure 19).

3.2.1.2.2 *DHR96* is targeted *in vivo*

Secondly, *DHR96* was tested, which is the cholesterol receptor and serves as a sensor for the nutritionally rich food conditions (Bujold et al., 2010; Horner et al., 2009; Sieber and Thummel, 2012). Likewise, under well-fed conditions, *mir-310s* deficient females had 1.5 fold higher *DHR96* mRNA levels in comparison to *controls.* In addition, the starvation condition pushed this relative overexpression to become above twofold. These findings demonstrate that the *in vivo Rab23* and *DHR96* expressions were regulated similarly by the *mir-310s* and suggest a connection between the increasing fold overexpressions of these genes and the increasing penetrance of the ovarian phenotypes upon nutritional starvation (Figure 19).

3.2.1.2.3 *ttk* is targeted *in vivo* only under dietary stress conditions

Thirdly, the probable *mir-310s* control on Ttk was analyzed that is a controller of Hh target gene expression, by its transcription factor activity (Sun and Deng, 2007). The expression analysis of *ttk* did not show *mir-310s* related regulation under well-fed conditions. However, *ttk* expression was measured to be under the *mir-310s* control under starvation conditions, where *mir-310s* deficiency caused 1.5 fold increase in *ttk* mRNA levels. Therefore, the conclusion followed that the adjustment of *ttk* mRNA levels upon starvation depend on the *mir-310s* (Figure 19).

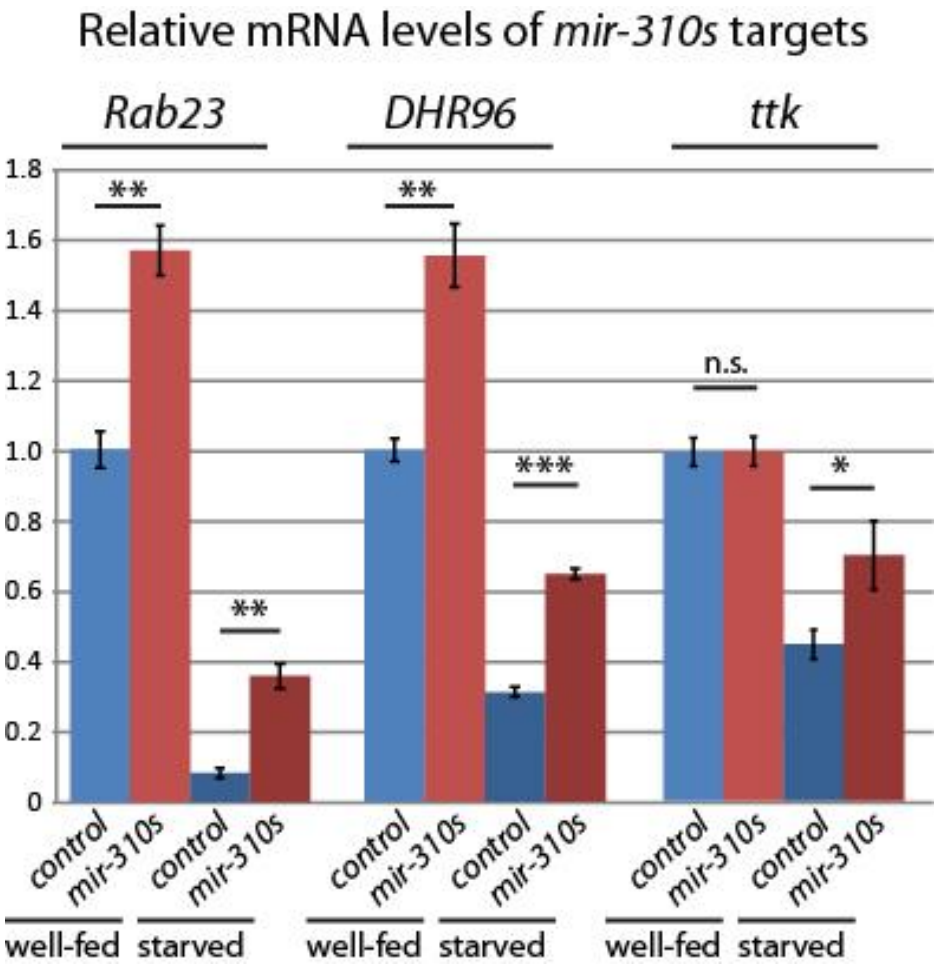

Figure 19. The three *mir-310s* candidate target genes have deregulated mRNA expression levels upon *mir-310s* loss

qRT-PCR analyses revealed the significantly higher amounts of all three putative *mir-310s* target genes in *mir-310s* mutant females. In well-fed conditions, for *Rab23* and *DHR96*, the absence of the *mir-310s* results in ~50% increase in relative mRNA amounts, whereas for *ttk* no change was measured. In starvation conditions, the loss of the *mir-310s* caused significant increases of ~400%, ~200%, and 150% for *Rab23, DHR96,* and *ttk* transcript levels, respectively (Çiçek et al., 2016).

Bar graph indicates AVE±SEM. p values were calculated using two-tailed Student's t-test. (*p<0.05, **p<0.005, ***p<0.0005)

In conclusion, the qRT-PCR data show that at least three elements of the evolutionary highly conserved Hh pathway are actively controlled by the *mir-310s in vitro* and *in vivo* and in the context of environmental nutritional conditions. In addition, the present expressions of the *mir-310s*, *Rab23,* and *DHR96* in the GSC niche; and of *ttk* in the FCs (Hartman et al., 2013; Sun and Deng, 2007) support the idea of the *mir-310s*-centered regulation of these genes, and hence of the Hh signaling, in the ovary.

3.2.1.3 Clonal *mir-310s* overexpression resembles *ttk* loss-of-function

It has been shown that the loss-of-function of *ttk* (loss of Ttk69 protein product of the gene) results in stalling of follicle epithelial cells in the endocycle and failure in switching to amplification cycle as a result of remaining Hh downstream target gene expression. The cell cycle stalled, Ttk69 lacking cells do not express the stage specific marker dE2F1 (Figure 20E and E') (Sun and Deng, 2007; Sun et al., 2008). Clonal overexpression of the *mir-310s* in the follicular epithelium resulted in similar changes in cell nuclei morphology. As seen in Figure 20C and D, the *mir-310s* overexpressing clones have distinct nuclei characteristics, such as the lack of the nuclear marker Lamin C and less condensed DNA (DAPI staining). This ectopic *in vivo* downregulation of *ttk* by the *mir-310s* indicates the probable endogenous role of the *mir-310s* as a potent regulator of *ttk* expression, hence as a controller of the on-off switch of the Hh signaling in the late follicular epithelium.

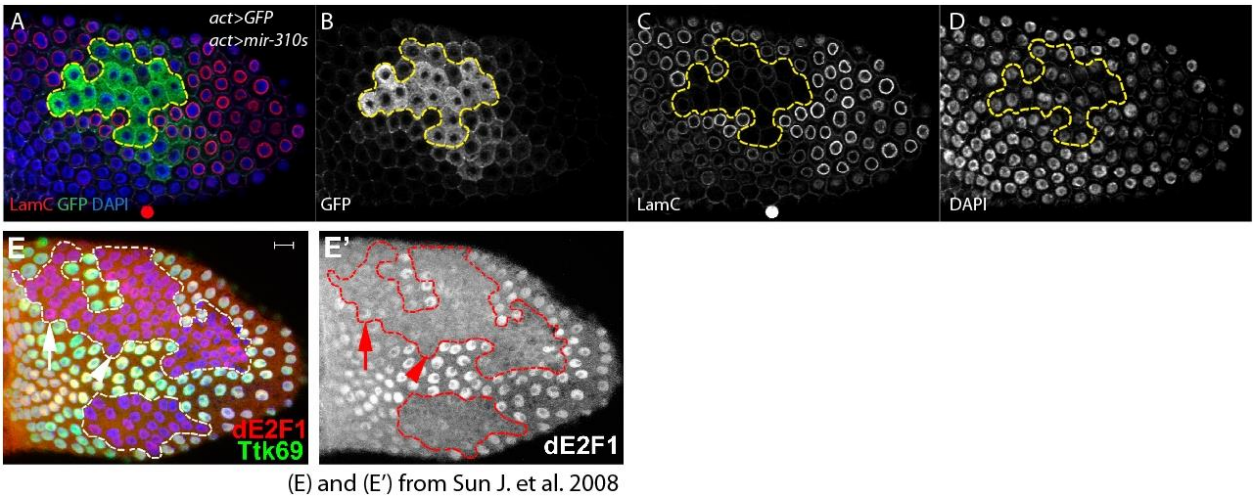

Figure 20. *mir-310s* overexpression in clones phenocopies *ttk* loss-of-function

(A-D) The *mir-310s* overexpressing FC clones (marked by GFP) have altered nuclei characteristics. Nuclear lamina marker LamC (C) and DAPI (D) show the resemblance of the clonal nuclei to the nuclei of FCs from earlier stage (still in endocycling stage) egg chambers.

(E-E') Studies have shown that loss of Ttk69 product of the *ttk* gene perturbs the endocycle to amplification switch in the follicular epithelium (Sun et al., 2008) resembling the clonal *mir-310s* overexpression (A).

Whereas the involvement of *DHR96* and *ttk* in Hh signaling are studied (Hartman et al., 2013; Sun and Deng, 2007; Sun et al., 2008), the participation of *Rab23* is not yet fully investigated in *Drosophila* (Pataki et al., 2010). For that reason, the investigation intensified on the *mir310s-Rab23* interaction with the focus on the probable involvement of *Rab23* in the Hh pathway.

3.2.1.4 Rab23 protein levels are under *mir-310s* control

In order to test the biological significance of the control of *Rab23* expression by the *mir-310s*, Rab23 expression was analyzed at the protein level. With the help of the *Rab23-YFP* line, the change in endogenous Rab23 protein levels were measured in context of *mir-310s* deficiency and different nutritional conditions. The endogenously tagged *Rab23-YFP* locus was assayed with *control* and *mir-310s* mutant background for analysis. Western blotting of whole fly extracts revealed the significantly higher Rab23 protein levels in *mir-310s* mutant background paralleling the mRNA levels. The magnitude of upregulation in case of *mir-310s* deficiency was twofold under

well-fed conditions; and was replaced by a sevenfold upregulation in nutritional restrictive conditions (Figure 21 and Table 9).

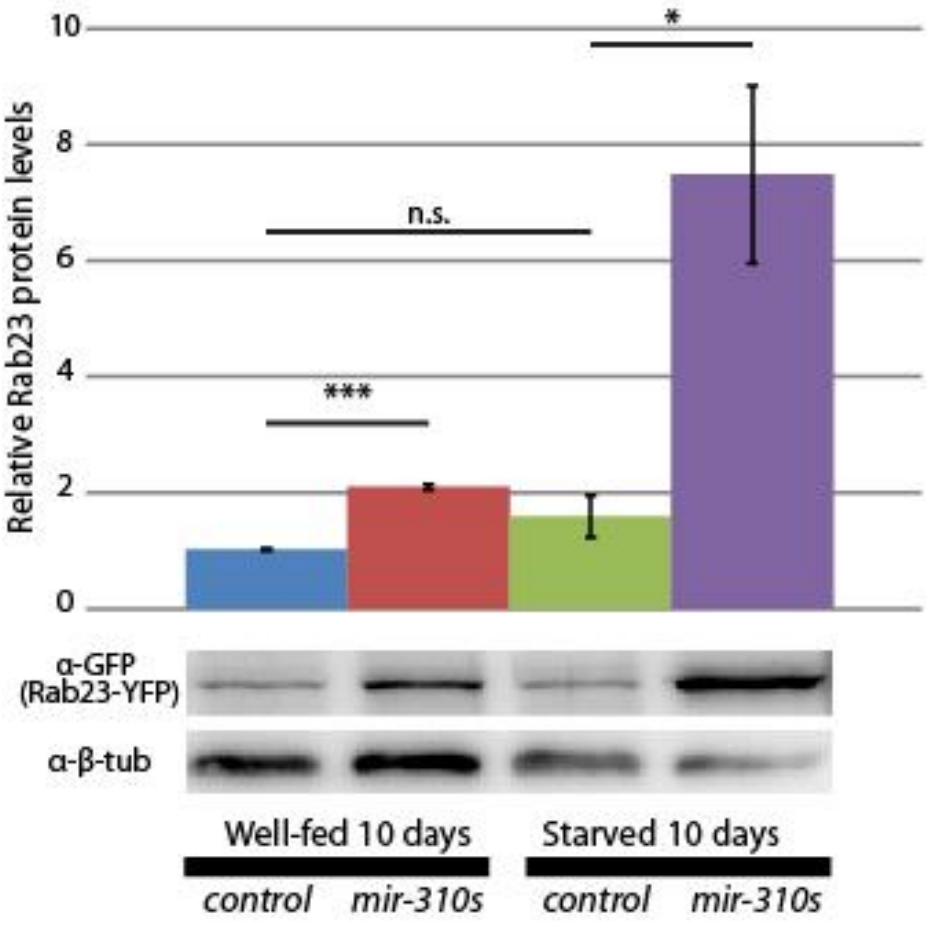

Figure 21. Rab23 protein levels are higher in *mir-310s* mutants.

Homozygous *Rab23-YFP* line is used for western blot analysis to measure the endogenous Rab23 protein levels. *mir-310s* mutant females have higher amounts of Rab23 protein both in well-fed and starved conditions with relative ratios of 200% and 700%.

Bar graph indicates AVE±SEM. p values were calculated using two-tailed Student's t-test. (*p<0.05, **p<0.005, ***p<0.0005)

The fact that the relative levels of Rab23 protein and mRNA levels did not match precisely implies that additional elements are involved in the nutrient-dependent control mechanism. This western

blot and the qRT-PCR analyses together showed the perturbed control over Rab23 expression as a cause of *mir-310s* loss-of-function. Besides, the widening gap between the *controls* and the *mir-310s* mutants in the expression levels upon nutritional restriction further paralleled with the higher penetrance of the mutant ovarian phenotypes under starvation. These analyses confirmed that *Rab23* is a direct *mir-310s* target and that the diet-sensitive regulation of *Rab23* mRNA and protein levels is under the control of the *mir-310s*.

3.2.2 *mir-310s, Rab23,* and *hh* expressions overlap spatially at the germarium anterior

3.2.2.1 *mir-310s* are expressed in the germarial soma

To create a better overview on the *mir-310s-Rab23* interaction and their involvement in the oogenesis, the endogenous spatial expression of the *mir-310s* and *Rab23* were analyzed. Firstly, the *mir-310s* expression pattern was visualized by driving nuclear LacZ and membrane GFP expression under control of endogenous *mir-310s* promoter using *mir-310s Gal4* line. The antibody staining revealed the *mir-310s* expression in the GSC niche cells (namely the CpCs and TF) (Figure 22), which are known to be Hh signal sending cells (Forbes et al., 1996a). In addition, the *mir-310s* expression was also observed in the ECs and the Hh signal receiving cells (Rojas-Rios et al., 2012), namely the stalk cells and the FCs (Figure 23B and C).

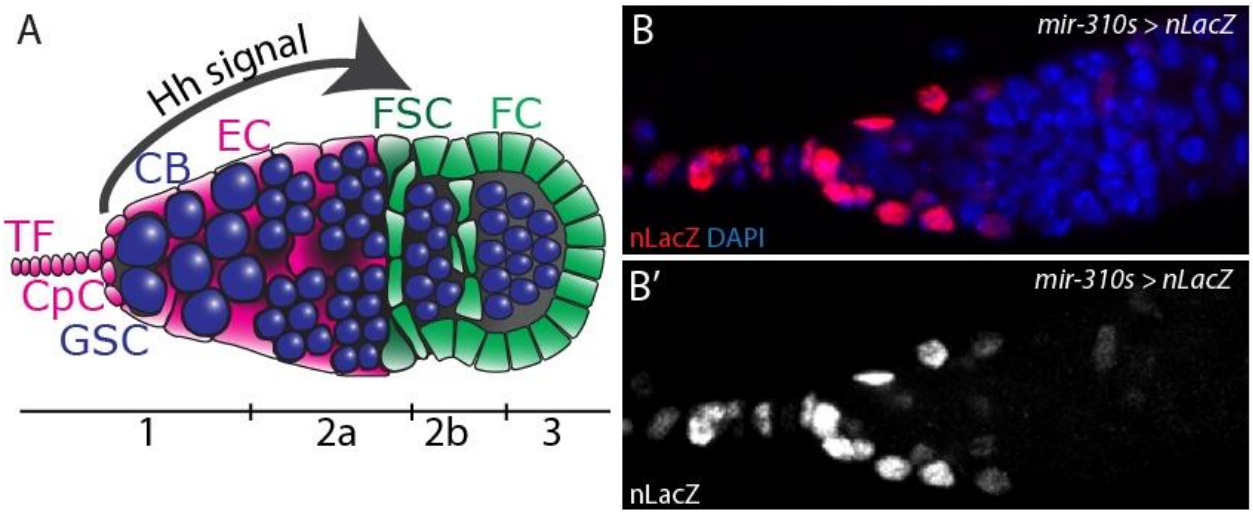

Figure 22. The *mir-310s* are expressed in the germarium, where Hh signaling acts

(A) Illustration represents the Hh signaling mechanism in the germarium involving its release from the GSC niche (TF and CpCs) and its reception by the FSCs and pre-follicular cells initiating their division and differentiation program (Forbes et al., 1996a; Forbes et al., 1996b). (TF: terminal filament, CpC: cap cell, FSC: follicle stem cell, FC: follicle cell)

(B) The *mir-310s* locus is transcriptionally active in the germarial soma. The *UAS nLacZ* reporter driven by the *mir-310s Gal4* identifies the expression pattern in the TF, CpCs and ECs (B'). The expression pattern of *mir-310s* in the ovary fits well with the known Hh ligand (Forbes et al., 1996a), hence further supports the involvement of the *mir-310s* in Hh signaling pathway (Çiçek et al., 2016).

Anterior is to the left. (B) represents maximum intensity projection of confocal Z-stacks.

3.2.2.2 The expression levels of the *mir-310s* are sensitive to nutritional stress

Together, the *mir-310s* loss of function phenotypes and their sensitivity to nutritional conditions raised the question of any change in the spatial or temporal expression pattern or the quantities of the *mir-310s*. To address this, the nuclear LacZ and membrane GFP expression patterns driven by *mir-310s* Gal4 were analyzed in starved flies. Analyses revealed no obvious changes in the *mir-310s* expression pattern. The driver was still dynamically active in the GSC niche, in stalks and in the late follicular epithelium (Figure 23D, E, and F).

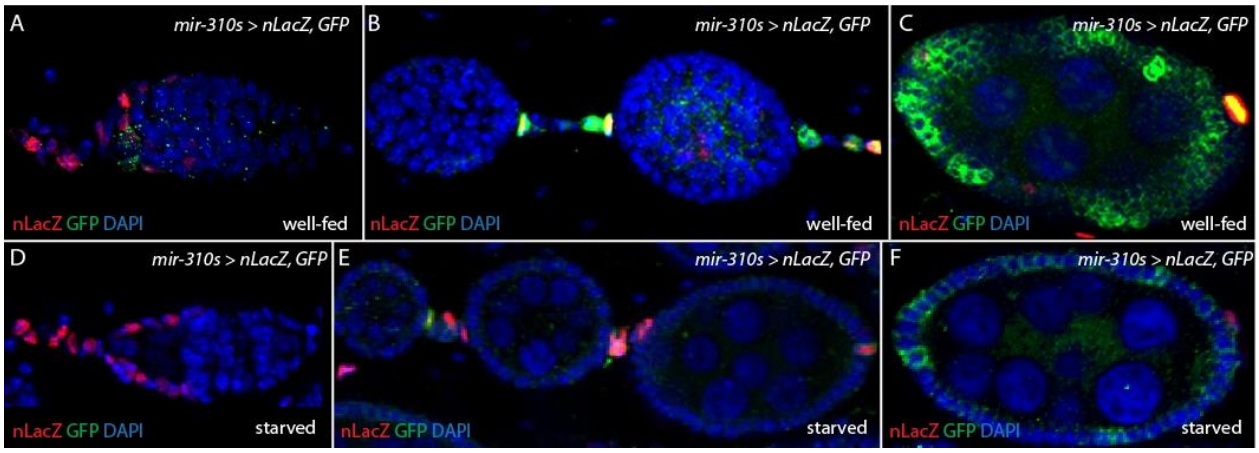

Figure 23. The *mir-310s* expression pattern does not change significantly upon starvation

(A-C) The *mir-310s* are expressed in the germarial somatic cells, including the GSC niche. In addition, the *mir-310s* promoter is also active in the stalk cells between adjacent egg chambers and in the follicular epithelium of the late egg chambers.

(D-F) In case of protein deprivation, the same sets of cells in the germarium as well as in the stalk and in the follicular epithelium are positive for the reporter expression indicating the not significantly affected expression pattern of the *mir-310s*.

Next, the change in the expression levels of the *mir-310s* were analyzed using fluorescent probe and PCR based Taqman® assays. Quantitative analysis revealed the gradual drop in the miRNA levels, which were still detectable after day 5 of starvation (Figure 24, Table 10).

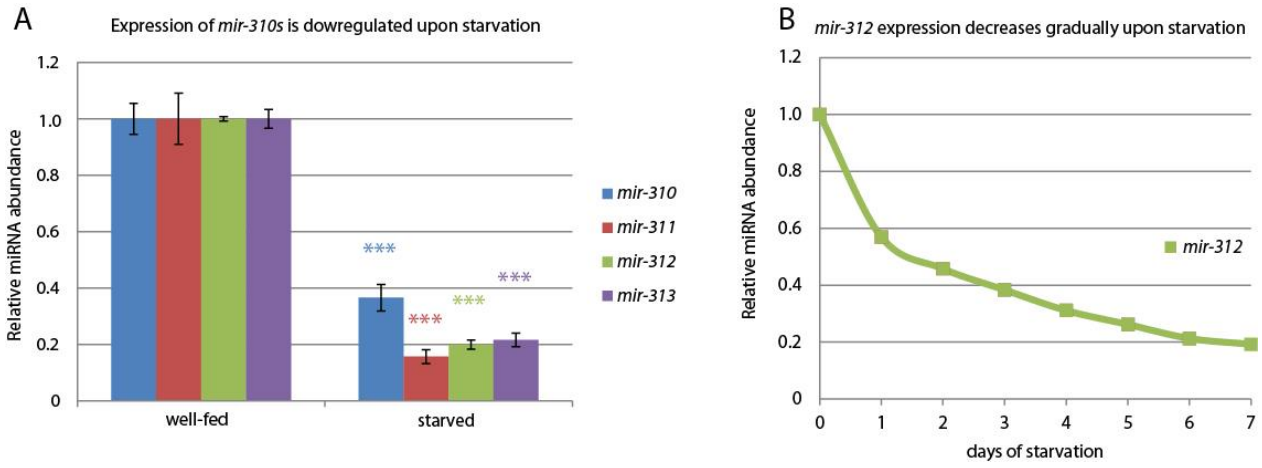

Figure 24 The *mir-310s* abundance gradually decreases upon nutritional restriction

(A) All members of the *mir-310s* are downregulated upon protein restriction. After 10 days of starvation, miRNA amounts drop and stabilize to 20-40% of their well-fed values.

(B) Closer inspection of one representative member of the *mir-310s* family, the *mir-312*, in daily basis reveals the gradual decrease in abundance starting with nutritional restriction.

Bar graph in (A) indicates AVE±SEM; and data points in (B) shows AVE. p values were determined using two-tailed Student's t-test. (*p<0.05, **p<0.005, ***p<0.0005)

3.2.2.3 Rab23, and Hh expressions overlap spatially at the germarium anterior

Upon investigation of *control* germaria, both the endogenous Rab23 and Hh were observed to be expressed in the GSC niche, specifically in the CpCs (Figure 25A). The fact that the *mir-310s*, Rab23, and Hh have spatially overlaying expression patterns further strengthened the probability of their interaction. In addition, to test this probability further, the status of the endogenous Rab23 was examined in *mir-310s* deficient background. In the *mir-310s* mutant background, Rab23 and for Hh ligand were expressed more prominently (especially in the CpCs) and spatially more widespread (Figure 25B). These observations suggest that the *mir-310s* target Rab23 in the germarial soma and imply that the *mir-310s* is involved in the cell-autonomous regulation of the Hh signaling in these cells, probably through Rab23.

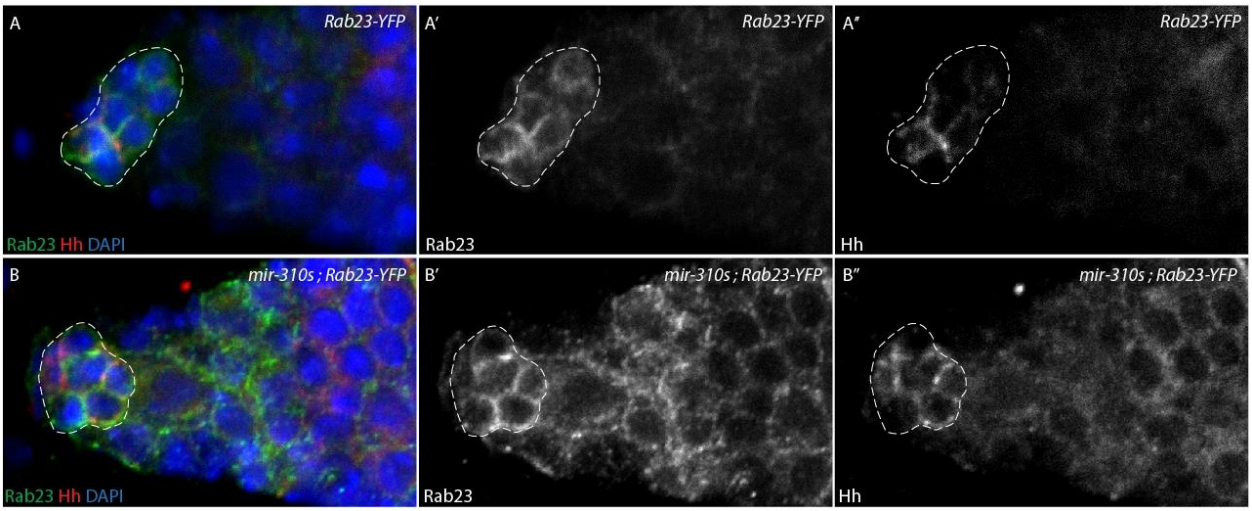

Figure 25. Rab23 and Hh ligand expressions in the germarium are *mir-310s* dependent

(A) Endogenously tagged *Rab23-YFP* demonstrates the Rab23 expression in the CpCs at the germarium anterior. Note that a subset of the Rab23 positive CpCs (A') are also positive for Hh (A'').

(B) The Rab23 (B') and Hh (B'') signals appear to be brighter and wider spread in case of *mir-310s* deficiency pointing to the negative regulatory role of the *mir-310s* on local protein abundance (Çiçek et al., 2016).

Anterior is to the left. (A) represents maximum intensity projection of confocal Z-stacks; (B) represents single optical section.

3.2.3 Hh pathway-associated *mir-310s* loss-of-function phenotypes can be rescued by Rab23 downregulation

To further test this hypothesis, specific phenotypes were investigated, which were reported to result from disturbed Hh signaling (Forbes et al., 1996a). Combinations of different mutations and RNAi transgenes were used to address the functional importance of the *mir-310s*-Rab23-Hh interaction. The Hh signal travels from signal sending cells (TF and CpCs) and acts long range on FSCs to initiate and control the follicle cell division, cyst encapsulation, and stalk cell specification (Chang et al., 2013; Forbes et al., 1996a; Forbes et al., 1996b; Tworoger et al., 1999).

3.2.3.1 *mir-310s* loss causes Hh-related cell specification defect

Firstly, stalk cells and their Hh dependent specification was analyzed during egg camber maturation. It has been shown that excessive Hh levels result in extra number of stalk cells, which form clusters in the stalk region. In addition, these cells are reported to bear characteristics of their precursor stage cells (Tworoger et al., 1999). Normally, late stage stalk cells do not express the cell adhesion molecule FasIII, which is a marker for the precursor pre-follicle cells. As reported before, in *controls*, only 5% of the late stalks were still expressing FasIII (Figure 26A). On the other hand, the analysis of the *mir-310s* mutants revealed a high, 65%, incidence of FasIII positive late stalks (Figure 26B). Interestingly, these FasIII expressing *mir-310s* mutant stalks were also positive for Hh ligand (Figure 26B''). The prevalence of ectopic FasIII expressing late stalk cells addressed to the known overactive Hh signaling phenotype. The *mir-310s* deficiency-caused higher Rab23 levels were tested to be the underlying reason for this phenotype. The soma-specific *actin Gal4* and *Rab23-RNAi* lines in the *mir-310s* background enabled the downregulation of high Rab23 levels. As a result, the stalk specification mutant phenotype was rescued by downregulation of excess Rab23 levels resulting in only 15% FasIII positive late stalk incidence (Figure 26C, Table 11).

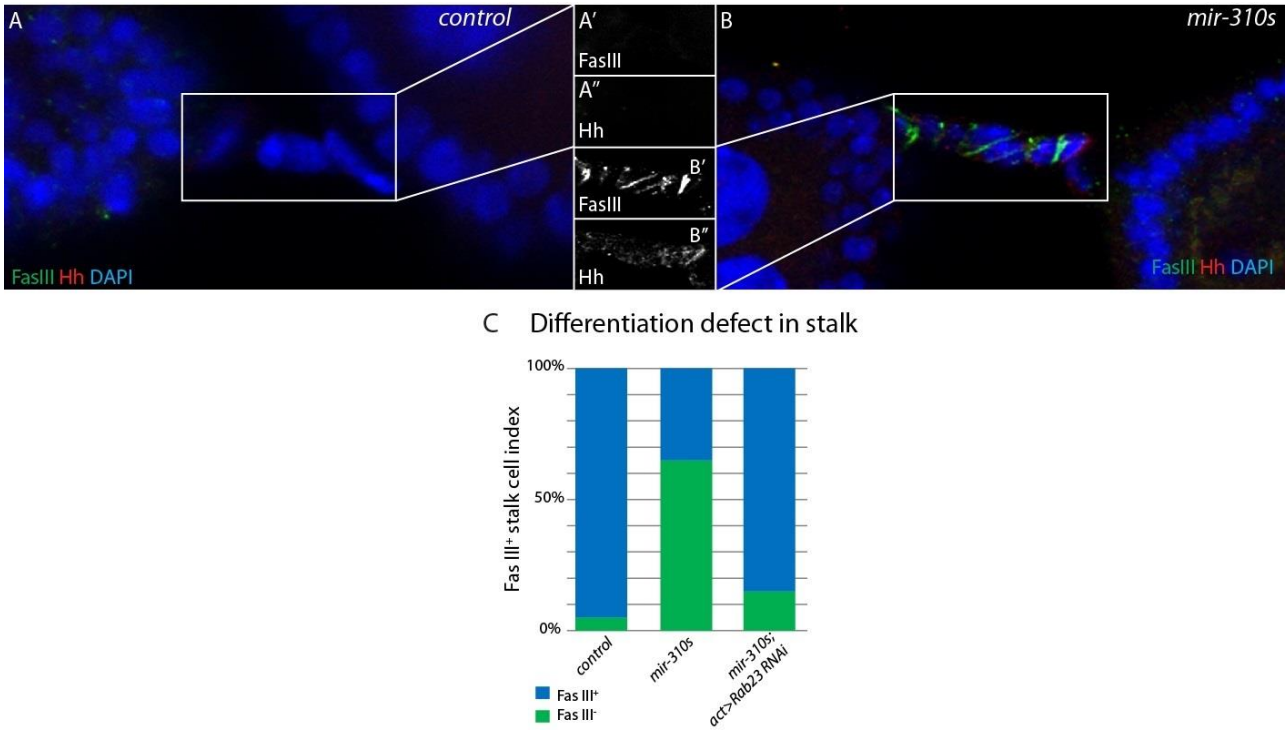

Figure 26. *mir-310s* loss causes cell-specification defect in stalks

(A) Stalk cells from late stage egg chambers cease to express an apical membrane marker, FasIII, specific for their precursor stages (A'); and they are negative for Hh ligand (A'') as reported before (Tworoger et al., 1999).

(B) The loss of the *mir-310s* causes perturbed organization and multilayered organization in the stalks, where these stalk cells continue expressing FasIII (green in B, B') and are positive for Hh ligand (red in B, B''). This phenotype resembles the defect in cell specification in case of Hh overexpression (Forbes et al., 1996a).

(C) The quantification of the FasIII expressing stalks in the *mir-310s* deficient ovarioles demonstrates the perturbed cell specification. Suppressing the upregulated Rab23 levels in *mir-310s* mutants somatically by *actin Gal4; UAS Rab23 RNAi* rescues this phenotype leaving only a small proportion (15%) of the late stage stalk cells still FasIII positive (Çiçek et al., 2016).

Anterior is to the left; images represent maximum intensity projections of confocal Z-stacks.

3.2.3.2 Loss of *mir-310s* perturbs cell/ tissue organization related to Hh pathway

Secondly, the germline cyst encapsulation process was investigated in *mir-310s* mutants. It is known that Hh overexpression perturbs the process of germline cyst being encapsulated by FSC progeny and their budding from the germarial region 2B-3. As a result germline cysts accumulate in the germarial region 2 without being surrounded by pre-follicular cells (Forbes et al., 1996a). The distribution of the germaria, which already completed the germline cyst encapsulation and which are still in the process or have failed to encapsulate was analyzed by marking the FSCs and their progeny, the pre-follicular cells, with FasIII. This distribution in *controls* showed that 85% of the germaria inhabited cysts enwrapped by FasIII positive cells (Figure 27A). However, less than 30% of the germaria in *mir-310s* deficient females had an encapsulated cyst (Figure 27B) pointing again to the perturbed Hh signaling. The RNAi approach to suppress the excess Rab23 amounts was again successful to rescue the phenotype confirming the Rab23 involvement in the Hh pathway and their control via the *mir-310s* (Figure 27C, Table 11).

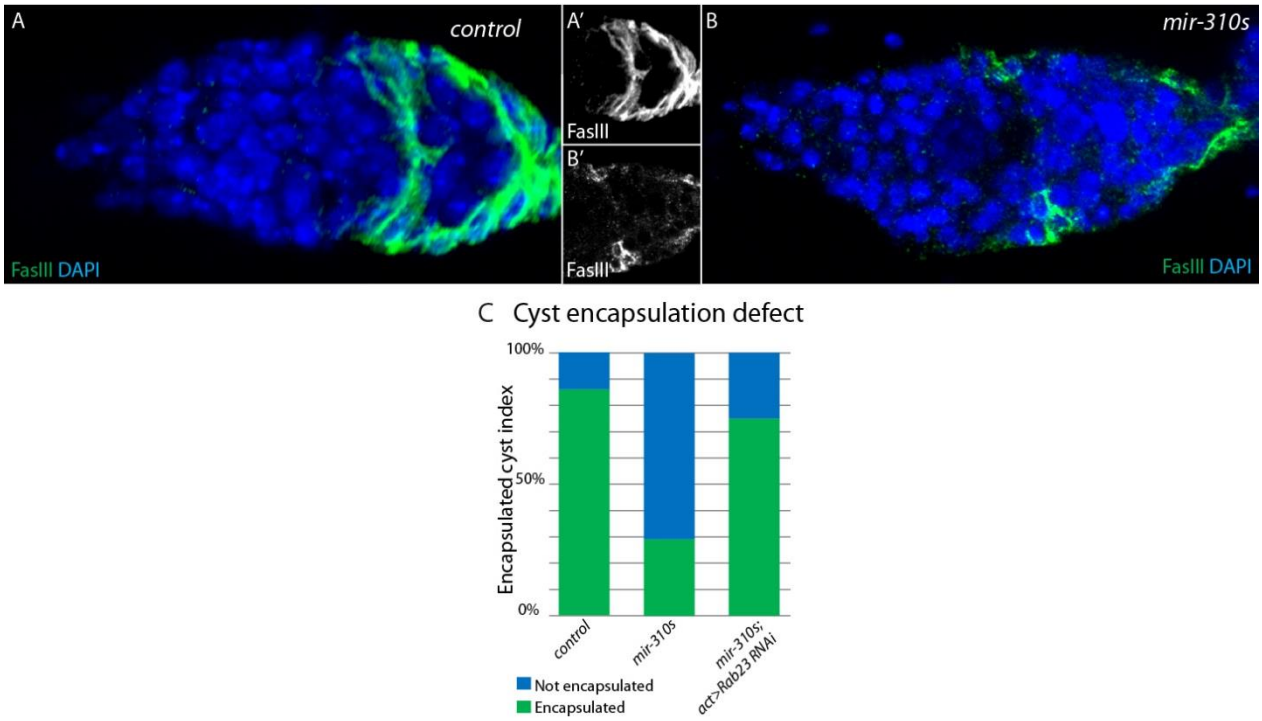

Figure 27. The *mir-310s* are required for cyst encapsulation

(A) The pre-follicular cells (marked with FasIII, A') encapsulate the germline cyst at region 2B of the germarium.

(B) The *mir-310s* mutant germarium fails to produce encapsulated cysts with the same rate as *controls*. At the germarial region 2A/2B boundary, pre-follicular cells (marked with FasIII (B')) have not intercalated between cysts by progressing towards the interior of the germarium and enwrap the cyst paralleling to a similar problem reported for *hh* mutants (Forbes et al., 1996a).

(C) The analysis of the encapsulated cyst distribution in *control* and *mir-310s* mutant germaria demonstrates the perturbed process because of *mir-310s* loss. Only ~30% of the *mir-310s* deficient germaria have proper enwrapped cysts, far less than the *control* ~85%. Downregulation of the *mir-310s* deficiency-upregulated Rab23 via *actin Gal4; UAS Rab23 RNAi* rescues this phenotype resulting in incidence of encapsulation at a rate of 75% (Çiçek et al., 2016).

Anterior is to the left; images represent maximum intensity projections of confocal Z-stacks.

3.2.3.3 Rab23 upregulation via *mir-310s* loss causes Hh-like cell proliferation phenotype

Thirdly, the involvement of the Hh signaling on the FC division was put on focus, where the Hh ligand accumulating on the FSCs initiate the proliferation program. Early studies have shown that the ectopic *hh* expression has the potential to drive extra somatic divisions of the pre-follicular cells (Forbes et al., 1996a; Forbes et al., 1996b). In addition, under nutritionally restrictive conditions, the division-stimulation potential of the excess Hh ligand release (from the TF and CpCs) and accumulation (on FSC) has been proven (Hartman et al., 2013). Therefore, the mitosis rates were examined in the early follicular epithelium of *mir-310s* deficient egg chambers under starvation conditions by quantifying mitotic stage 2 FCs using the mitosis marker, phosphohistone 3 (PH3). Under nutritionally restrictive conditions, *mir-310s* mutant egg chambers contained four times more mitotic FCs compared to *controls* (Figure 28A, B, and C). In order to test if the cause of this phenotype is the extra Rab23 abundance and the subsequent hyperactive Hh signaling acting on FSCs, Rab23 or Hh were overexpressed separately under nutritionally restrictive conditions to recapitulate a similar overproliferation phenotype. Usage of the CpCs specific driver, *bab1 Gal4*, ensured an overexpression pattern, which mimicked the endogenous spatial expression of both Rab23 and Hh ligand. The experiment was successful to reproduce the known hyperproliferative effect of the Hh ligand overexpression (Zhang and Kalderon, 2000) (Figure 28C). Similarly, fivefold higher mitosis rate was observed in the stage 2 egg chamber follicular epithelium. Importantly, the Rab23 overexpression also showed a very similar overactivation of the proliferation program in the FSCs, which caused the mitosis rate five times higher than the *controls* (Figure 28C). These results further supported the hypothesis that Rab23 being involved in Hh signaling in cell-autonomous manner. Subsequently, rescue experiments were performed by suppressing the extra Rab23 amounts and overactive Hh signaling driving *Rab23-RNAi* and *hh-RNAi* in the CpCs via *bab1 Gal4* in *mir-310s* mutant background. As a result, the mitotic FC numbers in the stage 2 egg chambers under starvation conditions went down to near *control* values rescuing the hyperproliferation phenotype caused by the *mir-310s* deficiency (Figure 28C, Table 11). Therefore, it is concluded that the excessive FC division rate caused by *mir-310s* loss under nutritional restriction occurs because of the upregulated *Rab23* expression and coupled hyperactivity of the Hh signaling in the signal sending cells.

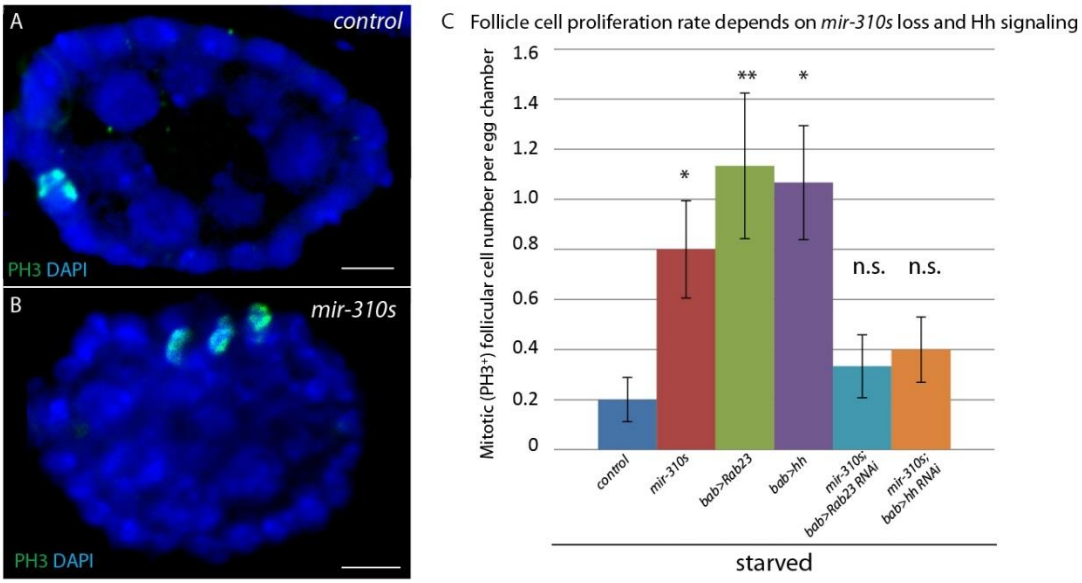

Figure 28. *mir-310s* loss causes higher mitosis rates in follicular epithelium

(A) *Control* stage 2 egg chamber with one FC at mitosis marked by PH3 (G') representing the low mitotic index values of *control* follicular epithelium under nutritional stress.

(B) *mir-310s* mutant stage 2 egg chamber with three mitotic FC marked by PH3 (H') representing the high mitosis rate in FCs under starvation conditions similar to the reported *hh* overexpression experiments (Forbes et al., 1996b).

(C) Quantification of mitotic FCs shows the low mitotic index upon nutritional restriction to 0.2 cells per stage 2 egg chamber in *controls*. The index value for *mir-310s* deficient egg chambers is however as high as 0.8 under the same restrictive conditions. Likewise, overexpression of *hh* and *Rab23* via *bab1 Gal4; UAS Rab23* and *bab1 Gal4; UAS hh, tub>Gal80^{ts}* (4 days at 29°C) causes high mitotic index values of 1.1 per egg chamber. This excess mitotic FC phenotype caused by *mir-310s* deficiency can be rescued by *bab1Gal4; UAS Rab23 RNAi* and *bab1 Gal4; UAS hh RNAi*, resulting in mitotic indexes of 0.3 and 0.4 respectively (Çiçek et al., 2016).

Anterior is to the left; images represent single optical sections; scale bar represents 5 µm. In (C) the bar graph indicates AVE±SEM. Significances were calculated with Mann-Whitney U test and z statistics (*p<0.05, **p<0.005, ***p<0.0005)

3.2.4 Rab23 is involved in the regulation of Hh signal sending in cell-autonomous manner

3.2.4.1 Rab23 and Hh colocalize subcellularly

Proteins from the Rab family are known for their membrane associations and regulate the specificity of intracellular trafficking (Zerial and McBride, 2001). These findings suggesting a cell-autonomous role for Rab23 in Hh signal sending cells, raised interest to further inspect the details of its mode of action subcellularly. In order to examine its subcellular localization and discover its interaction partners, the endogenously tagged Rab23 (*Rab23-YFP*) allele was used.

Firstly, the subcellular expression pattern of Rab23 and Hh was investigated at the CpCs. The majority of the GSC niche cells were positive for both proteins; in addition, small numbers of CpCs were observed as single positive for either Rab23 (green arrowhead) or Hh (red arrowhead) (Figure 29). In either case, both proteins revealed a heterogenous and punctuated distribution, which resulted in occurrence of few puncta, where respective Rab23 and Hh signals colocalized on yellow dot-like structures (yellow arrows) (Figure 29A). This heterogenous punctuated colocalization of both signals suggested Rab23-vesicle-mediated Hh ligand trafficking in the CpCs. The incomplete overlap of the subcellular distributions of Rab23 and Hh together with the arbitrary distribution of Rab23 or Hh positive CpC subsets, show the non-static nature of the GSC niche mode of action and dynamic involvement of Rab23 in the Hh signal sending process.

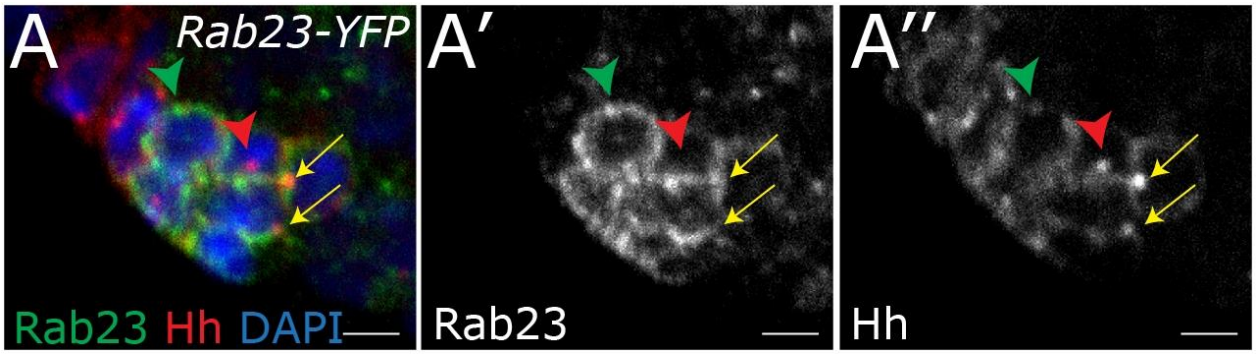

Figure 29. Rab23 and Hh selectively colocalize in subcellular compartments

(A) The *Rab23-YFP* germarial niche shows dynamic endogenous Rab23 (green arrowhead) and Hh (red arrowhead) expression in the CpC, where respective signals colocalize in subcellular puncta (yellow arrows) (Çiçek et al., 2016).

Anterior is to the left; image represents single optical section.

3.2.4.2 Rab23 has potential interaction partners in vesicle trafficking

Secondly, a co-immunoprecipitation experiment was performed in search for Rab23 interaction partners with the expectation of gathering information about the cellular microenvironment of the Hh ligand transport and release. For the experiment, endogenously tagged Rab23 locus was used (*Rab23-YFP-4xmyc*). Three biological replicates were analyzed by mass spectrometry. GO term analysis of the resulting candidate genes resulted in construction of functional interaction networks (Franceschini et al., 2013). Many protein groups were identified to be potential interaction partners of Rab23. However, among the candidates, a group of 12 proteins associated with COPI coated vesicles attracted attention (Figure 30), where they have been shown to be involved in Hh ligand release (Aikin et al., 2012; Lum et al., 2003; Nybakken et al., 2005) (see Table 12 and supplementary spreadsheets in the digital appendix for complete list of identified proteins). This finding corresponded to known Rab protein function of vesicular trafficking (Zerial and McBride, 2001) and further reinforced the predicted role of Rab23 in Hh ligand logistics.

A

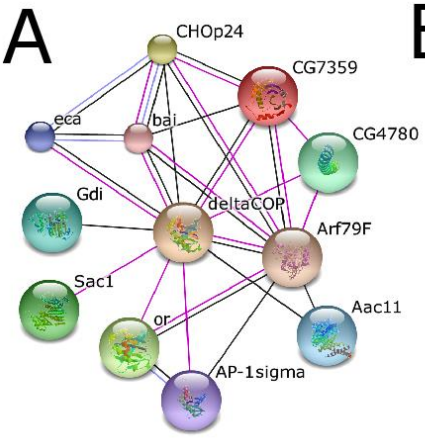

B

CG Number	Gene Name	GO Term
CG14813	deltaCOP	vesicle-mediated transport
CG3029	or	vesicle coating
CG11785	bai	Golgi vesicle transport
CG7359	Sec22	ER to Golgi vesicle-mediated transport
CG4780	Membrin	ER to Golgi vesicle-mediated transport
CG5864	AP-1sigma	vesicle-mediated transport
CG9128	Sac1	axon cargo transport
CG8385	Arf79F	post-Golgi vesicle-mediated transport
CG6582	Aac11	negative regulation of apoptotic process
CG3564	CHOp24	ER to Golgi vesicle-mediated transport
CG4422	Gdi	vesicle-mediated transport
CG33104	eca	ER to Golgi vesicle-mediated transport

Figure 30. Rab23 regulates Hh ligand logistics.

(A) Functional network and (B) associated GO terms of the COPI coatomer related proteins co-immunoprecipitated with Rab23 (Table 12) (Çiçek et al., 2016).

4 Discussion

In this study, the miRNAs from the *mir-310s* cluster are reported to be global regulators of energy homeostasis and associated processes across different organ systems. This novel miRNA regulated nutritional stress response mechanism is necessary for fine adjustment of an important signaling pathway to ensure proper oogenesis at right output rates. Specifically, three Hh pathway components are targeted by the *mir-310s* in a nutritional stress response context to ensure accuracy for the pathway activity. Furthermore one of the *mir-310s* targets, Rab23, regulates Hh ligand sending cell-autonomously.

4.1 *mir-310s* are involved in global control of nutrient and energy metabolism

To investigate global changes in protein expression upon miRNA deficiency, a proteomic approach was employed. For the first time, SILAC labeling in *Drosophila* was used in miRNA mutants to define affected gene clusters and interaction networks.

This experiment detected a large number of genes affected by *mir-310s* loss, where obtained clusters contain direct *mir-310s* targets as well as affected downstream pathway components combined. Note that due to technique limitations, identification of all low abundant targets, such as signaling components, was not possible, retrieving only a small fraction from the predicted target lists of the *mir-310s* supported with multiple algorithms (Betel et al., 2008; Enright et al., 2003; Kheradpour et al., 2007) (see supplementary spreadsheets in the digital appendix). For example, several of the *mir-310s'* predicted targets, which were not found in the proteomics experiment, have been confirmed by *in vitro* and *in vivo* techniques including *Drosophila* genetics. Extensive search for common GO terms in the retrieved groups and evaluation of the common cluster-associated functional pathways resulted in eight processes clearly affected by the loss of *mir-310s*.

Energy and lipid metabolism clusters were most prominent from identified groups, which immediately set up the course to find common affected processes. It is well known that the muscular and neural functions are sensitive to the energy and nutritional status of the organism. For example, the muscle mass of the fly is a known non-primary source for energy and nutrient scavenging (Arndt et al., 2010). Thus, it is foreseeable that clusters with muscle and neural developmental genes were affected by *mir-310s* loss. In addition, starvation-sensitive mitochondria-associated cluster can refer to deregulations in fatty acid and nucleotide synthesis

through Krebs cycle (Berg et al., 2002; Magwere et al., 2006). Many other affected genes, specific for these metabolic pathways, have also been identified in other clusters. This interconnection of affected groups further supports their relation to energy homeostasis. The connection between the affected cuticle-related cluster and nutritional status might not be obvious; however, studies in arthropods have shown that cuticular sugar and protein derivatives can be reconstituted for metabolic and synthetic purposes in development and starvation contexts (Hillerton, 1978; Speck and Urich, 1972).

Proteomic data confirmation was necessary to provide further proof of the diet-sensitive genes' deregulation at the mRNA level and to resolve the few protein expression discrepancies from the replicate experiments. The *mir-310s* deficiency-related deregulation of almost all 31 genes (previously shown to be sensitive to starvation (Farhadian et al., 2012)) were validated using qPCR. The expression control of the genes like *Larval serum protein 2 (Lsp2), Prophenoloxidase 1 (pro-PO-A1), Actin 88F, Odorant-binding protein 56e (Obp56e),* and *Cuticular proteins (Cpr62Bc and Cpr100A)* appeared to be *mir-310s* dependent. In addition, the *mir-310s* were found to control expression response of the genes *Larval serum protein 1 β (Lsp1β), Odorant-binding proteins (Obp56a and Obp99b),* and *Cuticular protein 72Ec (Cpr72Ec)* to nutritional restriction. These results further supported the hypothesis that *mir-310s* govern nutritional stress response, which correlates with physiological mutant phenotypes. This organismal effect of the *mir-310s* loss is ascribed to their highly dynamic and widespread expression pattern, regulating diet-sensitive processes directly through their target genes and indirectly through affected secondary processes.

Next, physiological characteristics of *mir-310s* mutants were analyzed to pinpoint perturbed processes in organismal level due to disturbed energy and nutrient homeostasis or perturbed response to dietary changes. The *mir-310s* loss results in shorter lifespan of the well-fed flies in both sexes. However, under starvation conditions *mir-310s* loss caused sex-specific effects in survival rates. Female *mir-310s* mutants outlived the *controls* under nutritional restriction, which led to the interpretation of this result that these mutants are well prepared for starvation further supported by the following findings. The crop is a food storage organ, which grows in size in females upon resumed feeding after starvation. *mir-310s* mutants have larger crops under normal feeding conditions, thus implying starved-like behavior of the miRNA mutants at all times. Increased crop diameter and accumulation of opaque food mass in the crops supports the idea that

under normal conditions *mir-310s* mutant females behave as if they are starved. However, further experiments (e.g. Capillary Feeder (CAFE) Assay (Ja et al., 2007)) need to be performed, in order to determine if the underlying reason is higher food consumption.

It is known that the nutritional restriction causes females to cease egg laying promptly. Therefore, the egg production of the *mir-310s* mutant females was analyzed to test the out-of-context starvation phenotype. *mir-310s* mutants lay significantly fewer eggs, which could be explained by active continuous starvation response in the absence of nutritional restriction.

Intrigued by deregulation of the lipid metabolism-associated genes upon *mir-310s* deficiency, total body fat content was analyzed in the mutant females. As expected, measurements of total fat content (triacylglycerol equivalents) displayed gross changes in both well-fed and starved conditions. The *mir-310s* mutant females accumulated less fat in well-fed conditions compared to *controls*. Interestingly, this phenotype was reversed under nutritional restriction, where the mutants accumulated significant amount of lipids. Therefore, the *mir-310s* are confirmed as necessary elements in starvation response possibly by regulating targets involved in lipid homeostasis and storage. Further experiments analyzing the *mir-310s* role in tissues controlling lipid storage (e.g. fat body) would hopefully explain the source of this oversensitivity.

4.2 The *mir-310s* control oogenesis via Hh signaling under favorable and restrictive nutritional conditions

miRNA target databases are very useful tools to search for putative target genes. However, depending on the miRNA sequence these lists can be too extensive to directly relate them with the biological context. Narrowing down these putative target lists was the initial step before systematic testing and following target confirmation.

The well-studied diet-sensitive *Drosophila* ovary, and more specifically the process of oogenesis, served as a platform to put the *mir-310s* in a pathway context, where the *mir-310s* mutant phenotypes are analyzed in this system, in order to find *in vivo mir-310s* targets.

Gross morphology of the *mir-310s* mutant ovaries depicted starvation-related nature of the mutation. Mutant ovaries contained late stage egg chambers and mature eggs even after 4-5 days of nutritional restriction. This non-responsiveness can be attributed to loss of synchrony in egg production and laying rates. In addition, distinct epithelial phenotypes were observed in a very high

penetrance under nutritional restriction. Starvation sensitivity of these specific cellular aberrations supported the hypothesis that the *mir-310s* have a role in oogenesis regulation and are clearly indispensable for nutritional stress response in this process.

In nutritionally rich conditions, *mir-310s* mutant ovaries showed subtle epithelial phenotypes (fused egg chambers, multilayered stalk and follicular epithelium with perturbed polarity). Similar phenotypes were shown upon misregulation of one of the best known evolutionary conserved developmental pathways, the Hh pathway (Forbes et al., 1996a; Forbes et al., 1996b; Zhang and Kalderon, 2001). The resemblance of *mir-310s* mutant phenotypes to those of Hh overexpression allowed narrowing down the search for direct miRNA target genes to the canonical pathway members and pathway-associated genes. Three genes, *Rab23, DHR96,* and *ttk*, were putative *mir-310s* targets and interacting with the Hh pathway components, taking into account their reported expression patterns in the ovary and loss- and gain-of-function phenotypes. Using a luciferase-based expression assay followed by qPCR, these genes were confirmed as *mir-310s* targets *in vitro* and *in vivo*. Relevantly, the *in vivo* mRNA levels gave clues about the diet-sensitive nature of *mir-310s* control over these genes. These findings have shown that establishing accurate *Rab23* and *DHR96* mRNA levels in starvation and well-fed conditions depend on *mir-310s* presence. On the other hand, *ttk* mRNA levels rely on *mir-310s* tuning activity only under dietary restrictive conditions. In conclusion, these data suggested that in the ovary the accurate Hh signaling strength was established through adjustment of *Rab23, DHR96,* and *ttk* expression levels by *mir-310s* according to changing dietary conditions.

The spatial expression profile of the *mir-310s* also supported its involvement in the Hh signaling. The nuclear LacZ and membrane GFP reporter expression patterns driven by *mir-310s* Gal4 line proved to be useful to detect the *mir-310s* locus activity in the interfollicular stalks and follicular epithelial cells. The spatial distribution of *mir-310s* expression in germarium showed strong activity at the GSC niche (in TF and CpCs) and in ECs at some extend. Note that the nLacZ and mGFP were not temporally and spatially coexpressed in these cell types. This indicated a highly dynamic transcriptional activity of the locus, visualized by the reporter proteins' differential turnover rates. Especially the *mir-310s* expression pattern in the germarium was coinciding almost perfectly with the known expression pattern of the *hh* gene (Forbes et al., 1996a; Forbes et al., 1996b). On the other hand, the stalk cells and the follicle cells (including FSCs) are known to

express the Hh receptor Ptc and respond to Hh signal (Forbes et al., 1996b). The mutual expression of the *mir-310s* in the Hh signal sending and receiving cells in the ovary supported the hypothesis that the *mir-310s* play a role in its regulation. In addition, the fact that the *mir-310s* are expressed in both the signaling source and the target cell types, necessitated the involvement of cell specific targets.

Following the hypothesis that the *mir-310s* are necessary for proper dietary stress response in the ovary, possible changes in their spatial expression were investigated. However, no obvious difference in reporter expression pattern was observed in the well-fed and starved *mir-310s>nLacZ mGFP* ovaries. This result postulated that the *mir-310s* have a location-specific role in specifically these cell types controlling Hh signal sending and receiving.

To obtain a quantitative measure for the starvation effect on the *mir-310s* locus activity, a PCR based Taqman assay was performed. The relative mature miRNA levels demonstrated a gradual decline (tested for *mir-312*) and a steady expression level after 5 days of starvation (tested for all *mir-310s* members).

Decline of the target *Rab23, DHR96,* and *ttk* levels together with the negative regulator *mir-310s* levels upon starvation seems to be counterintuitive. However, the proposed model explains the *mir-310s* control over their three target genes under nutritional restriction, ensuring their dowregulation for the proper dietary stress response. The result of this specific control mechanism is the establishment of lower Hh signaling strength, which has to be achieved to keep the low levels of downstream signaling activity and low rate of oogenesis in general (Figure 31).

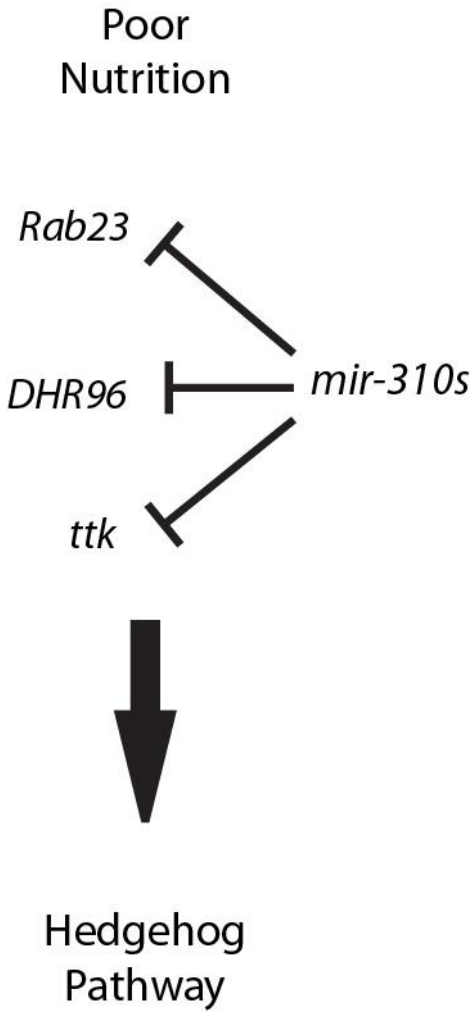

Figure 31. Under nutritional restriction, the *mir-310s* are responsible to downregulate its target genes to control the Hh signaling strength

4.3 *Drosophila* Rab23 is a novel element in the Hh pathway actively regulated by the *mir-310s*

In order to monitor the tissue-specific spatial changes in Rab23 protein expression upon *mir-310s* loss the endogenous *Rab23-YFP* expression pattern was analyzed in *control* and *mir-310s* deficient backgrounds. *mir-310s* mutation caused more expansive expression pattern and higher signal intensity of Rab23 in CpCs and ECs, which correlates with the expression pattern of the *mir-310s* and is confirmed by the relative Rab23 protein levels. This result, together with the *in vitro* assay

and upregulated *Rab23* mRNA levels, proves that *Rab23* is an *in vivo* target of the *mir-310s* in the germarium. In addition, stronger staining for the Hh ligand in the *mir-310s* mutant germaria (with upregulated Rab23 levels) further reinforced the proposed role of Rab23 as positive regulator of Hh ligand release and its intracellular mobility.

To further test the hypothesis of the Rab23 and *mir-310s* involvement in the Hh pathway, *mir-310s* mutants were investigated for cell-specific quantifiable phenotypes, which were reported for perturbed Hh signaling. Overactive Hh signaling in germarium causes cell specification defects in stalk cells, where they fail to undergo differentiation and express their precursor stage cell-specific marker FasIII (Tworoger et al., 1999). The *mir-310s* mutant stalk cells displayed similar phenotype with 65% penetrance, which could be rescued by downregulating Rab23 (*mir-310s ; act>Rab23 RNAi*). A very similar result was observed on the tissue organization related phenotype, where the germline cyst encapsulation is perturbed and results in stalled cysts at the germarial 2B-3 region (Forbes et al., 1996a). Analysis has shown that more than 70% of *mir-310s* mutant germaria harbored such stalled non-encapsulated germline cysts. Similarly, Rab23 downregulation successfully rescued this phenotype proving that the excess Rab23 levels (as a result of *mir-310s* loss) are responsible for this phenotype. Last but not least, the excessive pre-follicular cell proliferation phenotype was analyzed, which is caused by overexpression of Hh (Forbes et al., 1996a; Forbes et al., 1996b) potent enough to exert this effect even under nutritional restriction (Hartman et al., 2013). The *mir-310s* mutant egg chambers contained fourfold higher numbers of mitotic cells compared to *controls*, very similar to Hh overactivation. This effect was reproduced by overexpressing Hh or Rab23 specifically in the GSC niche cells, which resulted in excessive numbers of mitotic cells per chamber (~5 fold higher than the *control*). Successful rescue of this phenotype by Rab23 or Hh downregulation in *mir-310s* mutant background clearly showed the *mir-310s*' involvement in Rab23, and hence Hh signaling, regulation. Therefore, Rab23 was confirmed as a cell-autonomous positive regulator of Hh signal sending, and that the *mir-310s* are indeed responsible to tune Rab23 levels in well-fed and starved conditions in order to achieve accurate levels of Hh signaling activity.

To further investigate the cell-autonomous involvement of Rab23 in Hh ligand release by CpCs, the subcellular localizations of endogenous Rab23 and Hh ligand were investigated. Imaging of *Rab23-YFP* ovaries stained with anti-GFP and anti-Hh antibodies revealed punctate signals for

both Rab23 and Hh. Initial analysis demonstrated heterogeneous distribution of the respective signals, where some CpCs were positive for either Rab23 or Hh, and some were coexpressing both proteins. Importantly, these coexpression puncta pointed to subcellular compartments, to which both proteins were presumably colocalizing. This finding was the first clue for a direct interaction between Rab23 and Hh ligand, and suggests that Rab23 is involved in Hh ligand logistics at the signal-sending cell by direct interaction or through other elements of specific or general transport mechanisms in the cell. Although this data strongly proposes a direct interaction or at least a very close proximity for Rab23 and Hh ligand, further biochemical approaches have to be undertaken in order to confirm this finding.

To better understand the molecular environment of Rab23 a co-immunoprecipitation experiment was performed using the *Rab23-YFP-4xmyc* line to identify its interaction partners. Among a large number of identified proteins, members of the COPI vesicle coatomer proteins were detected, which are essential for vesicle formation and budding. In similar context, Rab proteins are membrane-associated proteins important for vesicle trafficking (Zerial and McBride, 2001). It was also shown previously that COPI proteins regulate Hh ligand release (Aikin et al., 2012; Lum et al., 2003; Nybakken et al., 2005). The identification of COPI associated proteins as potential Rab23 interaction partners shaped the hypothesis that Rab23 is involved in Hh ligand logistics in the CpCs and positively regulates its anterograde transport and release. Further experiments using known secretory vesicle markers would shed light on the directionality and composition of the Hh transporting vesicles that are trafficked by Rab23 in the CpCs.

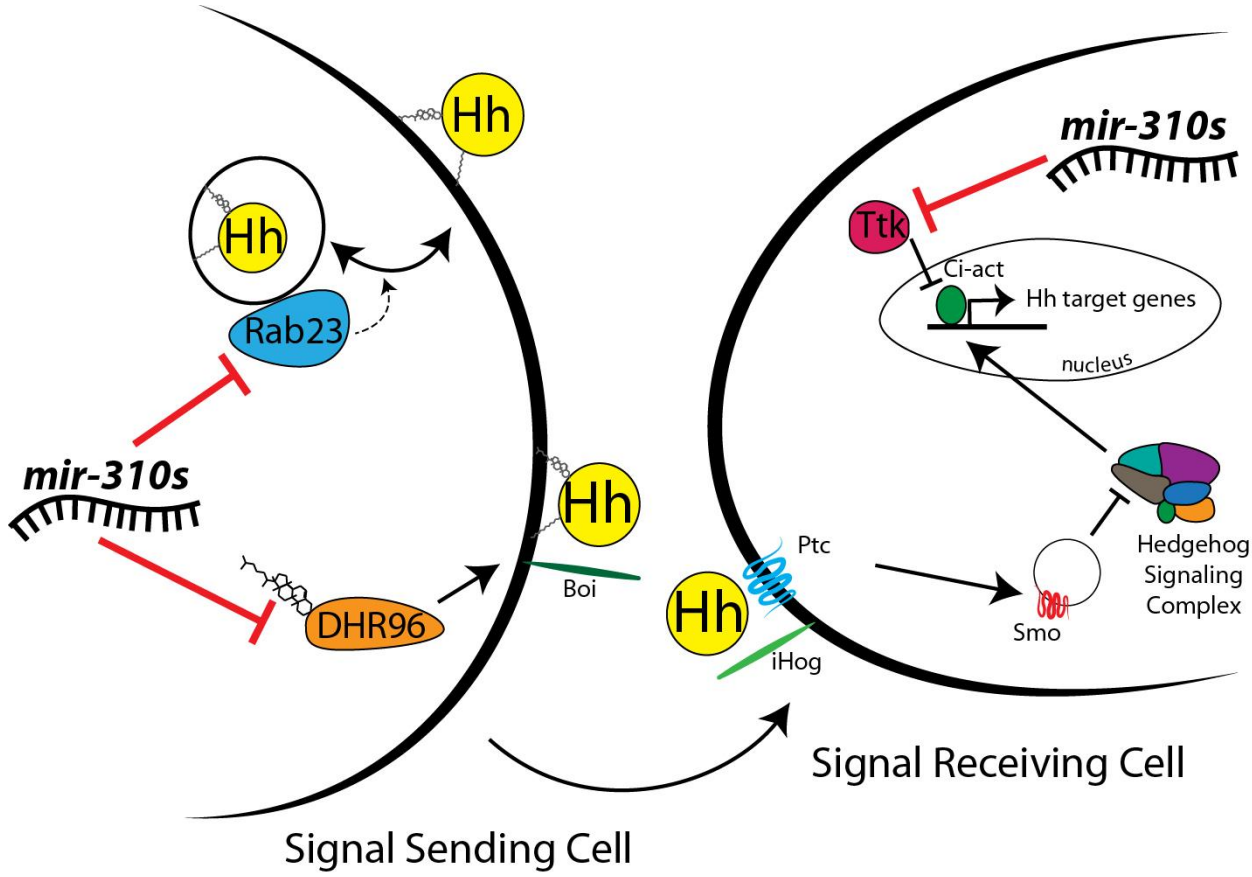

Figure 32. The *mir-310s* target *Rab23, DHR96,* and *ttk* in the Hh pathway

In summary, the *mir-310s* are identified as novel regulators of global energy homeostasis. This finding was supported by the proteomic data and gross physiological and morphological phenotypes of *mir-310s* mutants. *mir-310s* loss caused ovary specific defects, which assumed higher penetrance upon nutritional restriction. Three direct *mir-310s* targets were identified, which are involved in the Hh pathway regulation. The target genes, *Rab23, DHR96,* and *ttk*, were confirmed to be under tight and prompt control of the *mir-310s* and nutritional status. Here, it is shown that the Hh pathway signaling strength has to be regulated by the *mir-310s* via these targets to ensure accurate dietary response in the ovary for proper FSC division and differentiation (Figure 32). Lastly, Rab23 is proposed as a novel regulator of Hh ligand availability possibly by controlling intracellular trafficking of Hh ligand transporting vesicles. Taking everything into account, these findings suggest a miRNA-based tuning mechanism, where *mir-310s* are essential regulators that

guarantee accurate amounts of Hh signal sending and receiving under different environmental nutritional setups.

Conclusions

In this study, the *mir-310s* are identified as global regulators of energy homeostasis, where they tune dietary-sensitive processes in terms of global protein and mRNA expression. Importantly, genes associated with energy and lipid metabolism are deregulated by *mir-310s* loss. Phenotypically, *mir-310s* loss causes diet-sensitive defects such as increased crop size, lower fecundity, and increased fat accumulation under nutritionally restrictive conditions.

The *mir-310s* are also required for maintenance of oogenesis, which is sensitive to nutritional conditions. Mutants exhibit epithelial phenotypes worsening dramatically upon nutritional restriction. *mir-310s* loss causes accumulating stalk cells, formation of multilayered follicular epithelia, and appearance of fused egg chambers resembling reported perturbations in the evolutionary conserved Hedgehog (Hh) pathway.

Three genes interacting with the Hh pathway (*Rab23, DHR96,* and *ttk*) are confirmed as *in vivo* targets of the *mir-310s*. In *Drosophila*, the cholesterol receptor DHR96 and transcription factor Ttk have been shown to regulate Hh ligand release and downstream gene activity, respectively. Here, intracellular trafficking-associated Rab23 is shown as a novel Hh pathway interactor in *Drosophila*. The cell-autonomous role of Rab23 as positive regulator of Hh ligand sending is supported by colocalization of Rab23 and Hh ligand in the signal sending cells and Rab23 coimmunoprecipitated COPI coatomer-associated proteins indicating the vesicle transport control by Rab23. Presumably, Rab23 interacts with Hh-loaded vesicles and facilitates its intracellular transport and positively regulates its recruitment to the cell membrane and release.

In summary, *mir-310s* are found as potent regulators of *Rab23, DHR96,* and *ttk* expression levels, ensuring low transcript levels at dietary-restrictive conditions, which is essential to sustain low Hh signaling strength under nutritional stress.

References

Adams, M.D., Celniker, S.E., Holt, R.A., Evans, C.A., Gocayne, J.D., Amanatides, P.G., Scherer, S.E., Li, P.W., Hoskins, R.A., Galle, R.F., *et al.* (2000). The genome sequence of Drosophila melanogaster. Science *287*, 2185-2195.

Aikin, R., Cervantes, A., D'Angelo, G., Ruel, L., Lacas-Gervais, S., Schaub, S., and Therond, P. (2012). A genome-wide RNAi screen identifies regulators of cholesterol-modified hedgehog secretion in Drosophila. PloS one *7*, e33665.

Al-Anzi, B., Armand, E., Nagamei, P., Olszewski, M., Sapin, V., Waters, C., Zinn, K., Wyman, R.J., and Benzer, S. (2010). The leucokinin pathway and its neurons regulate meal size in Drosophila. Current biology : CB *20*, 969-978.

Alexandre, C., Jacinto, A., and Ingham, P.W. (1996). Transcriptional activation of hedgehog target genes in Drosophila is mediated directly by the cubitus interruptus protein, a member of the GLI family of zinc finger DNA-binding proteins. Genes & development *10*, 2003-2013.

Alexandre, C., Lecourtois, M., and Vincent, J. (1999). Wingless and Hedgehog pattern Drosophila denticle belts by regulating the production of short-range signals. Development *126*, 5689-5698.

Arndt, V., Dick, N., Tawo, R., Dreiseidler, M., Wenzel, D., Hesse, M., Furst, D.O., Saftig, P., Saint, R., Fleischmann, B.K., *et al.* (2010). Chaperone-assisted selective autophagy is essential for muscle maintenance. Current biology : CB *20*, 143-148.

Ashburner, M. (1989). Drosophila. A laboratory handbook (Cold Spring Harbor Laboratory Press).

Baker, K.D., and Thummel, C.S. (2007). Diabetic larvae and obese flies-emerging studies of metabolism in Drosophila. Cell metabolism *6*, 257-266.

Barrio, L., Dekanty, A., and Milan, M. (2014). MicroRNA-mediated regulation of Dp53 in the Drosophila fat body contributes to metabolic adaptation to nutrient deprivation. Cell reports *8*, 528-541.

Begg, M., and Robertson, F.W. (1948). Nutritional requirements of Drosophila melanogaster. Nature *161*, 769.

Behm-Ansmant, I., Rehwinkel, J., Doerks, T., Stark, A., Bork, P., and Izaurralde, E. (2006). mRNA degradation by miRNAs and GW182 requires both CCR4:NOT deadenylase and DCP1:DCP2 decapping complexes. Genes & development *20*, 1885-1898.

Berg, J.M., Tymoczko, J.L., and Stryer, L. (2002). The Citric Acid Cycle Is a Source of Biosynthetic Precursors. Biochemistry; New York: W H Freeman *5th edition*, Section 17.13.

Betel, D., Wilson, M., Gabow, A., Marks, D.S., and Sander, C. (2008). The microRNA.org resource: targets and expression. Nucleic acids research *36*, D149-153.

Bhattacharyya, S.N., Habermacher, R., Martine, U., Closs, E.I., and Filipowicz, W. (2006). Relief of microRNA-mediated translational repression in human cells subjected to stress. Cell *125*, 1111-1124.

Bohnsack, M.T., Czaplinski, K., and Gorlich, D. (2004). Exportin 5 is a RanGTP-dependent dsRNA-binding protein that mediates nuclear export of pre-miRNAs. Rna *10*, 185-191.

Bracht, J., Hunter, S., Eachus, R., Weeks, P., and Pasquinelli, A.E. (2004). Trans-splicing and polyadenylation of let-7 microRNA primary transcripts. Rna *10*, 1586-1594.

Brennecke, J., Stark, A., Russell, R.B., and Cohen, S.M. (2005). Principles of microRNA-target recognition. PLoS biology *3*, e85.

Briscoe, J., and Therond, P.P. (2013). The mechanisms of Hedgehog signalling and its roles in development and disease. Nature reviews Molecular cell biology *14*, 416-429.

Brogiolo, W., Stocker, H., Ikeya, T., Rintelen, F., Fernandez, R., and Hafen, E. (2001). An evolutionarily conserved function of the Drosophila insulin receptor and insulin-like peptides in growth control. Current biology : CB *11*, 213-221.

Bujold, M., Gopalakrishnan, A., Nally, E., and King-Jones, K. (2010). Nuclear receptor DHR96 acts as a sentinel for low cholesterol concentrations in Drosophila melanogaster. Molecular and cellular biology *30*, 793-805.

Cai, X., Hagedorn, C.H., and Cullen, B.R. (2004). Human microRNAs are processed from capped, polyadenylated transcripts that can also function as mRNAs. Rna *10*, 1957-1966.

Calin, G.A., and Croce, C.M. (2006). MicroRNA signatures in human cancers. Nature reviews Cancer *6*, 857-866.

Calin, G.A., Liu, C.G., Sevignani, C., Ferracin, M., Felli, N., Dumitru, C.D., Shimizu, M., Cimmino, A., Zupo, S., Dono, M., *et al.* (2004). MicroRNA profiling reveals distinct signatures in B cell chronic lymphocytic leukemias. Proceedings of the National Academy of Sciences of the United States of America *101*, 11755-11760.

Canavoso, L.E., Jouni, Z.E., Karnas, K.J., Pennington, J.E., and Wells, M.A. (2001). Fat metabolism in insects. Annual review of nutrition *21*, 23-46.

Castle, W.E., Carpenter, F.W., Clark, A.H., Mast, S.O., and Barrows, W.M. (1906). The Effects of Inbreeding, Cross-Breeding, and Selection upon the Fertility and Variability of Drosophila. Proceedings of the American Academy of Arts and Sciences *41*, 731-786.

Chamoun, Z., Mann, R.K., Nellen, D., von Kessler, D.P., Bellotto, M., Beachy, P.A., and Basler, K. (2001). Skinny hedgehog, an acyltransferase required for palmitoylation and activity of the hedgehog signal. Science *293*, 2080-2084.

Chan, C.C., Scoggin, S., Wang, D., Cherry, S., Dembo, T., Greenberg, B., Jin, E.J., Kuey, C., Lopez, A., Mehta, S.Q., *et al.* (2011). Systematic discovery of Rab GTPases with synaptic functions in Drosophila. Current biology : CB *21*, 1704-1715.

Chang, Y.C., Jang, A.C., Lin, C.H., and Montell, D.J. (2013). Castor is required for Hedgehog-dependent cell-fate specification and follicle stem cell maintenance in Drosophila oogenesis. Proceedings of the National Academy of Sciences of the United States of America *110*, E1734-1742.

Chen, J.K., Taipale, J., Cooper, M.K., and Beachy, P.A. (2002). Inhibition of Hedgehog signaling by direct binding of cyclopamine to Smoothened. Genes & development *16*, 2743-2748.

Chendrimada, T.P., Gregory, R.I., Kumaraswamy, E., Norman, J., Cooch, N., Nishikura, K., and Shiekhattar, R. (2005). TRBP recruits the Dicer complex to Ago2 for microRNA processing and gene silencing. Nature *436*, 740-744.

Choi, W.Y., Giraldez, A.J., and Schier, A.F. (2007). Target protectors reveal dampening and balancing of Nodal agonist and antagonist by miR-430. Science *318*, 271-274.

Çiçek, I.Ö., Karaca, S., Brankatschk, M., Eaton, S., Urlaub, H., and Shcherbata, H.R. (2016). Hedgehog Signaling strength is Orchestrated by the mir-310 Cluster of microRNAs in Response to Diet. Genetics.

Conlon, I., and Raff, M. (1999). Size control in animal development. Cell *96*, 235-244.

Cox, J., and Mann, M. (2008). MaxQuant enables high peptide identification rates, individualized p.p.b.-range mass accuracies and proteome-wide protein quantification. Nature biotechnology *26*, 1367-1372.

Decotto, E., and Spradling, A.C. (2005). The Drosophila ovarian and testis stem cell niches: similar somatic stem cells and signals. Developmental cell *9*, 501-510.

Denli, A.M., Tops, B.B., Plasterk, R.H., Ketting, R.F., and Hannon, G.J. (2004). Processing of primary microRNAs by the Microprocessor complex. Nature *432*, 231-235.

Dews, M., Homayouni, A., Yu, D., Murphy, D., Sevignani, C., Wentzel, E., Furth, E.E., Lee, W.M., Enders, G.H., Mendell, J.T., *et al.* (2006). Augmentation of tumor angiogenesis by a Myc-activated microRNA cluster. Nature genetics *38*, 1060-1065.

Ding, X.C., Weiler, J., and Grosshans, H. (2009). Regulating the regulators: mechanisms controlling the maturation of microRNAs. Trends in biotechnology *27*, 27-36.

Doench, J.G., and Sharp, P.A. (2004). Specificity of microRNA target selection in translational repression. Genes & development *18*, 504-511.

Drummond-Barbosa, D., and Spradling, A.C. (2001). Stem cells and their progeny respond to nutritional changes during Drosophila oogenesis. Developmental biology *231*, 265-278.

Du, T., and Zamore, P.D. (2005). microPrimer: the biogenesis and function of microRNA. Development *132*, 4645-4652.

Eagle, H. (1955). THE MINIMUM VITAMIN REQUIREMENTS OF THE L AND HELA CELLS IN TISSUE CULTURE, THE PRODUCTION OF SPECIFIC VITAMIN DEFICIENCIES, AND THEIR CURE. The Journal of Experimental Medicine *102*, 595-600.

Eaton, S. (2008). Multiple roles for lipids in the Hedgehog signalling pathway. Nature reviews Molecular cell biology *9*, 437-445.

Edgecomb, R.S., Harth, C.E., and Schneiderman, A.M. (1994). Regulation of feeding behavior in adult Drosophila melanogaster varies with feeding regime and nutritional state. The Journal of experimental biology *197*, 215-235.

Eggenschwiler, J.T., Espinoza, E., and Anderson, K.V. (2001). Rab23 is an essential negative regulator of the mouse Sonic hedgehog signalling pathway. Nature *412*, 194-198.

Enright, A.J., John, B., Gaul, U., Tuschl, T., Sander, C., and Marks, D.S. (2003). MicroRNA targets in Drosophila. Genome biology *5*, R1.

Eugster, C., Panakova, D., Mahmoud, A., and Eaton, S. (2007). Lipoprotein-heparan sulfate interactions in the Hh pathway. Developmental cell *13*, 57-71.

Farhadian, S.F., Suarez-Farinas, M., Cho, C.E., Pellegrino, M., and Vosshall, L.B. (2012). Post-fasting olfactory, transcriptional, and feeding responses in Drosophila. Physiology & behavior *105*, 544-553.

Fire, A., Xu, S., Montgomery, M.K., Kostas, S.A., Driver, S.E., and Mello, C.C. (1998). Potent and specific genetic interference by double-stranded RNA in Caenorhabditis elegans. Nature *391*, 806-811.

Forbes, A.J., Lin, H., Ingham, P.W., and Spradling, A.C. (1996a). hedgehog is required for the proliferation and specification of ovarian somatic cells prior to egg chamber formation in Drosophila. Development *122*, 1125-1135.

Forbes, A.J., Nakano, Y., Taylor, A.M., and Ingham, P.W. (1993). Genetic analysis of hedgehog signalling in the Drosophila embryo. Dev Suppl, 115-124.

Forbes, A.J., Spradling, A.C., Ingham, P.W., and Lin, H. (1996b). The role of segment polarity genes during early oogenesis in Drosophila. Development *122*, 3283-3294.

Forstemann, K., Tomari, Y., Du, T., Vagin, V.V., Denli, A.M., Bratu, D.P., Klattenhoff, C., Theurkauf, W.E., and Zamore, P.D. (2005). Normal microRNA maturation and germ-line stem cell maintenance requires Loquacious, a double-stranded RNA-binding domain protein. PLoS biology *3*, e236.

Franceschini, A., Szklarczyk, D., Frankild, S., Kuhn, M., Simonovic, M., Roth, A., Lin, J., Minguez, P., Bork, P., von Mering, C., *et al.* (2013). STRING v9.1: protein-protein interaction networks, with increased coverage and integration. Nucleic acids research *41*, D808-815.

Gilboa, L., and Lehmann, R. (2006). Soma-germline interactions coordinate homeostasis and growth in the Drosophila gonad. Nature *443*, 97-100.

Giraldez, A.J., Mishima, Y., Rihel, J., Grocock, R.J., Van Dongen, S., Inoue, K., Enright, A.J., and Schier, A.F. (2006). Zebrafish MiR-430 promotes deadenylation and clearance of maternal mRNAs. Science *312*, 75-79.

Gregory, R.I., Chendrimada, T.P., Cooch, N., and Shiekhattar, R. (2005). Human RISC couples microRNA biogenesis and posttranscriptional gene silencing. Cell *123*, 631-640.

Gregory, R.I., Yan, K.P., Amuthan, G., Chendrimada, T., Doratotaj, B., Cooch, N., and Shiekhattar, R. (2004). The Microprocessor complex mediates the genesis of microRNAs. Nature *432*, 235-240.

Griffiths-Jones, S., Saini, H.K., van Dongen, S., and Enright, A.J. (2008). miRBase: tools for microRNA genomics. Nucleic acids research *36*, D154-158.

Group, T.E.C.W. (2006). Nutrition and reproduction in women. Human Reproduction Update *12*, 193-207.

Grun, D., Wang, Y.L., Langenberger, D., Gunsalus, K.C., and Rajewsky, N. (2005). microRNA target predictions across seven Drosophila species and comparison to mammalian targets. PLoS computational biology *1*, e13.

Gunesdogan, U., Jackle, H., and Herzig, A. (2010). A genetic system to assess in vivo the functions of histones and histone modifications in higher eukaryotes. EMBO reports *11*, 772-776.

Hammond, M.P., and Laird, C.D. (1985). Chromosome structure and DNA replication in nurse and follicle cells of Drosophila melanogaster. Chromosoma *91*, 267-278.

Han, J., Lee, Y., Yeom, K.H., Kim, Y.K., Jin, H., and Kim, V.N. (2004). The Drosha-DGCR8 complex in primary microRNA processing. Genes & development *18*, 3016-3027.

Hartman, T.R., Strochlic, T.I., Ji, Y., Zinshteyn, D., and O'Reilly, A.M. (2013). Diet controls Drosophila follicle stem cell proliferation via Hedgehog sequestration and release. The Journal of cell biology *201*, 741-757.

Hartman, T.R., Zinshteyn, D., Schofield, H.K., Nicolas, E., Okada, A., and O'Reilly, A.M. (2010). Drosophila Boi limits Hedgehog levels to suppress follicle stem cell proliferation. The Journal of cell biology *191*, 943-952.

Haslam, D.W., and James, W.P.T. (2005). Obesity. Lancet *366*, 1197-1209.

He, L., Thomson, J.M., Hemann, M.T., Hernando-Monge, E., Mu, D., Goodson, S., Powers, S., Cordon-Cardo, C., Lowe, S.W., Hannon, G.J., *et al.* (2005). A microRNA polycistron as a potential human oncogene. Nature *435*, 828-833.

Hildebrandt, A., Bickmeyer, I., and Kuhnlein, R.P. (2011). Reliable Drosophila body fat quantification by a coupled colorimetric assay. PloS one *6*, e23796.

Hillerton, J.E. (1978). Changes in the structure and composition of the extensible cuticle of Rhodnius prolixus through the 5th larval instar. Journal of Insect Physiology *24*, 399-412.

Holman, R.T. (1971). Essential fatty acid deficiency. Progress in the Chemistry of Fats and other Lipids *9*, 275-348.

Horner, M.A., Pardee, K., Liu, S., King-Jones, K., Lajoie, G., Edwards, A., Krause, H.M., and Thummel, C.S. (2009). The Drosophila DHR96 nuclear receptor binds cholesterol and regulates cholesterol homeostasis. Genes & development *23*, 2711-2716.

Hornstein, E., Mansfield, J.H., Yekta, S., Hu, J.K., Harfe, B.D., McManus, M.T., Baskerville, S., Bartel, D.P., and Tabin, C.J. (2005). The microRNA miR-196 acts upstream of Hoxb8 and Shh in limb development. Nature *438*, 671-674.

Humphreys, D.T., Westman, B.J., Martin, D.I., and Preiss, T. (2005). MicroRNAs control translation initiation by inhibiting eukaryotic initiation factor 4E/cap and poly(A) tail function. Proceedings of the National Academy of Sciences of the United States of America *102*, 16961-16966.

Hutvagner, G., McLachlan, J., Pasquinelli, A.E., Balint, E., Tuschl, T., and Zamore, P.D. (2001). A cellular function for the RNA-interference enzyme Dicer in the maturation of the let-7 small temporal RNA. Science *293*, 834-838.

Hutvagner, G., and Zamore, P.D. (2002). A microRNA in a multiple-turnover RNAi enzyme complex. Science *297*, 2056-2060.

Ingham, P.W. (1993). Localized hedgehog activity controls spatial limits of wingless transcription in the Drosophila embryo. Nature *366*, 560-562.

Ingham, P.W., and Fietz, M.J. (1995). Quantitative effects of hedgehog and decapentaplegic activity on the patterning of the Drosophila wing. Current biology : CB *5*, 432-440.

Ingham, P.W., and McMahon, A.P. (2001). Hedgehog signaling in animal development: paradigms and principles. Genes & development *15*, 3059-3087.

Ingham, P.W., Nakano, Y., and Seger, C. (2011). Mechanisms and functions of Hedgehog signalling across the metazoa. Nature reviews Genetics *12*, 393-406.

Ja, W.W., Carvalho, G.B., Mak, E.M., de la Rosa, N.N., Fang, A.Y., Liong, J.C., Brummel, T., and Benzer, S. (2007). Prandiology of Drosophila and the CAFE assay. Proceedings of the National Academy of Sciences of the United States of America *104*, 8253-8256.

Jiang, F., Ye, X., Liu, X., Fincher, L., McKearin, D., and Liu, Q. (2005). Dicer-1 and R3D1-L catalyze microRNA maturation in Drosophila. Genes & development *19*, 1674-1679.

Ketting, R.F., Fischer, S.E., Bernstein, E., Sijen, T., Hannon, G.J., and Plasterk, R.H. (2001). Dicer functions in RNA interference and in synthesis of small RNA involved in developmental timing in C. elegans. Genes & development *15*, 2654-2659.

Kheradpour, P., Stark, A., Roy, S., and Kellis, M. (2007). Reliable prediction of regulator targets using 12 Drosophila genomes. Genome research *17*, 1919-1931.

Kiriakidou, M., Nelson, P.T., Kouranov, A., Fitziev, P., Bouyioukos, C., Mourelatos, Z., and Hatzigeorgiou, A. (2004). A combined computational-experimental approach predicts human microRNA targets. Genes & development *18*, 1165-1178.

Kirilly, D., Spana, E.P., Perrimon, N., Padgett, R.W., and Xie, T. (2005). BMP signaling is required for controlling somatic stem cell self-renewal in the Drosophila ovary. Developmental cell *9*, 651-662.

Kloosterman, W.P., Wienholds, E., Ketting, R.F., and Plasterk, R.H. (2004). Substrate requirements for let-7 function in the developing zebrafish embryo. Nucleic acids research *32*, 6284-6291.

Konig, A., and Shcherbata, H. (2015). Soma influences GSC progeny differentiation via the cell adhesion-mediated steroid-let-7-Wingless signaling cascade that regulates chromatin dynamics. Biology Open.

Konig, A., and Shcherbata, H.R. (2013). Visualization of adult stem cells within their niches using the Drosophila germline as a model system. Methods in molecular biology *1035*, 25-33.

Krek, A., Grun, D., Poy, M.N., Wolf, R., Rosenberg, L., Epstein, E.J., MacMenamin, P., da Piedade, I., Gunsalus, K.C., Stoffel, M., *et al.* (2005). Combinatorial microRNA target predictions. Nature genetics *37*, 495-500.

Kuhnlein, R.P. (2011). The contribution of the Drosophila model to lipid droplet research. Progress in lipid research *50*, 348-356.

Kyhse-Andersen, J. (1984). Electroblotting of multiple gels: a simple apparatus without buffer tank for rapid transfer of proteins from polyacrylamide to nitrocellulose. Journal of biochemical and biophysical methods *10*, 203-209.

Laemmli, U.K. (1970). Cleavage of structural proteins during the assembly of the head of bacteriophage T4. Nature *227*, 680-685.

Landthaler, M., Yalcin, A., and Tuschl, T. (2004). The human DiGeorge syndrome critical region gene 8 and Its D. melanogaster homolog are required for miRNA biogenesis. Current biology : CB *14*, 2162-2167.

Laus, M.F., Vales, L.D., Costa, T.M., and Almeida, S.S. (2011). Early postnatal protein-calorie malnutrition and cognition: a review of human and animal studies. International journal of environmental research and public health *8*, 590-612.

Lee, R.C., Feinbaum, R.L., and Ambros, V. (1993). The C. elegans heterochronic gene lin-4 encodes small RNAs with antisense complementarity to lin-14. Cell *75*, 843-854.

Lee, Y., Ahn, C., Han, J., Choi, H., Kim, J., Yim, J., Lee, J., Provost, P., Radmark, O., Kim, S., *et al.* (2003). The nuclear RNase III Drosha initiates microRNA processing. Nature *425*, 415-419.

Lee, Y., Kim, M., Han, J., Yeom, K.H., Lee, S., Baek, S.H., and Kim, V.N. (2004). MicroRNA genes are transcribed by RNA polymerase II. The EMBO journal *23*, 4051-4060.

Leung, A.K., and Sharp, P.A. (2010). MicroRNA functions in stress responses. Molecular cell *40*, 205-215.

Lewis, B.P., Burge, C.B., and Bartel, D.P. (2005). Conserved seed pairing, often flanked by adenosines, indicates that thousands of human genes are microRNA targets. Cell *120*, 15-20.

Lewis, B.P., Shih, I.H., Jones-Rhoades, M.W., Bartel, D.P., and Burge, C.B. (2003). Prediction of mammalian microRNA targets. Cell *115*, 787-798.

Li, Y., Wang, F., Lee, J.A., and Gao, F.B. (2006). MicroRNA-9a ensures the precise specification of sensory organ precursors in Drosophila. Genes & development *20*, 2793-2805.

Liu, J., Rivas, F.V., Wohlschlegel, J., Yates, J.R., 3rd, Parker, R., and Hannon, G.J. (2005). A role for the P-body component GW182 in microRNA function. Nature cell biology *7*, 1261-1266.

Lu, J., Fu, Y., Kumar, S., Shen, Y., Zeng, K., Xu, A., Carthew, R., and Wu, C.I. (2008). Adaptive evolution of newly emerged micro-RNA genes in Drosophila. Molecular biology and evolution *25*, 929-938.

Lu, J., Getz, G., Miska, E.A., Alvarez-Saavedra, E., Lamb, J., Peck, D., Sweet-Cordero, A., Ebert, B.L., Mak, R.H., Ferrando, A.A., *et al.* (2005). MicroRNA expression profiles classify human cancers. Nature *435*, 834-838.

Lum, L., Yao, S., Mozer, B., Rovescalli, A., Von Kessler, D., Nirenberg, M., and Beachy, P.A. (2003). Identification of Hedgehog pathway components by RNAi in Drosophila cultured cells. Science *299*, 2039-2045.

Lund, E., Guttinger, S., Calado, A., Dahlberg, J.E., and Kutay, U. (2004). Nuclear export of microRNA precursors. Science *303*, 95-98.

Maggert, K.A., Gong, W.J., and Golic, K.G. (2008). Methods for homologous recombination in Drosophila. Methods in molecular biology *420*, 155-174.

Magwere, T., Goodall, S., Skepper, J., Mair, W., Brand, M.D., and Partridge, L. (2006). The Effect of Dietary Restriction on Mitochondrial Protein Density and Flight Muscle Mitochondrial Morphology in Drosophila. The Journals of Gerontology Series A: Biological Sciences and Medical Sciences *61*, 36-47.

Maniataki, E., and Mourelatos, Z. (2005). A human, ATP-independent, RISC assembly machine fueled by pre-miRNA. Genes & development *19*, 2979-2990.

Margolis, J., and Spradling, A. (1995). Identification and behavior of epithelial stem cells in the Drosophila ovary. Development *121*, 3797-3807.

Maroney, P.A., Yu, Y., Fisher, J., and Nilsen, T.W. (2006). Evidence that microRNAs are associated with translating messenger RNAs in human cells. Nature structural & molecular biology *13*, 1102-1107.

Marrone, A.K., Edeleva, E.V., Kucherenko, M.M., Hsiao, N.H., and Shcherbata, H.R. (2012). Dg-Dys-Syn1 signaling in Drosophila regulates the microRNA profile. BMC cell biology *13*, 26.

Martinez, J., and Tuschl, T. (2004). RISC is a 5' phosphomonoester-producing RNA endonuclease. Genes & development *18*, 975-980.

Martinez, N.J., Ow, M.C., Barrasa, M.I., Hammell, M., Sequerra, R., Doucette-Stamm, L., Roth, F.P., Ambros, V.R., and Walhout, A.J. (2008). A C. elegans genome-scale microRNA network contains composite feedback motifs with high flux capacity. Genes & development *22*, 2535-2549.

McGuire, S. (2013). WHO, World Food Programme, and International Fund for Agricultural Development. 2012. The State of Food Insecurity in the World 2012. Economic growth is necessary but not sufficient to accelerate reduction of hunger and malnutrition. Rome, FAO. Advances in Nutrition *4*, 126-127.

Mendell, J.T., and Olson, E.N. (2012). MicroRNAs in stress signaling and human disease. Cell *148*, 1172-1187.

Miller, A. (1950). The internal anatomy and histology of the imago of Drosophila melanogaster. Biology of Drosophila, 420-534.

Miska, E.A., Alvarez-Saavedra, E., Abbott, A.L., Lau, N.C., Hellman, A.B., McGonagle, S.M., Bartel, D.P., Ambros, V.R., and Horvitz, H.R. (2007). Most Caenorhabditis elegans microRNAs are individually not essential for development or viability. PLoS genetics *3*, e215.

Morris, L.X., and Spradling, A.C. (2011). Long-term live imaging provides new insight into stem cell regulation and germline-soma coordination in the Drosophila ovary. Development *138*, 2207-2215.

Morrison, S.J., and Spradling, A.C. (2008). Stem cells and niches: mechanisms that promote stem cell maintenance throughout life. Cell *132*, 598-611.

Ng, M., Fleming, T., Robinson, M., Thomson, B., Graetz, N., Margono, C., Mullany, E.C., Biryukov, S., Abbafati, C., Abera, S.F., *et al.* (2014). Global, regional, and national prevalence of overweight and obesity in children and adults during 1980-2013: a systematic analysis for the Global Burden of Disease Study 2013. Lancet *384*, 766-781.

Nottrott, S., Simard, M.J., and Richter, J.D. (2006). Human let-7a miRNA blocks protein production on actively translating polyribosomes. Nature structural & molecular biology *13*, 1108-1114.

Nusslein-Volhard, C., and Wieschaus, E. (1980). Mutations affecting segment number and polarity in Drosophila. Nature *287*, 795-801.

Nybakken, K., Vokes, S.A., Lin, T.Y., McMahon, A.P., and Perrimon, N. (2005). A genome-wide RNA interference screen in Drosophila melanogaster cells for new components of the Hh signaling pathway. Nature genetics *37*, 1323-1332.

Nystul, T., and Spradling, A. (2007). An epithelial niche in the Drosophila ovary undergoes long-range stem cell replacement. Cell stem cell *1*, 277-285.

Nystul, T., and Spradling, A. (2010). Regulation of epithelial stem cell replacement and follicle formation in the Drosophila ovary. Genetics *184*, 503-515.

O'Donnell, K.A., Wentzel, E.A., Zeller, K.I., Dang, C.V., and Mendell, J.T. (2005). c-Myc-regulated microRNAs modulate E2F1 expression. Nature *435*, 839-843.

O'Reilly, A.M., Lee, H.H., and Simon, M.A. (2008). Integrins control the positioning and proliferation of follicle stem cells in the Drosophila ovary. The Journal of cell biology *182*, 801-815.

Panakova, D., Sprong, H., Marois, E., Thiele, C., and Eaton, S. (2005). Lipoprotein particles are required for Hedgehog and Wingless signalling. Nature *435*, 58-65.

Pancratov, R., Peng, F., Smibert, P., Yang, S., Jr., Olson, E.R., Guha-Gilford, C., Kapoor, A.J., Liang, F.X., Lai, E.C., Flaherty, M.S., *et al.* (2013). The miR-310/13 cluster antagonizes beta-catenin function in the regulation of germ and somatic cell differentiation in the Drosophila testis. Development *140*, 2904-2916.

Pataki, C., Matusek, T., Kurucz, E., Ando, I., Jenny, A., and Mihaly, J. (2010). Drosophila Rab23 is involved in the regulation of the number and planar polarization of the adult cuticular hairs. Genetics *184*, 1051-1065.

Petersen, C.P., Bordeleau, M.E., Pelletier, J., and Sharp, P.A. (2006). Short RNAs repress translation after initiation in mammalian cells. Molecular cell *21*, 533-542.

Pillai, R.S., Bhattacharyya, S.N., Artus, C.G., Zoller, T., Cougot, N., Basyuk, E., Bertrand, E., and Filipowicz, W. (2005). Inhibition of translational initiation by Let-7 MicroRNA in human cells. Science *309*, 1573-1576.

Piper, M.D., Blanc, E., Leitao-Goncalves, R., Yang, M., He, X., Linford, N.J., Hoddinott, M.P., Hopfen, C., Soultoukis, G.A., Niemeyer, C., *et al.* (2014). A holidic medium for Drosophila melanogaster. Nature methods *11*, 100-105.

Porter, J.A., Ekker, S.C., Park, W.J., von Kessler, D.P., Young, K.E., Chen, C.H., Ma, Y., Woods, A.S., Cotter, R.J., Koonin, E.V., *et al.* (1996a). Hedgehog patterning activity: role of a lipophilic modification mediated by the carboxy-terminal autoprocessing domain. Cell *86*, 21-34.

Porter, J.A., Young, K.E., and Beachy, P.A. (1996b). Cholesterol modification of hedgehog signaling proteins in animal development. Science *274*, 255-259.

Promega (2009). siCHECK™ Vectors Technical Bulletin.

Richards, G.S., and Degnan, B.M. (2009). The dawn of developmental signaling in the metazoa. Cold Spring Harbor symposia on quantitative biology *74*, 81-90.

Robbins, D.J., Nybakken, K.E., Kobayashi, R., Sisson, J.C., Bishop, J.M., and Therond, P.P. (1997). Hedgehog elicits signal transduction by means of a large complex containing the kinesin-related protein costal2. Cell *90*, 225-234.

Rojas-Rios, P., Guerrero, I., and Gonzalez-Reyes, A. (2012). Cytoneme-mediated delivery of hedgehog regulates the expression of bone morphogenetic proteins to maintain germline stem cells in Drosophila. PLoS biology *10*, e1001298.

Rong, Y.S., and Golic, K.G. (2000). Gene targeting by homologous recombination in Drosophila. Science *288*, 2013-2018.

Ross, S.A., and Davis, C.D. (2011). MicroRNA, nutrition, and cancer prevention. Adv Nutr *2*, 472-485.

Rottiers, V., and Naar, A.M. (2012). MicroRNAs in metabolism and metabolic disorders. Nature reviews Molecular cell biology *13*, 239-250.

Royzman, I., and Orr-Weaver, T.L. (1998). S phase and differential DNA replication during Drosophila oogenesis. Genes to cells : devoted to molecular & cellular mechanisms *3*, 767-776.

Russell, R.C., Fang, C., and Guan, K.L. (2011). An emerging role for TOR signaling in mammalian tissue and stem cell physiology. Development *138*, 3343-3356.

Rybak, A., Fuchs, H., Smirnova, L., Brandt, C., Pohl, E.E., Nitsch, R., and Wulczyn, F.G. (2008). A feedback loop comprising lin-28 and let-7 controls pre-let-7 maturation during neural stem-cell commitment. Nature cell biology *10*, 987-993.

Sahai-Hernandez, P., Castanieto, A., and Nystul, T.G. (2012). Drosophila models of epithelial stem cells and their niches. Wiley interdisciplinary reviews Developmental biology *1*, 447-457.

Sahai-Hernandez, P., and Nystul, T.G. (2013). A dynamic population of stromal cells contributes to the follicle stem cell niche in the Drosophila ovary. Development *140*, 4490-4498.

Saito, K., Ishizuka, A., Siomi, H., and Siomi, M.C. (2005). Processing of pre-microRNAs by the Dicer-1-Loquacious complex in Drosophila cells. PLoS biology *3*, e235.

Sambrook, J., Russell, D.W.D.W., and Laboratory, C.S.H. (2001). Molecular cloning : a laboratory manual, 3rd. ed edn (Cold Spring Harbor Laboratory).

Sang, J.H. (1956). The Quantitative Nutritional Requirements of Drosophila-Melanogaster. Journal of Experimental Biology *33*, 45-72.

Sang, J.H., and King, R.C. (1961). Nutritional Requirements of Axenically Cultured Drosophila Melanogaster Adults. Journal of Experimental Biology *38*, 793-&.

Schneeberger, M., Gomez-Valades, A.G., Ramirez, S., Gomis, R., and Claret, M. (2015). Hypothalamic miRNAs: emerging roles in energy balance control. Frontiers in neuroscience *9*, 41.

Schwarz, D.S., Hutvagner, G., Du, T., Xu, Z., Aronin, N., and Zamore, P.D. (2003). Asymmetry in the assembly of the RNAi enzyme complex. Cell *115*, 199-208.

Scott, R.C., Schuldiner, O., and Neufeld, T.P. (2004). Role and regulation of starvation-induced autophagy in the Drosophila fat body. Developmental cell *7*, 167-178.

Sen, G.L., and Blau, H.M. (2005). Argonaute 2/RISC resides in sites of mammalian mRNA decay known as cytoplasmic bodies. Nature cell biology *7*, 633-636.

Shevchenko, A., Tomas, H., Havlis, J., Olsen, J.V., and Mann, M. (2006). In-gel digestion for mass spectrometric characterization of proteins and proteomes. Nature protocols *1*, 2856-2860.

Sieber, M.H., and Thummel, C.S. (2012). Coordination of triacylglycerol and cholesterol homeostasis by DHR96 and the Drosophila LipA homolog magro. Cell metabolism *15*, 122-127.

Song, X., and Xie, T. (2002). DE-cadherin-mediated cell adhesion is essential for maintaining somatic stem cells in the Drosophila ovary. Proceedings of the National Academy of Sciences of the United States of America *99*, 14813-14818.

Song, X., and Xie, T. (2003). Wingless signaling regulates the maintenance of ovarian somatic stem cells in Drosophila. Development *130*, 3259-3268.

Speck, U., and Urich, K. (1972). Resorption des alten Panzers vor der Häutung bei dem FlußkrebsOrconectes limosus. J Comp Physiol *78*, 210-220.

Spradling, A.C. (1993). Developmental genetics of oogenesis, pp. 1-70.

Stegman, M.A., Vallance, J.E., Elangovan, G., Sosinski, J., Cheng, Y., and Robbins, D.J. (2000). Identification of a tetrameric hedgehog signaling complex. The Journal of biological chemistry *275*, 21809-21812.

Stern, D. (2001). Body-size evolution: how to evolve a mammoth moth. Current biology : CB *11*, R917-919.

Sun, J., and Deng, W.M. (2007). Hindsight mediates the role of notch in suppressing hedgehog signaling and cell proliferation. Developmental cell *12*, 431-442.

Sun, J., Smith, L., Armento, A., and Deng, W.M. (2008). Regulation of the endocycle/gene amplification switch by Notch and ecdysone signaling. The Journal of cell biology *182*, 885-896.

Sury, M.D., Chen, J.X., and Selbach, M. (2010). The SILAC fly allows for accurate protein quantification in vivo. Molecular & cellular proteomics : MCP *9*, 2173-2183.

Tabata, T., and Kornberg, T.B. (1994). Hedgehog is a signaling protein with a key role in patterning Drosophila imaginal discs. Cell *76*, 89-102.

Tatum, E.L. (1939). Nutritional Requirements of Drosophila Melanogaster. Proceedings of the National Academy of Sciences of the United States of America *25*, 490-497.

Teleman, A.A., Maitra, S., and Cohen, S.M. (2006). Drosophila lacking microRNA miR-278 are defective in energy homeostasis. Genes & development *20*, 417-422.

Thomas-Orillard, M. (1984). Modifications of Mean Ovariole Number, Fresh Weight of Adult Females and Developmental Time in DROSOPHILA MELANOGASTER Induced by Drosophila C Virus. Genetics *107*, 635-644.

Towbin, H., Staehelin, T., and Gordon, J. (1979). Electrophoretic transfer of proteins from polyacrylamide gels to nitrocellulose sheets: procedure and some applications. Proceedings of the National Academy of Sciences of the United States of America *76*, 4350-4354.

Tsurudome, K., Tsang, K., Liao, E.H., Ball, R., Penney, J., Yang, J.S., Elazzouzi, F., He, T., Chishti, A., Lnenicka, G., *et al.* (2010). The Drosophila miR-310 cluster negatively regulates synaptic strength at the neuromuscular junction. Neuron *68*, 879-893.

Tworoger, M., Larkin, M.K., Bryant, Z., and Ruohola-Baker, H. (1999). Mosaic analysis in the drosophila ovary reveals a common hedgehog-inducible precursor stage for stalk and polar cells. Genetics *151*, 739-748.

UniProt, C. (2014). Activities at the Universal Protein Resource (UniProt). Nucleic acids research *42*, D191-198.

Venter, J.C., Adams, M.D., Myers, E.W., Li, P.W., Mural, R.J., Sutton, G.G., Smith, H.O., Yandell, M., Evans, C.A., Holt, R.A., *et al.* (2001). The sequence of the human genome. Science *291*, 1304-1351.

Vokes, S.A., Ji, H., Wong, W.H., and McMahon, A.P. (2008). A genome-scale analysis of the cis-regulatory circuitry underlying sonic hedgehog-mediated patterning of the mammalian limb. Genes & development *22*, 2651-2663.

Wigglesworth, V.B. (1949). The utilization of reserve substances in Drosophila during flight. The Journal of experimental biology *26*, 150-163, illust.

Wightman, B., Ha, I., and Ruvkun, G. (1993). Posttranscriptional regulation of the heterochronic gene lin-14 by lin-4 mediates temporal pattern formation in C. elegans. Cell *75*, 855-862.

Wolpert, L., Beddinton, R., Brockes, J., Jessell, T., Lawrence, P., and Meyerowitz, E. (1998). Principles of development. Current Biology Ltd London.

Wu, C.I., Shen, Y., and Tang, T. (2009). Evolution under canalization and the dual roles of microRNAs: a hypothesis. Genome research *19*, 734-743.

Wu, L., Fan, J., and Belasco, J.G. (2006). MicroRNAs direct rapid deadenylation of mRNA. Proceedings of the National Academy of Sciences of the United States of America *103*, 4034-4039.

Xie, X., Lu, J., Kulbokas, E.J., Golub, T.R., Mootha, V., Lindblad-Toh, K., Lander, E.S., and Kellis, M. (2005). Systematic discovery of regulatory motifs in human promoters and 3' UTRs by comparison of several mammals. Nature *434*, 338-345.

Xu, P., Vernooy, S.Y., Guo, M., and Hay, B.A. (2003). The Drosophila microRNA Mir-14 suppresses cell death and is required for normal fat metabolism. Current biology : CB *13*, 790-795.

Yao, S., Lum, L., and Beachy, P. (2006). The ihog cell-surface proteins bind Hedgehog and mediate pathway activation. Cell *125*, 343-357.

Yatsenko, A.S., Marrone, A.K., and Shcherbata, H.R. (2014). miRNA-based buffering of the cobblestone-lissencephaly-associated extracellular matrix receptor dystroglycan via its alternative 3'-UTR. Nature communications *5*, 4906.

Yekta, S., Shih, I.H., and Bartel, D.P. (2004). MicroRNA-directed cleavage of HOXB8 mRNA. Science *304*, 594-596.

Yi, R., Qin, Y., Macara, I.G., and Cullen, B.R. (2003). Exportin-5 mediates the nuclear export of pre-microRNAs and short hairpin RNAs. Genes & development *17*, 3011-3016.

Young, V.R. (1994). Adult amino acid requirements: the case for a major revision in current recommendations. The Journal of nutrition *124*, 1517S-1523S.

Zecca, M., Basler, K., and Struhl, G. (1995). Sequential organizing activities of engrailed, hedgehog and decapentaplegic in the Drosophila wing. Development *121*, 2265-2278.

Zerial, M., and McBride, H. (2001). Rab proteins as membrane organizers. Nature reviews Molecular cell biology *2*, 107-117.

Zhang, W., Zhao, Y., Tong, C., Wang, G., Wang, B., Jia, J., and Jiang, J. (2005). Hedgehog-regulated Costal2-kinase complexes control phosphorylation and proteolytic processing of Cubitus interruptus. Developmental cell *8*, 267-278.

Zhang, Y., and Kalderon, D. (2000). Regulation of cell proliferation and patterning in Drosophila oogenesis by Hedgehog signaling. Development *127*, 2165-2176.

Zhang, Y., and Kalderon, D. (2001). Hedgehog acts as a somatic stem cell factor in the Drosophila ovary. Nature *410*, 599-604.

Acknowledgements

First of all, I want to thank my supervisor Halyna R. Shcherbata for giving me the opportunity to pursue my doctoral studies in her lab and for her great supervision, guidance, and understanding throughout these 3.5 years.

Next, I want to thank all current and former Shcherbata Lab members, Andriy Yatsenko, Mariya Kucherenko, Annekatrin König, Yuanbin Xie, Evgeniia Edeleva, April Marrone, and Nai-Hua Hsiao for their technical support, valuable scientific input, and especially for their company creating a family like working environment.

My research was substantially supported by the fly community via sharing resources freely. In addition, I have to give credit to my helpful collaborators Samir Karaca, Henning Urlaub, Marko Brankatschk, and Suzanne Eaton for their contribution. I am thankful to the whole Herbert Jäckle Department for the friendly atmosphere and intellectual discussions we shared throughout my studies, especially to Philip Hehlert and Ronald Kühnlein for their technical contribution. In addition, I want to thank my thesis committee members Roland Dosch and Andreas Wodarz for their valuable input to my doctoral studies and Reinhard Schuh, Michael Kessel, and Henrik Bringmann to spare the time and effort to be in my extended thesis committee.

My studies were supported by the Ph.D. program "Molecular Biology" – International Max Planck Research School at the Georg August University Göttingen and Max Planck Society. I especially thank Steffen Burkhardt and Kerstin Grüniger, who helped me to experience a smooth adaptation to Göttingen and graduate education.

I want to thank all my friends from the Molecular Biology Program for making these years fun, and especially my Turkish friends for making it feel like home.

Special thanks goes to my high school biology teacher Ludger Heilos, to whom I owe my enthusiasm to study biology.

Finally, I want to thank my family. I am truly grateful to my parents Mürşide Çiçek and Necip Feyyaz Çiçek for their continuous and unconditioned love and support, to my brother Osman Ali Çiçek for his advice and for boosting up my mood whenever I needed, and to Mariia Levchenko for her encouragement, patience, and love.

Appendix

Supplementary Figure

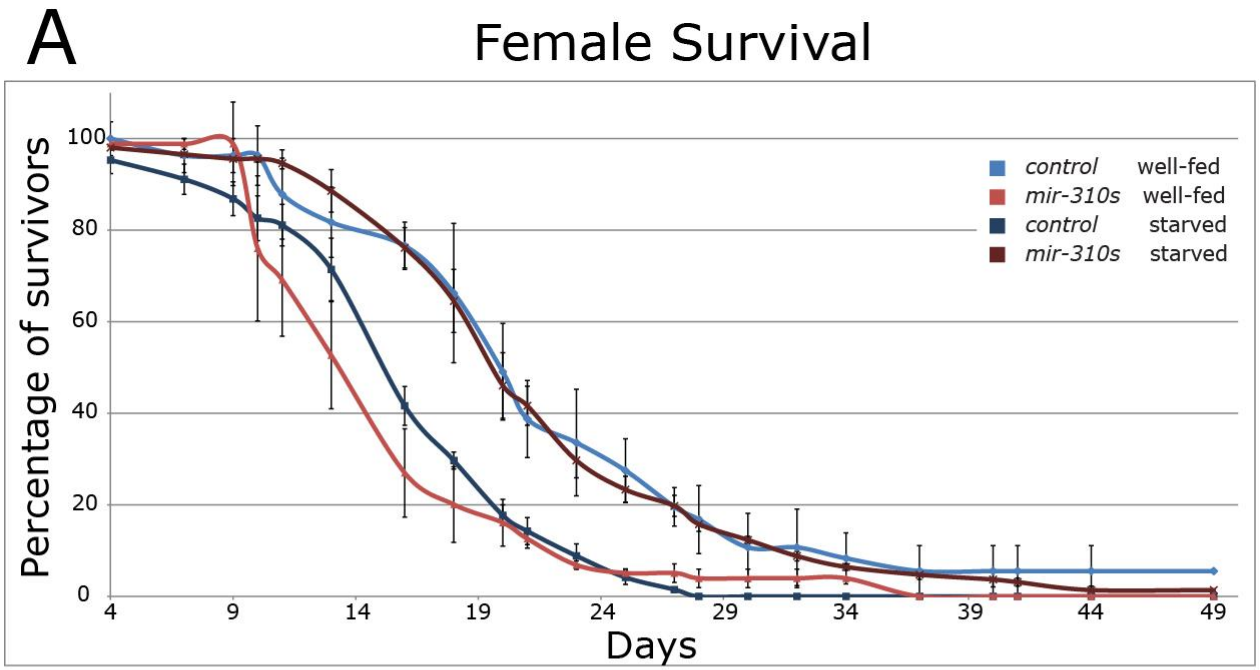

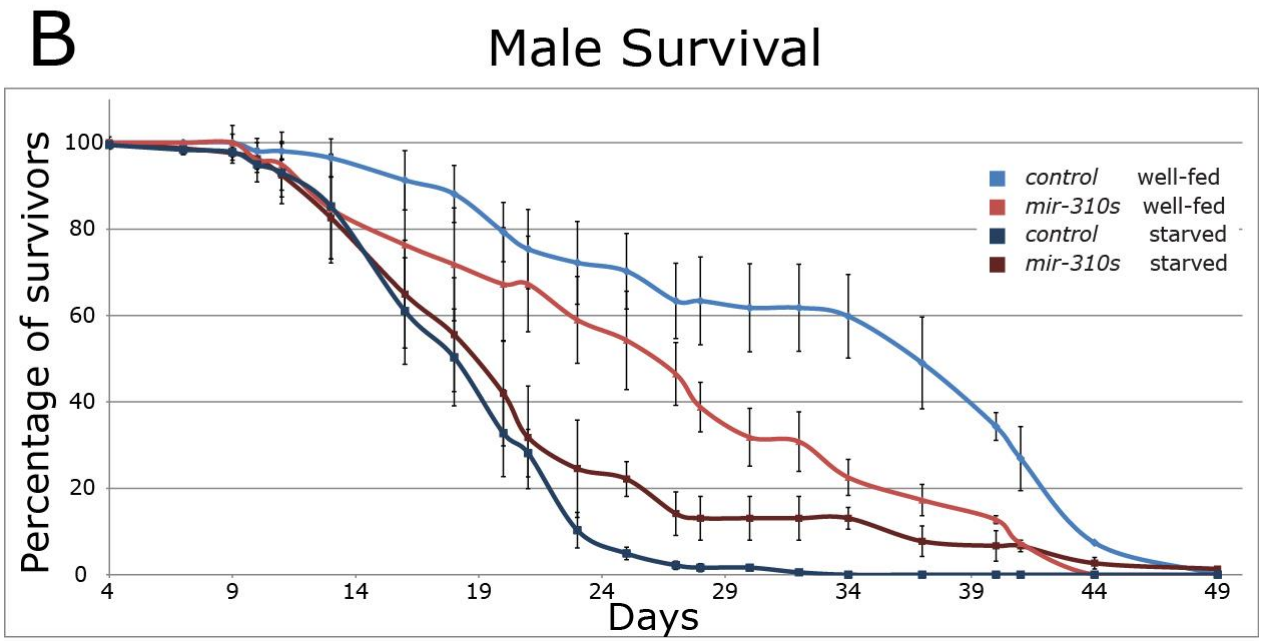

Figure 33. Adult lifespan is affected by *mir-310s* loss

(A) *mir-310s* deficiency results in shorter lifespan in female flies under well-fed conditions. However, *mir-310s* mutant females survive the starvation conditions longer than *controls.*

(B) *mir-310s* deficiency causes shorter male life span in well-fed and starvation conditions.

Supplementary Tables

Table 4. Genes with deregulated protein expression in *mir-310s* mutants identified via SILAC labeling

CG numbers	Gene names
CG17870	14-3-3zeta
CG8431	Aats-cys
CG5394	Aats-glupro
CG11198	ACC
CG10067	Act57B
CG7478	Act79B
CG18290	Act87E
CG5178	Act88F
CG9127	ade2
CG31628	ade3
CG3989	ade5
CG3481	Adh
CG6612	Adk3
CG3752	Aldh
CG1977	alpha-Spec
CG18212	alt
CG1462	Aph-4
CG15828	Apoltp
CG5711	Arr1
CG5670	Atpalpha
CG7610	ATPsyn-gamma
CG32234	axo
CG11785	bai
CG5870	beta-Spec
CG16884	BG:DS00180.3
CG7088	bnb
CG6815	bor
CG10302	bsf
CG9242	bur
CG3725	Ca-P60A, CG3725
CG6702	Cbp53E
CG6022	Cchl
CG9012	Chc
CG1744	chp
CG2028	CkIalpha
CG3244	Clect27
CG1618	comt
CG11949	cora
CG12045	Cpr100A
CG9079	Cpr47Ea
CG8505	Cpr49Ae
CG8511	Cpr49Ag
CG10112	Cpr51A
CG1919	Cpr62Bc
CG4784	Cpr72Ec
CG31150	crossveinless d
CG3050	Cyp6d5
CG8790	Dic1
CG5170	Dp1
CG4584	dUTPase
CG3747	Eaat1
CG1873	Ef1alpha100E
CG3835	EG:87B1.3
CG3699	EG:BACR7A4.14
CG9805	eIF3-S10
CG9677	eIF3-S6
CG4954	eIF3-S8
CG6917	Est-6
CG7400	Fatp
CG6544	fau
CG4609	fax
CG31692	fbp
CG3763	Fbp2
CG2216	Fer1HCH
CG7445	fln
CG2637	Fs(2)Ket
CG9092	Gal

Appendix

CG9232	Galt
CG10287	Gasp
CG1106	Gel
CG9206	Gl
CG9480	Glycogenin
CG8256	Gpo-1
CG4181	GstD2
CG11512	GstD4
CG17530	GstE6
CG8938	GstS1
CG8094	Hex-C
His2B	His2B
His4	His4
CG3949	hoip
CG4463	Hsp23
CG4183	Hsp26
CG4466	Hsp27
CG4475	Idgf2
CG10978	jagn
CG9423	Kap-alpha3
CG12008	kst
CG9432	l(2)01289
CG15081	l(2)03709
CG7532	l(2)34Fc
CG10691	l(2)37Cc
CG3082	l(2)k09913

CG10236	LanA
CG13393	lethal (2) k12914
CG4178	Lsp1beta
CG6806	Lsp2
CG8696	LvpH
CG30360	Mal-A6
CG4916	me31B
CG5889	Men-b
CG30021	metro
CG1742	Mgstl
CG17927	MHC
CG5596	Mlc1
CG2184	Mlc2
CG6214	MRP
CG32531	mRpS14
CG34073	mt:ATPase6
CG6851	Mtch
CG9193	mus209
CG5330	Nap1
CG12202	Nat1
CG2286	ND75
CG12908	Ndg
CG5125	ninaC
CG7917	Nlp
CG3620	norpA
CG1634	Nrg

CG43079	nrm
CG9261	Nrv2
CG8663	nrv3
CG15457	Obp19c
CG2297	Obp44a
CG11797	Obp56a
CG8462	Obp56e
CG18111	Obp99a
CG7592	Obp99b
CG17052	obst-A
CG8479	opa1-like
CG5119	pAbp
CG12151	Pdp
CG8844	Pdsw
CG42314	PMCA
CG6647	porin
CG9842	Pp2B-14D
CG33103	Ppn
CG5779	proPO-A1
CG12405	Prx2540-1
CG11765	Prx2540-2
CG4067	pug
CG18572	r
CG7576	Rab3
CG11064	Rfabg
CG9412	rin

Appendix

CG7014	RpS5b
CG3283	SdhB
CG6666	SdhC
CG6781	se
CG6782	sea, CG6782
CG9539	Sec61alpha
CG16944	sesB
CG18102	shi
CG18591	SmE
CG1982	Sodh-1
CG3926	Spat
CG4659	Srp54k
CG5064	Srp68
CG8396	Ssb-c31a
CG5474	SsRbeta
CG2194	su(r)
CG10622	Sucb
CG2827	Tal
CG9035	Tapdelta
CG4581	Thiolase
CG4898	Tm1
CG4843	Tm2
CG12408	TpnC4
CG2981	TpnC41C
CG7930	TpnC73F
CG10686	tral

CG33950	trol
CG9138	uif
CG15261	UK114
CG7107	up
CG3524	v(2)k05816
CG12403	Vha68-1
CG7178	wupA
CG2985	Yp1
CG2979	Yp2
CG11129	Yp3
CG14168	Zasp67
CG15792	zip
CG10031	CG10031
CG10340	CG10340
CG10527	CG10527
CG10638	CG10638
CG10924	CG10924
CG10932	CG10932
CG11089	CG11089
CG11594	CG11594
CG11899	CG11899
CG11920	CG11920
CG11999	CG11999
CG12079	CG12079
CG12163	CG12163
CG12171	CG12171

CG12203	CG12203
CG12896	CG12896
CG1444	CG1444
CG14661	CG14661
CG14715	CG14715
CG14757	CG14757
CG15369	CG15369
CG15881	CG15881
CG1648	CG1648
CG16758	CG16758
CG16985	CG16985
CG17029	CG17029
CG18547	CG18547
CG1885	CG1885
CG2082	CG2082
CG2233	CG2233
CG2233	CG2233
CG2310	CG2310
CG2852	CG2852
CG2943	CG2943
CG3011	CG3011
CG30222	CG30222
CG31195	CG31195
CG31198	CG31198
CG33138	CG33138
CG34026	CG34026

Appendix

CG34215	CG34215
CG3523	CG3523
CG3566	CG3566
CG3609	CG3609
CG3902	CG3902
CG3999	CG3999
CG4169	CG4169
CG4239	CG4239
CG4729	CG4729
CG4769	CG4769
CG5177	CG5177
CG5590	CG5590
CG31233	CG5839
CG5885	CG5885
CG5945	CG5945
CG5958	CG5958
CG6084	CG6084

CG6287	CG6287
CG6370	CG6370
CG6455	CG6455
CG6512	CG6512
CG6776	CG6776
CG6878	CG6878
CG6950	CG6950
CG7322	CG7322
CG7580	CG7580
CG7637	CG7637
CG7646	CG7646
CG8036	CG8036
CG8108	CG8108
CG8132	CG8132
CG8503	CG8503
CG8628	CG8628
CG8778	CG8778

CG8858	CG8858
CG9090	CG9090
CG9119	CG9119
CG9297	CG9297
CG9331	CG9331
CG9577	CG9577
CG9674	CG9674
CG9897	CG9897
CG9914	CG9914

For full list of identified proteins see supplementary spreadsheets in the digital appendix (Çiçek et al., 2016).

Table 5. Relative transcript levels of the starvation-sensitive genes due to *mir-310s* loss and/or nutritional deprivation

Genotype/ Condition	Target Gene	C_T AVE±SEM[b]	ΔC_T AVE±SEM[b]	$\Delta\Delta C_T$ AVE±SEM[b]	Relative mRNA level[a,c] AVE± SEM[b]	Log_{10} Relative mRNA level AVE± SEM[b]
Plate 1						
control well-fed	*Act88F*	2.76E+01 ±5.57E-02	9.47 ±6.27E-02	3.18E-07 ±5.57E-02	1.00 ±3.80E-02	-9.57E-08 ±1.68E-02
control starved		2.16E+01 ±1.79E-02	3.58 ±2.69E-02	-5.88 ±1.79E-02	5.90E+01 ±7.30E-01 $p^{control\ well\text{-}fed}$=1.52E-07	1.77 ±5.38E-03
mir-310s well-fed		2.50E+01 ±3.11E-02	6.45 ±4.29E-02	-3.02 ±3.11E-02	8.09 ±1.73E-01 $p^{control\ well\text{-}fed}$=2.30E-06	9.08E-01 ±9.37E-03
mir-310s starved		2.40E+01 ±9.20E-03	5.79 ±1.19E-02	-3.68 ±9.20E-03	1.28E+01 ±8.18E-02 $p^{control\ well\text{-}fed}$=2.05E-08	1.11 ±2.77E-03
control well-fed	*ade2*	2.29E+01 ±3.16E-02	4.70 ±4.28E-02	1.59E-07 ±3.16E-02	1.00 ±2.18E-02	-4.78E-08 ±9.52E-03
control starved		2.32E+01 ±4.70E-02	5.17 ±5.12E-02	4.65E-01 ±4.70E-02	7.25E-01 ±2.35E-02 $p^{control\ well\text{-}fed}$=1.01E-03	-1.40E-01 ±1.42E-02
mir-310s well-fed		2.19E+01 ±2.31E-02	3.32 ±3.75E-02	-1.38 ±2.31E-02	2.61 ±4.15E-02 $p^{control\ well\text{-}fed}$=4.30E-06	4.16E-01 ±6.95E-03
mir-310s starved		2.25E+01 ±1.49E-02	4.36 ±1.67E-02	-3.45E-01 ±1.49E-02	1.27 ±1.32E-02 $p^{control\ well\text{-}fed}$=4.48E-04	1.04E-01 ±4.49E-03
control well-fed	*ade3*	2.34E+01 ±1.77E-02	5.21 ±3.38E-02	-1.59E-07 ±1.77E-02	1.00 ±1.22E-02	4.78E-08 ±5.33E-03
control starved		2.49E+01 ±2.39E-02	6.91 ±3.13E-02	1.70 ±2.39E-02	3.09E-01 ±5.09E-03 $p^{control\ well\text{-}fed}$=8.01E-07	-5.11E-01 ±7.19E-03
mir-310s well-fed		2.27E+01 ±1.78E-02	4.15 ±3.45E-02	-1.06 ±1.78E-02	2.08 ±2.56E-02 $p^{control\ well\text{-}fed}$=2.82E-06	3.18E-01 ±5.36E-03
mir-310s starved		2.39E+01 ±2.81E-02	5.73 ±2.91E-02	5.16E-01 ±2.81E-02	6.99E-01 ±1.37E-02 $p^{control\ well\text{-}fed}$=8.16E-05	-1.55E-01 ±8.46E-03
control well-fed	*Arr1*	2.30E+01 ±9.35E-03	4.80 ±3.03E-02	0.00 ±9.35E-03	1.00 ±6.49E-03	0.00 ±2.82E-03
control starved		2.03E+01 ±4.21E-02	2.27 ±4.67E-02	-1.83 ±7.03E-01	3.56 ±1.49 $p^{control\ well\text{-}fed}$=4.02E-05	5.52E-01 ±1.27E-02
mir-310s well-fed		2.28E+01 ±1.09E-01	4.27 ±1.13E-01	-9.41E-01 ±5.17E-01	1.92 ±8.63E-01 $p^{control\ well\text{-}fed}$=2.35E-01	2.83E-01 ±1.56E-01
mir-310s starved		2.14E+01 ±3.34E-02	3.19 ±3.43E-02	-8.18E-01 ±8.12E-01	1.76 ±8.43E-01 $p^{control\ well\text{-}fed}$=2.11E-01	2.46E-01 ±2.44E-01
control	*CG3699*	2.39E+01	5.72	-1.59E-07	1.00	4.78E-08

well-fed		±5.05E-02	±5.81E-02	±5.05E-02	±3.55E-02	±1.52E-02
control starved		2.53E+01 ±2.82E-02	7.28 ±3.47E-02	1.56 ±2.82E-02	3.38E-01 ±6.55E-03 $p^{control\ well\text{-}fed}$=5.16E-05	-4.71E-01 ±8.49E-03
mir-310s well-fed		2.50E+01 ±7.56E-03	6.43 ±3.05E-02	7.14E-01 ±7.56E-03	6.09E-01 ±3.19E-03 $p^{control\ well\text{-}fed}$=3.88E-04	-2.15E-01 ±2.28E-03
mir-310s starved		2.52E+01 ±7.45E-03	7.03 ±1.06E-02	1.31 ±7.45E-03	4.03E-01 ±2.08E-03 $p^{control\ well\text{-}fed}$=7.28E-05	-3.95E-01 ±2.24E-03
control well-fed	*CG3902*	2.29E+01 ±1.99E-03	4.78 ±2.89E-02	1.59E-07 ±1.99E-03	1.00 ±1.38E-03	-4.78E-08 ±5.99E-04
control starved		2.43E+01 ±2.56E-02	6.32 ±3.26E-02	1.54 ±2.56E-02	3.44E-01 ±6.17E-03 $p^{control\ well\text{-}fed}$=5.18E-08	-4.63E-01 ±7.72E-03
mir-310s well-fed		2.26E+01 ±1.72E-02	4.04 ±3.41E-02	-7.34E-01 ±1.72E-02	1.66 ±1.98E-02 $p^{control\ well\text{-}fed}$=4.79E-06	2.21E-01 ±5.16E-03
mir-310s starved		2.33E+01 ±1.23E-02	5.18 ±1.45E-02	3.97E-01 ±1.23E-02	7.60E-01 ±6.46E-03 $p^{control\ well\text{-}fed}$=3.42E-06	-1.19E-01 ±3.71E-03
control well-fed	*Rpl32*	1.82E+01 ±2.88E-02	0.00 ±2.88E-02			
control starved		1.80E+01 ±2.02E-02	6.36E-07 ±2.02E-02			
mir-310s well-fed		1.86E+01 ±2.95E-02	1.91E-06 ±2.95E-02			
mir-310s starved		1.82E+01 ±7.58E-03	6.36E-07 ±7.58E-03			
No Reverse Transcriptase						
control well-fed	*Rpl32*	3.34E+01 ±2.44E-01	1.53E+01 ±2.44E-01	1.53E+01 ±2.44E-01	2.53E-05 ±4.68E-06	-4.60 ±7.35E-02
control starved		3.30E+01 ±2.87E-01	1.50E+01 ±2.87E-01	1.50E+01 ±2.87E-01	3.06E-05 ±5.89E-06	-4.51 ±8.65E-02
mir-310s well-fed		3.28E+01 ±1.09E-01	1.43E+01 ±1.09E-01	1.43E+01 ±1.09E-01	5.06E-05 ±3.98E-06	-4.30 ±3.29E-02
mir-310s starved		3.37E+01 ±1.36E-01	1.56E+01 ±1.36E-01	1.56E+01 ±1.36E-01	2.08E-05 ±1.95E-06	-4.68 4.10E-02
Plate 2						
control well-fed	*CG3999*	2.69E+01 ±1.07E-02	9.08 ±2.33E-02	-6.36E-07 ±1.07E-02	1.00 ±7.44E-03	1.91E-07 ±3.22E-03
control starved		2.85E+01 ±2.78E-02	1.08E+01 ±2.98E-02	1.72 ±2.78E-02	3.04E-01 ±5.90E-03 $p^{control\ well\text{-}fed}$=2.08E-07	-5.17E-01 ±8.36E-03
mir-310s well-fed		2.68E+01 ±3.90E-02	8.55 ±4.82E-02	-5.30E-01 ±3.90E-02	1.44 ±3.95E-02 $p^{control\ well\text{-}fed}$=3.79E-04	1.60E-01 ±1.17E-02
mir-310s starved		2.76E+01 ±4.55E-02	9.69 ±4.81E-02	6.09E-01 ±4.55E-02	6.56E-01 ±2.10E-02 $p^{control\ well\text{-}fed}$=1.03E-04	-1.83E-01 ±1.37E-02
control well-fed	*CG9914*	3.08E+01 ±4.14E-02	1.30E+01 ±4.63E-02	-9.54E-07 ±4.14E-02	1.00 ±2.83E-02	2.87E-07 ±1.25E-02

control starved		3.19E+01 ±2.46E-02	1.42E+01 ±2.69E-02	1.20 ±2.46E-02	4.34E-01 ±7.41E-03 $p^{control\ well\text{-}fed}$=4.19E-05	-3.62E-01 ±7.42E-03
mir-310s well-fed		3.08E+01 ±2.57E-02	1.25E+01 ±3.83E-02	-4.46E-01 ±2.57E-02	1.36 ±2.44E-02 $p^{control\ well\text{-}fed}$=6.35E-04	1.34E-01 ±7.74E-03
mir-310s starved		3.06E+01 ±5.07E-02	1.27E+01 ±5.30E-02	-2.91E-01 ±5.07E-02	1.22 ±4.31E-02 $p^{control\ well\text{-}fed}$=1.22E-02	8.76E-02 ±1.53E-02
control well-fed	*CG11089*	2.22E+01 ±2.57E-02	4.41 ±3.30E-02	-7.95E-07 ±2.57E-02	1.00 ±1.80E-02	2.39E-07 ±7.73E-03
control starved		2.30E+01 ±1.08E-02	5.33 ±1.54E-02	9.29E-01 ±1.08E-02	5.25E-01 ±3.96E-03 $p^{control\ well\text{-}fed}$=1.33E-05	-2.80E-01 ±3.27E-03
mir-310s well-fed		2.15E+01 ±9.71E-03	3.30 ±3.00E-02	-1.10 ±9.71E-03	2.15 ±1.44E-02 $p^{control\ well\text{-}fed}$=9.64E-07	3.32E-01 ±2.92E-03
mir-310s starved		2.30E+01 ±1.41E-02	5.10 ±2.10E-02	6.99E-01 ±1.41E-02	6.16E-01 ±6.07E-03 $p^{control\ well\text{-}fed}$=3.49E-05	-2.10E-01 ±4.26E-03
control well-fed	*CG15369*	3.29E+01 ±8.65E-03	1.51E+01 ±2.24E-02	-3.18E-07 ±8.65E-03	1.00 ±5.97E-03	9.57E-08 ±2.60E-03
control starved		3.17E+01 ±1.71E-01	1.40E+01 ±1.72E-01	-1.12 ±1.71E-01	2.18 ±2.56E-01 $p^{control\ well\text{-}fed}$=9.14E-03	3.38E-01 ±5.15E-02
mir-310s well-fed		3.29E+01 ±8.31E-02	1.47E+01 ±8.78E-02	-4.16E-01 ±8.31E-02	1.33 ±7.67E-02 $p^{control\ well\text{-}fed}$=1.17E-02	1.25E-01 ±2.50E-02
mir-310s starved		3.11E+01 ±8.40E-02	1.32E+01 ±8.54E-02	-1.86 ±8.40E-02	3.64 ±2.06E-01 $p^{control\ well\text{-}fed}$=2.12E-04	5.61E-01 ±2.53E-02
control well-fed	*CG16884*	3.60E+01 ±1.55E-01	1.82E+01 ±1.57E-01	0.00 ±1.55E-01	1.00 ±1.03E-01	0.00 ±4.68E-02
control starved		3.48E+01 ±6.19E-02	1.70E+01 ±6.29E-02	-1.13 ±6.19E-02	2.20 ±9.23E-02 $p^{control\ well\text{-}fed}$=1.02E-03	3.41E-01 ±1.86E-02
mir-310s well-fed		3.63E+01 ±5.23E-02	1.81E+01 ±5.95E-02	-8.92E-02 ±5.23E-02	1.06 ±3.80E-02 $p^{control\ well\text{-}fed}$=6.50E-01	2.69E-02 ±1.57E-02
mir-310s starved		3.49E+01 ±1.49E-01	1.71E+01 ±1.50E-01	-1.13 ±1.49E-01	2.18 ±2.27E-01 $p^{control\ well\text{-}fed}$=8.67E-03	3.39E-01 ±4.48E-02
control well-fed	*CG30360*	2.19E+01 ±1.06E-02	4.11 ±2.32E-02	-7.95E-07 ±1.06E-02	1.00 ±7.30E-03	2.39E-07 ±3.18E-03
control starved		2.30E+01 ±1.63E-02	5.32 ±1.96E-02	1.22 ±1.63E-02	4.30E-01 ±4.86E-03 $p^{control\ well\text{-}fed}$=3.35E-07	-3.67E-01 ±4.91E-03
mir-310s well-fed		2.27E+01 ±1.47E-02	4.50 ±3.19E-02	3.92E-01 ±1.47E-02	7.62E-01 ±7.78E-03 $p^{control\ well\text{-}fed}$=2.40E-05	-1.18E-01 ±4.41E-03
mir-310s starved		2.34E+01 ±2.02E-02	5.52 ±2.55E-02	1.41 ±2.02E-02	3.76E-01 ±5.23E-03 $p^{control\ well\text{-}fed}$=2.58E-07	-4.24E-01 ±6.08E-03

control well-fed	*Rpl32*	1.78E+01 ±2.07E-02	-6.36E-07 ±2.07E-02			
control starved		1.77E+01 ±1.09E-02	0.00 ±1.09E-02			
mir-310s well-fed		1.82E+01 ±2.84E-02	-1.27E-06 ±2.84E-02			
mir-310s starved		1.79E+01 ±1.55E-02	6.36E-07 ±1.55E-02			
No Reverse Transcriptase						
control well-fed	*Rpl32*	3.28E+01 ±1.19E-01	1.50E+01 ±1.19E-01	1.50E+01 ±1.19E-01	3.07E-05 ±2.64E-06	-4.51 ±3.59E-02
control starved		3.28E+01 ±1.03E-01	1.51E+01 ±1.03E-01	1.51E+01 ±1.03E-01	2.92E-05 ±2.16E-06	-4.53 ±3.10E-02
mir-310s well-fed		3.22E+01 ±9.10E-02	1.40E+01 ±9.10E-02	1.40E+01 ±9.10E-02	6.13E-05 ±3.82E-06	-4.21 ±2.74E-02
mir-310s starved		3.27E+01 ±2.33E-01	1.49E+01 ±2.33E-01	1.49E+01 ±2.33E-01	3.37E-05 ±5.94E-06	-4.47 ±7.00E-02
Plate 3						
control well-fed	*CG31233*	2.54E+01 ±1.38E-02	7.51 ±2.92E-02	0.00 ±1.38E-02	1.00 ±9.53E-03	0.00 ±4.14E-03
control starved		2.36E+01 ±1.64E-03	5.80 ±9.31E-03	-1.72 ±1.64E-03	3.29 ±3.73E-03 $p^{control\ well\text{-}fed}$=2.41E-09	5.17E-01 ±4.93E-04
mir-310s well-fed		2.59E+01 ±3.60E-02	7.76 ±1.04E-01	2.41E-01 ±3.60E-02	8.46E-01 ±2.13E-02 $p^{control\ well\text{-}fed}$=2.79E-03	-7.25E-02 ±1.09E-02
mir-310s starved		2.43E+01 ±1.91E-02	6.43 ±2.24E-02	-1.08 ±1.91E-02	2.12 ±2.82E-02 $p^{control\ well\text{-}fed}$=2.96E-06	3.26E-01 ±5.74E-03
control well-fed	*Cpr62Bc*	3.45E+01 ±7.64E-02	1.66E+01 ±8.06E-02	6.36E-07 ±7.64E-02	1.00 ±5.16E-02	-1.91E-07 ±2.30E-02
control starved		3.15E+01 ±3.45E-02	1.37E+01 ±3.57E-02	-2.93 ±3.45E-02	7.64 ±1.84E-01 $p^{control\ well\text{-}fed}$=4.10E-06	8.83E-01 ±1.04E-02
mir-310s well-fed		3.20E+01 ±5.19E-02	1.38E+01 ±1.11E-01	-2.79 ±5.19E-02	6.90 ±2.46E-01 $p^{control\ well\text{-}fed}$=1.94E-05	8.39E-01 ±1.56E-02
mir-310s starved		3.01E+01 ±1.61E-02	1.23E+01 ±2.00E-02	-4.31 ±1.61E-02	1.98E+01 ±2.22E-01 $p^{control\ well\text{-}fed}$=1.29E-07	1.30 ±4.84E-03
control well-fed	*Cpr72Ec*	3.25E+01 ±8.92E-02	1.46E+01 ±9.28E-02	-3.18E-07 ±8.92E-02	1.00 ±6.37E-02	9.57E-08 ±2.68E-02
control starved		3.29E+01 ±1.73E-02	1.51E+01 ±1.96E-02	5.13E-01 ±1.73E-02	7.01E-01 ±8.41E-03 $p^{control\ well\text{-}fed}$=9.22E-03	-1.54E-01 ±5.22E-03
mir-310s well-fed		2.80E+01 ±9.14E-03	9.84 ±9.80E-02	-4.76 ±9.14E-03	2.70E+01 ±1.71E-01 $p^{control\ well\text{-}fed}$=1.46E-08	1.43 ±2.75E-03
mir-310s starved		2.62E+01 ±3.01E-02	8.39 ±3.24E-02	-6.21 ±3.01E-02	7.40E+01 ±1.54 $p^{control\ well\text{-}fed}$=1.19E-06	1.87 ±9.07E-03
control well-fed	*Cpr100A*	3.18E+01 ±1.13E-01	1.39E+01 ±1.16E-01	0.00 ±1.13E-01	1.00 ±8.06E-02	0.00 ±3.41E-02

control starved		2.79E+01 ±1.96E-02	1.01E+01 ±2.17E-02	-3.78 ±1.96E-02	1.38E+01 ±1.89E-01 $p^{control\ well\text{-}fed}$=4.00E-07	1.14 ±5.91E-03
mir-310s well-fed		2.78E+01 ±4.13E-02	9.63 ±1.06E-01	-4.27 ±4.13E-02	1.93E+01 ±5.45E-01 $p^{control\ well\text{-}fed}$=4.90E-06	1.29 ±1.24E-02
mir-310s starved		2.84E+01 ±3.03E-02	1.06E+01 ±3.25E-02	-3.31 ±3.03E-02	9.93 ±2.10E-01 $p^{control\ well\text{-}fed}$=2.43E-06	9.97E-01 ±9.11E-03
control well-fed	*Gal*	2.76E+01 ±6.26E-02	9.77 ±6.77E-02	-3.18E-07 ±6.26E-02	1.00 ±4.26E-02	9.57E-08 ±1.89E-02
control starved		2.79E+01 ±4.60E-02	1.01E+01 ±4.69E-02	3.15E-01 ±4.60E-02	8.04E-01 ±2.55E-02 $p^{control\ well\text{-}fed}$=1.65E-02	-9.50E-02 ±1.38E-02
mir-310s well-fed		2.86E+01 ±1.76E-02	1.04E+01 ±9.91E-02	6.79E-01 ±1.76E-02	6.25E-01 ±7.62E-03 $p^{control\ well\text{-}fed}$=9.55E-04	-2.04E-01 ±5.31E-03
mir-310s starved		2.80E+01 ±1.89E-02	1.01E+01 ±2.23E-02	3.70E-01 ±1.89E-02	7.74E-01 ±1.02E-02 $p^{control\ well\text{-}fed}$=6.50E-03	-1.11E-01 ±5.68E-03
control well-fed	*Gasp*	2.99E+01 ±4.09E-02	1.20E+01 ±4.83E-02	3.18E-07 ±4.09E-02	1.00 ±2.79E-02	-9.57E-08 ±1.23E-02
control starved		2.61E+01 ±1.95E-02	8.34 ±2.16E-02	-3.67 ±1.95E-02	1.27E+01 ±1.73E-01 $p^{control\ well\text{-}fed}$=2.97E-07	1.10 ±5.88E-03
mir-310s well-fed		2.90E+01 ±2.72E-02	1.08E+01 ±1.01E-01	-1.16 ±2.72E-02	2.23 ±4.20E-02 $p^{control\ well\text{-}fed}$=1.66E-05	3.49E-01 ±8.20E-03
mir-310s starved		2.76E+01 ±1.90E-02	9.77 ±2.24E-02	-2.24 ±1.90E-02	4.72 ±6.19E-02 $p^{control\ well\text{-}fed}$=6.65E-07	6.74E-01 ±5.72E-03
control well-fed	*Rpl32*	1.79E+01 ±2.57E-02	0.00 ±2.57E-02			
control starved		1.78E+01 ±9.16E-03	6.36E-07 ±9.16E-03			
mir-310s well-fed		1.81E+01 ±9.76E-02	0.00 ±9.76E-02			
mir-310s starved		1.78E+01 ±1.18E-02	0.00 ±1.18E-02			
No Reverse Transcriptase						
control well-fed	*Rpl32*	3.30E+01 ±6.88E-02	1.51E+01 ±6.88E-02	1.51E+01 ±6.88E-02	2.81E-05 ±1.34E-06	-4.55 2.07E-02
control starved		3.29E+01 ±1.01E-01	1.51E+01 ±1.01E-01	1.51E+01 ±1.01E-01	2.90E-05 ±2.03E-06	-4.54 3.04E-02
mir-310s well-fed		3.23E+01 ±2.68E-01	1.42E+01 ±2.68E-01	1.42E+01 ±2.68E-01	5.32E-05 ±9.93E-06	-4.27 8.06E-02
mir-310s starved		3.30E+01 ±9.89E-03	1.52E+01 ±9.89E-03	1.52E+01 ±9.89E-03	2.67E-05 ±1.83E-07	-4.57 2.98E-03
Plate 4						
control well-fed	*GstD4*	2.55E+01 ±3.46E-02	8.26 ±3.85E-02	-3.18E-07 ±3.46E-02	1.00 ±2.42E-02	9.57E-08 ±1.04E-02
control starved		2.56E+01 ±2.51E-02	8.55 ±2.63E-02	2.91E-01 ±2.51E-02	8.17E-01 ±1.43E-02	-8.77E-02 ±7.57E-03

					$p^{control\ well\text{-}fed}$=2.85E-03	
mir-310s well-fed		2.54E+01 ±1.23E-02	7.72 ±3.97E-02	-5.38E-01 ±1.23E-02	1.45 ±1.24E-02 $p^{control\ well\text{-}fed}$=7.65E-05	1.62E-01 ±3.71E-03
mir-310s starved		2.59E+01 ±1.08E-02	8.72 ±1.58E-02	4.55E-01 ±1.08E-02	7.30E-01 ±5.46E-03 $p^{control\ well\text{-}fed}$=3.97E-04	-1.37E-01 ±3.26E-03
control well-fed	*Lsp1beta*	2.69E+01 ±3.96E-02	9.65 ±4.31E-02	-6.36E-07 ±3.96E-02	1.00 ±2.73E-02	1.91E-07 ±1.19E-02
control starved		3.17E+01 ±9.43E-03	1.47E+01 ±1.23E-02	5.08 ±9.43E-03	2.95E-02 ±1.93E-04 $p^{control\ well\text{-}fed}$=3.72E-06	-1.53 ±2.84E-03
mir-310s well-fed		2.39E+01 ±2.93E-02	6.26 ±4.78E-02	-3.39 ±2.93E-02	1.05E+01 ±2.12E-01 $p^{control\ well\text{-}fed}$=1.54E-06	1.02 ±8.82E-03
mir-310s starved		2.40E+01 ±2.88E-02	6.85 ±3.11E-02	-2.80 ±2.88E-02	6.98 ±1.38E-01 $p^{control\ well\text{-}fed}$=1.83E-06	8.44E-01 ±8.67E-03
control well-fed	*Lsp2*	1.98E+01 ±1.86E-02	2.57 ±2.52E-02	-6.36E-07 ±1.86E-02	1.00 ±1.28E-02	1.91E-07 ±5.61E-03
control starved		2.87E+01 ±4.05E-02	1.17E+01 ±4.12E-02	9.17 ±4.05E-02	1.74E-03 ±4.95E-05 $p^{control\ well\text{-}fed}$=1.64E-07	-2.76 ±1.22E-02
mir-310s well-fed		2.19E+01 ±2.81E-03	4.30 ±3.78E-02	1.72 ±2.81E-03	3.03E-01 ±5.89E-04 $p^{control\ well\text{-}fed}$=6.91E-07	-5.19E-01 ±8.45E-04
mir-310s starved		2.34E+01 ±2.49E-02	6.17 ±2.74E-02	3.59 ±2.49E-02	8.28E-02 ±1.44E-03 $p^{control\ well\text{-}fed}$=2.36E-07	-1.08 ±7.49E-03
control well-fed	*LvpH*	2.17E+01 ±4.82E-02	4.53 ±5.10E-02	-4.77E-07 ±4.82E-02	1.00 ±3.29E-02	1.44E-07 ±1.45E-02
control starved		2.18E+01 ±2.57E-02	4.76 ±2.69E-02	2.35E-01 ±2.57E-02	8.50E-01 ±1.52E-02 $p^{control\ well\text{-}fed}$=1.41E-02	-7.06E-02 ±7.74E-03
mir-310s well-fed		2.23E+01 ±2.06E-02	4.63 ±4.30E-02	1.01E-01 ±2.06E-02	9.32E-01 ±1.34E-02 $p^{control\ well\text{-}fed}$=1.26E-01	-3.04E-02 ±6.21E-03
mir-310s starved		2.29E+01 ±2.60E-03	5.74 ±1.19E-02	1.21 ±2.60E-03	4.32E-01 ±7.80E-04 $p^{control\ well\text{-}fed}$=6.58E-05	-3.64E-01 ±7.84E-04
control well-fed	*Mgstl*	2.29E+01 ±1.60E-02	5.71 ±2.33E-02	-4.77E-07 ±1.60E-02	1.00 ±1.11E-02	1.44E-07 ±4.82E-03
control starved		2.34E+01 ±1.61E-02	6.38 ±1.79E-02	6.76E-01 ±1.61E-02	6.26E-01 ±6.96E-03 $p^{control\ well\text{-}fed}$=8.94E-06	-2.04E-01 ±4.83E-03
mir-310s well-fed		2.24E+01 ±5.28E-03	4.78 ±3.81E-02	-9.32E-01 ±5.28E-03	1.91 ±6.99E-03 $p^{control\ well\text{-}fed}$=2.62E-07	2.80E-01 ±1.59E-03
mir-310s starved		2.24E+01 ±1.72E-01	5.22 ±1.72E-01	-4.89E-01 ±1.72E-01	1.40 ±1.76E-01 $p^{control\ well\text{-}fed}$=7.43E-02	1.47E-01 ±5.17E-02
control well-fed	*mus209*	2.19E+01 ±1.36E-02	4.70 ±2.17E-02	-6.36E-07 ±1.36E-02	1.00 ±9.37E-03	1.91E-07 ±4.08E-03

control starved		2.44E+01 ±9.25E-03	7.39 ±1.21E-02	2.69 ±9.25E-03	1.55E-01 ±9.93E-04 $p^{control\ well\text{-}fed}$=9.25E-08	-8.10E-01 ±2.78E-03
mir-310s well-fed		2.19E+01 ±5.19E-03	4.24 ±3.81E-02	-4.61E-01 ±5.19E-03	1.38 ±4.96E-03 $p^{control\ well\text{-}fed}$=3.74E-06	1.39E-01 ±1.56E-03
mir-310s starved		2.34E+01 ±3.90E-03	6.20 ±1.22E-02	1.51 ±3.90E-03	3.52E-01 ±9.51E-04 $p^{control\ well\text{-}fed}$=2.67E-07	-4.54E-01 ±1.18E-03
control well-fed	*Rpl32*	1.72E+01 ±1.69E-02	-6.36E-07 ±1.69E-02			
control starved		1.70E+01 ±7.88E-03	6.36E-07 ±7.88E-03			
mir-310s well-fed		1.76E+01 ±3.77E-02	0.00 ±3.77E-02			
mir-310s starved		1.72E+01 ±1.16E-02	1.27E-06 ±1.16E-02			
No Reverse Transcriptase						
control well-fed	*Rpl32*	3.19+E01	1.47E+01	1.47E+01	3.70E-05	-4.43
control starved		3.30E+01	1.33E+01	1.33E+01	9.94E-05	-4.00
mir-310s well-fed		3.03E+01	1.27E+01	1.27E+01	1.50E-04	-3.82
mir-310s starved		3.05E+01	1.33E+01	1.33E+01	9.94E-05	-4.00
Plate 5						
control well-fed	*Obp44a*	2.69E+01 ±3.37E-02	8.55 ±3.55E-02	-3.18E-07 ±3.37E-02	1.00 ±2.36E-02	9.57E-08 ±1.01E-02
control starved		2.67E+01 ±1.68E-02	8.41 ±5.16E-02	-1.33E-01 ±1.68E-02	1.10 ±1.29E-02 $p^{control\ well\text{-}fed}$=2.30E-02	4.01E-02 ±5.07E-03
mir-310s well-fed		2.68E+01 ±3.72E-02	7.95 ±5.92E-02	-6.01E-01 ±3.72E-02	1.52 ±3.89E-02 $p^{control\ well\text{-}fed}$=3.42E-04	1.81E-01 ±1.12E-02
mir-310s starved		2.66E+01 ±1.28E-02	8.12 ±3.78E-02	-4.28E-01 ±1.28E-02	1.35 ±1.19E-02 $p^{control\ well\text{-}fed}$=1.98E-04	1.29E-01 ±3.84E-03
control well-fed	*Obp56a*	2.57E+01 ±2.06E-02	7.32 ±2.34E-02	-1.59E-07 ±2.06E-02	1.00 ±1.43E-02	4.78E-08 ±6.20E-03
control starved		2.49E+01 ±7.92E-03	6.70 ±4.94E-02	-6.17E-01 ±7.92E-03	1.53 ±8.39E-03 $p^{control\ well\text{-}fed}$=5.50E-06	1.86E-01 ±2.38E-03
mir-310s well-fed		2.79E+01 ±2.00E-02	9.05 ±5.02E-02	1.73 ±2.00E-02	3.02E-01 ±4.16E-03 $p^{control\ well\text{-}fed}$=1.22E-06	-5.21E-01 ±6.01E-03
mir-310s starved		2.75E+01 ±5.34E-02	9.00 ±6.41E-02	1.68 ±5.34E-02	3.11E-01 ±1.17E-02 $p^{control\ well\text{-}fed}$=3.07E-06	-5.07E-01 ±1.61E-02
control well-fed	*Obp56e*	2.46E+01 ±3.45E-02	6.25 ±3.63E-02	0.00 ±3.45E-02	1.00 ±2.41E-02	0.00 ±1.04E-02
control starved		2.56E+01 ±1.69E-02	7.36 ±5.16E-02	1.11 ±1.69E-02	4.64E-01 ±5.41E-03	-3.34E-01 ±5.10E-03

					$p^{control\ well\text{-}fed}$=2.63E-05	
mir-310s well-fed		2.76E+01 ±1.19E-02	8.76 ±4.76E-02	2.51 ±1.19E-02	1.76E-01 ±1.45E-03 $p^{control\ well\text{-}fed}$=4.35E-06	-7.55E-01 ±3.59E-03
mir-310s starved		2.69E+01 ±2.14E-02	8.36 ±4.15E-02	2.11 ±2.14E-02	2.32E-01 ±3.47E-03 $p^{control\ well\text{-}fed}$=5.96E-06	-6.35E-01 ±6.45E-03
control well-fed	*Obp99b*	2.56E+01 ±2.63E-02	7.30 ±2.85E-02	1.59E-07 ±2.63E-02	1.00 ±1.83E-02	-4.78E-08 ±7.90E-03
control starved		2.93E+01 ±5.85E-02	1.10E+01 ±7.62E-02	3.75 ±5.85E-02	7.44E-02 ±3.05E-03 $p^{control\ well\text{-}fed}$=9.65E-07	-1.13 ±1.76E-02
mir-310s well-fed		2.17E+01 ±5.31E-03	2.88 ±4.64E-02	-4.42 ±5.31E-03	2.14E+01 ±7.86E-02 $p^{control\ well\text{-}fed}$=1.48E-09	1.33 ±1.60E-03
mir-310s starved		2.39E+01 ±6.43E-03	5.36 ±3.61E-02	-1.94 ±6.43E-03	3.83 ±1.71E-02 $p^{control\ well\text{-}fed}$=3.68E-08	5.83E-01 ±1.94E-03
control well-fed	*Obst-A*	2.99E+01 ±3.09E-02	1.15E+01 ±3.29E-02	-3.18E-07 ±3.09E-02	1.00 ±2.16E-02	9.57E-08 ±9.31E-03
control starved		2.86E+01 ±5.96E-02	1.04E+01 ±7.70E-02	-1.15 ±5.96E-02	2.21 ±8.97E-02 $p^{control\ well\text{-}fed}$=1.92E-04	3.45E-01 ±1.79E-02
mir-310s well-fed		2.88E+01 ±4.78E-02	9.92 ±6.64E-02	-1.62 ±4.78E-02	3.07 ±1.04E-01 $p^{control\ well\text{-}fed}$=3.97E-05	4.88E-01 ±1.44E-02
mir-310s starved		2.80E+01 ±2.56E-02	9.46 ±4.38E-02	-2.07 ±2.56E-02	4.20 ±7.39E-02 $p^{control\ well\text{-}fed}$=2.00E-06	6.24E-01 ±7.71E-03
control well-fed	*pro-PO-A1*	2.67E+01 ±3.29E-02	8.33 ±3.47E-02	3.18E-07 ±3.29E-02	1.00 ±2.26E-02	-9.57E-08 ±9.89E-03
control starved		2.67E+01 ±4.36E-02	8.46 ±6.54E-02	1.27E-01 ±4.36E-02	9.16E-01 ±2.75E-02 $p^{control\ well\text{-}fed}$=7.73E-02	-3.83E-02 ±1.31E-02
mir-310s well-fed		3.62E+01 ±2.55E-01	1.73E+01 ±2.59E-01	8.99 ±2.55E-01	1.96E-03 ±3.78E-04 $p^{control\ well\text{-}fed}$=1.56E-06	-2.71 ±7.68E-02
mir-310s starved		3.62E+01 ±5.30E-01	1.77E+01 ±5.31E-01	9.39 ±5.30E-01	1.50E-03 ±6.56E-04 $p^{control\ well\text{-}fed}$=1.56E-06	-2.83 ±1.59E-01
control well-fed	*Rpl32*	1.83E+01 ±1.11E-02	0.00 ±1.11E-02			
control starved		1.82E+01 ±4.88E-02	0.00 ±4.88E-02			
mir-310s well-fed		1.89E+01 ±4.61E-02	-6.36E-07 ±4.61E-02			
mir-310s starved		1.85E+01 ±3.56E-02	0.00 ±3.56E-02			
No Reverse Transcriptase						
control well-fed -RT	*Rpl32*	3.06E+01 ±1.02E-01	1.22E+01 ±1.02E-01	1.22E+01 ±1.02E-01	9.15E-05	-4.04
control starved -RT		3.08E+01 ±1.01E-01	1.27E+01 ±1.01E-01	1.27E+01 ±1.01E-01	1.05E-04	-3.98

mir-310s well-fed -RT		3.06E+01 ±1.08E-01	1.20E+01 ±1.08E-01	1.20E+01 ±1.08E-01	1.39E-04	-3.86
mir-310s starved -RT		2.99E+01 ±7.07E-01	1.17E+01 ±7.07E-01	1.17E+01 ±7.07E-01	9.03E-05	-4.04
Plate 6						
control well-fed	*Sucb*	2.38E+01 ±3.20E-02	5.40 ±4.19E-02	1.11E-06 ±3.20E-02	1.00 ±2.20E-02	-3.35E-07 ±9.62E-03
control starved		2.43E+01 ±2.38E-02	6.23 ±5.19E-02	8.30E-01 ±2.38E-02	5.62E-01 ±9.29E-03 $p^{control\ well\text{-}fed}$=5.23E-05	-2.50E-01 ±7.16E-03
mir-310s well-fed		2.39E+01 ±3.60E-02	5.24 ±6.33E-02	-1.59E-01 ±3.60E-02	1.12 ±2.80E-02 $p^{control\ well\text{-}fed}$=3.08E-02	4.78E-02 ±1.08E-02
mir-310s starved		2.43E+01 ±1.63E-02	5.99 ±4.23E-02	5.95E-01 ±1.63E-02	6.62E-01 ±7.46E-03 $p^{control\ well\text{-}fed}$=1.30E-04	-1.79E-01 ±4.90E-03
control well-fed	*Rpl32*	1.84E+01 ±2.71E-02	1.27E-06 ±2.71E-02			
control starved		1.81E+01 ±4.62E-02	-6.36E-07 ±4.62E-02			
mir-310s well-fed		1.86E+01 ±5.21E-02	6.36E-07 ±5.21E-02			
mir-310s starved		1.83E+01 ±3.91E-02	-6.36E-07 ±3.91E-02			
No Reverse Transcriptase						
control well-fed	*Rpl32*	3.06E+01 ±1.02E-01	1.22E+01 ±1.02E-01	1.22E+01 ±1.02E-01	2.11E-05 ±1.45E-05	-3.68 3.08E-02
control starved		3.08E+01 ±1.01E-01	1.27E+01 ±1.01E-01	1.27E+01 ±1.01E-01	1.51E-05 ±1.03E-05	-3.82 3.05E-02
mir-310s well-fed		3.06E+01 ±1.08E-01	1.20E+01 ±1.08E-01	1.20E+01 ±1.08E-01	2.45E-05 ±1.81E-05	-3.61 3.24E-02
mir-310s starved		2.99E+01 ±7.07E-01	1.17E+01 ±7.07E-01	1.17E+01 ±7.07E-01	3.05E-04 ±1.43E-04	-3.52 2.13E-01

[a] The mRNA levels were calculated using the formula $2^{-\Delta\Delta CT}$.

[b] Standard error of the mean (SEM) values are based on three replicates

[c] p values were calculated using two-tailed non-paired Student's t-test for significance testing.

(Çiçek et al., 2016)

Appendix

Table 6. *mir-310s* deficiency causes global phenotypes related to nutritional stress and epithelial defects in the ovary

Genotype/Condition Phenotype	*control* well-fed	*mir-310s* well-fed	*control* starved	*mir-310s* starved
Female Survival[a]: LD_{50}, days (AVE±SEM) n=number of females analyzed	20.44±1.68 n=35	13.28±1.64 n=63 $p^{control\ well\text{-}fed}$=0.038 $p^{control\ starved}$=0.29	15.39±0.58 n=72 $p^{control\ well\text{-}fed}$=0.047	19.82±0.89 n=207 $p^{control\ starved}$=0.01 $p^{mir\text{-}310s\ well\text{-}fed}$=0.02 $p^{control\ well\text{-}fed}$=0.76
Crop diameter[b]: (in mm) (AVE±SEM) n=number of crops analyzed	0.65±0.05 n=12	0.85±0.04 n=10 $p^{control\ well\text{-}fed}$=0.007	0.44±0.05 n=10	0.44±0.04 n=10 $p^{control\ starved}$=1,00
Fecundity[c]: Eggs laid per fly per day (AVE±SEM) n=number of females analyzed	16.48±1.76 n=49	6.03±0.4 n=50 p=0.004		
Lipid Accumulation: µg TAG equivalents per mg protein (AVE±SEM) n=number of females analyzed	3 days 386.77±35.68 n=30	3 days 210.67±28.57 n=20 $p^{control\ well\text{-}fed}$=0.008	10 days 582.07±217.43 n = 30 $p^{control\ well\text{-}fed}$=0.04	10 days 1581.0±202.03 n=30 $p^{control\ well\text{-}fed}$=0.0002 $p^{control\ starved}$=0.006
Follicular Epithelial Defects[d]: Fused Egg Chambers Frequency n=ovarioles analyzed	5% n=20	70% n=20		
Supernumerary / Multilayered Stalks Frequency n=ovarioles analyzed	25% n=20	95% n=19		
Defective/Multilayered Follicular Epithelium Frequency n=ovarioles analyzed	25% n=20	80% n=20		

[a] Three biological replicates were examined

[b] Maximum crop diameters are determined using bright field images and Adobe Photoshop Software.

[c] Female flies were set on apple juice/sugar/agar plates with a drop of fresh yeast paste for egg laying analysis.

Appendix

[d] Percentage of incidence of the listed phenotypes per ovariole is shown.

Two-tailed non-paired Student's t-test was used for p value determination.

(Çiçek et al., 2016)

Table 7. The *mir-310s* downregulate *Rab23, DHR96,* and *ttk in vitro*

3' UTR Reporter	*control* Plate 1 (*Rab23 and DHR96)*	*Rab23*	*DHR96*	*control* Plate 2 (*ttk)*	*ttk*
Luciferase Signal (*Renilla/Firefly*) AVE±SEM	9.92E-02 ±3.94E-03	3.98E-02 ±2.49E-03	6.42E-02 ±1.73E-03	1.29E-01 ±1.25E-02	7.74E-02 ±8.1E-03
Relative Luciferase Signal AVE±SEM	1.00 ±3.98E-02	4.01E-01 ±2.5E-02 p=9.11E-03	6.47E-01 ±1.75E-02 p=2.22E-02	1.00 ±9.73E-02	6.01E-01 ±6.29E-02 p=4.52E-02

Two biological replicates were performed for each gene in two plates. Control readings from respective plates served to normalize the luciferase signals.

Two-tailed non-paired Student's t-test was used to determine the p values.

(Çiçek et al., 2016)

Table 8. Relative transcript levels of putative *mir-310s* targets are determined using qRT-PCR

Genotype/ Condition	C_T *Rab23* AVE±SEM[b]	C_T *Rpl32* AVE±SEM[b]	Δ C_T AVE±SEM[b]	ΔΔ C_T AVE±SEM[b]	Relative ***Rab23*** mRNA level[a,c] AVE± SEM[b]
control well-fed	2.42E+01 ±2.7E-01	1.85E+01 ±1.97E-01	5.71 ±8.18E-02	0.00 ±8.18E-02	1.00 ±5.18E-02
mir-310s well-fed	2.41E+01 ±1.04E-01	1.9E+01 ±5.34E-02	5.06 ±6.22E-02	-6.48E-01 ±7.23E-02	1.57 ±7.08E-02 $p^{control\ well\text{-}fed}$ =2.9E-03
control starved	2.8E+01 ±3.1E-01	1.86E+01 ±1.21E-01	9.32 ±1.79E-01	3.61 ±2.67E-01	8.17E-02 ±1.4E-02
mir-310s starved	2.59E+01 ±1.98E-01	1.87E+01 ±9.29E-02	7.2 ±1.15E-01	1.49 ±1.52E-01	3.56E-01 ±3.47E-02 $p^{control\ starved}$ =5.64E-04
	C_T *DHR96* AVE±SEM	C_T *Rpl32* AVE±SEM	Δ C_T AVE±SEM	ΔΔ C_T AVE±SEM	Relative ***DHR96*** mRNA level AVE± SEM
control well-fed	2.66E+01 ±1.87E-01	1.83E+01 ±1.34E-01	8.24 ±1.21E-01	0.00 ±6.43E-02	1.00 ±3.23E-02
mir-310s well-fed	2.66E+01 ±1.52E-01	1.90E+01 ±5.72E-02	7.61 ±8.62E-02	-6.35E-01 ±1.11E-01	1.55 ±9.1E-02 $p^{control\ well\text{-}fed}$ =5.52E-03
control starved	2.85E+01 ±1.14E+01	1.86E+01 ±1.14E-01	9.93 ±9.17E-02	1.69 ±9.36E-02	3.12E-01 ±1.43E-02
mir-310s starved	2.75E+01 ±1.1E-01	1.86E+01 ±5.7E-02	8.87 ±5.79E-02	6.28E-01 ±6.06E-02	6.47E-01 ±1.53E-02 $p^{control\ starved}$ =1.3E-04
	C_T *ttk* AVE±SEM	C_T *Rpl32* AVE±SEM	Δ C_T AVE±SEM	ΔΔ C_T AVE±SEM	Relative ***ttk*** mRNA level AVE± SEM
control well-fed	2.56E+01 ±2.48E-01	1.89E+01 ±2.06E-01	6.67 ±1.72E-01	0.00 ±5.53E-02	1.00 ±4.04E-02
mir-310s well-fed	2.64E+01 ±9.0E-02	1.97E+01 ±2.12E-01	6.66 ±1.61E-01	-4.0E-03 ±1.22E-01	1.002 ±8.94E-02 $p^{control\ well\text{-}fed}$=9.54E-01
control starved	2.69E+01 ±1.18E-01	1.91E+01 ±1.08E-01	7.82 ±1.03E-01	1.16 ±3.42E-01	0.45 ±4.2E-02
mir-310s starved	2.64E+01 ±1.13E-01	1.93E+01 ±1.53E-01	7.17 ±1.61E-01	5.06E-01 ±1.39E-01	0.70 ±9.93E-02 $p^{control\ starved}$=2.14E-02

[a] The relative *Rab23, DHR96,* and *ttk* mRNA levels were determined using the formula $2^{-\Delta\Delta CT}$.

[b] Three biological replicates were used to determine average (AVE) and standard error of the mean (SEM) values.

[c] For significance testing two-tailed, non-paired Student's t-test was used.

(Çiçek et al., 2016)

Table 9. *mir-310s* mutants have increased Rab23 protein levels under well-fed and starved conditions

Genotype/ Condition	Total Pixel/Signal Intensity $^{Rab23\text{-}YFP}$ AVE±SEM[b]	Total Pixel/Signal Intensity $^{\beta\text{-}tub}$ AVE±SEM[b]	Relative protein level[a] AVE±SEM[b]
control; Rab23-YFP well-fed	4.39E+03 ±9.95E+02	3.95E+04 ±9.06E+03	1.00 ±1.49E-02
mir-310s; Rab23-YFP well-fed	1.19E+04 ±2.10E+03	5.20E+04 ±9.63E+03	2.07 ±4.79E-02 $p^{control\ well\text{-}fed}$=2,87E-05
control; Rab23-YFP starved	9.51E+03 ±1.29E+03	5.78E+04 ±1.05E+04	1.57 ±3.61E-01 $p^{control\ well\text{-}fed}$=1.9E-01
mir-310s; Rab23-YFP starved	6.18E+04 ±1.36E+04	8.78E+04 ±3.13E+04	7.38 ±1.51 $p^{control\ starved}$=1.99E-02

Total intensities were determined by Adobe Photoshop Software.

[a] Relative Rab23 protein levels were determined by normalizing first to the β-tubulin of each sample and then to the well-fed *control* sample.

[b] Three replicates were used to determine averages (AVE) and the standard errors of the means (SEM).

Two-tailed non-paired Student's t-test was used for p value calculation and statistical testing.

(Çiçek et al., 2016)

Table 10. Relative miRNA expression levels measured by Taqman assays show gradual decrease upon starvation

Genotype/ Condition	C_T *mir-310* AVE±SEM[b]	C_T *2S rRNA* AVE±SEM[b]	Δ C_T AVE±SEM[b]	ΔΔ C_T AVE±SEM[b]	Relative ***mir-310*** miRNA level[a,c] AVE± SEM[b]
control well-fed	2.45E+01 ±2.81E-01	1.23E+01 ±3.00E-01	1.25 E+01 ±2.26E-01	0.00 ±7.26E-02	1.00 ±5.47E-02
control starved	2.70E+01 ±1.42E-01	1.33E+01 ±8.34E-02	1.37E+01 ±8.58E-02	1.45 ±1.63E-01	3.66E-01 ±4.68E-02 $p^{control\ well\text{-}fed}$ =7.72E-05
mir-310s well-fed	3.80E+01 ±1.02	1.28E+01 ±1.01E-01	2.53E+01 ±1.02	1.30E+01 ±1.02	1.22E-04 ±1.02E-04
Genotype/ Condition	C_T *mir-311* AVE±SEM[b]	C_T *2S rRNA* AVE±SEM[b]	Δ C_T AVE±SEM[b]	ΔΔ C_T AVE±SEM[b]	Relative ***mir-311*** miRNA level[a,c] AVE± SEM[b]
control well-fed	2.40E+01 ±2.76E-01	Same as in *mir-310*	1.18 E+01 ±2.24E-01	0.00 ±6.55E-02	1.00 ±9.08E-02
control starved	2.77E+01 ±1.85E-01	Same as in *mir-310*	1.44E+01 ±1.06E-01	2.67 ±2.23E-01	1.57E-01 ±2.42E-02 $p^{control\ well\text{-}fed}$ =2.99E-06
mir-310s well-fed	3.65E+01 ±2.73E-01	Same as in *mir-310*	2.38E+01 ±2.91E-01	1.20E+01 ±2.73E-01	2.46E-04 ±4.38E-05
Genotype/ Condition	C_T *mir-312* AVE±SEM[b]	C_T *2S rRNA* AVE±SEM[b]	Δ C_T AVE±SEM[b]	ΔΔ C_T AVE±SEM[b]	Relative ***mir-312*** miRNA level[a,c] AVE± SEM[b]
control well-fed	2.53E+01 ±2.98E-01	1.19E+01 ±3.25E-01	1.35 E+01 ±2.22E-01	0.00 ±1.14E-02	1.00 ±8.03E-03
control starved	2.87E+01 ±1.68E-01	1.29E+01 ±6.99E-02	1.58E+01 ±1.16E-01	2.32 ±1.14E-01	2.00E-01 ±1.57E-02 $p^{control\ well\text{-}fed}$ =6.77E-09
mir-310s well-fed	3.68E+01 ±1.09E-01	1.26E+01 ±7.74E-02	2.42E+01 ±1.34E-01	1.07E+01 ±1.09E-01	7.62E-04 ±4.38E-05
Genotype/ Condition	C_T *mir-313* AVE±SEM[b]	C_T *2S rRNA* AVE±SEM[b]	Δ C_T AVE±SEM[b]	ΔΔ C_T AVE±SEM[b]	Relative ***mir-313*** miRNA level[a,c] AVE± SEM[b]
control well-fed	2.78E+01 ±2.62E-01	Same as in *mir-312*	1.60 E+01 ±2.10E-01	0.00 ±5.07E-02	1.00 ±3.38E-02
control starved	3.10E+01 ±2.22E-01	Same as in *mir-312*	1.81E+01 ±1.44E-01	2.21 ±1.83E-01	2.16E-01 ±2.45E-02 $p^{control\ well\text{-}fed}$ =1.61E-06
mir-310s well-fed	3.68E+01 ±1.41E-01	Same as in *mir-312*	2.42 E+01 ±1.61E-01	8.35 ±1.41E-01	2.26E-03 ±2.89E-04
Single Day Starvation *mir-312* Expression Profile					
Genotype/ Condition	C_T *mir-312* AVE±SEM[d]	C_T *2S rRNA* AVE±SEM[d]	Δ C_T AVE±SEM[d]	ΔΔ C_T AVE±SEM[d]	Relative ***mir-312*** miRNA level[a,c] AVE± SEM[d]
control well-fed[1-4d]	2.79E+01 ±2.18E-02	1.29E+01 ±4.86E-02	1.50E+01 ±5.33E-02	0.00 ±2.18E-02	1.00 ±1.51E-02
control 1d starved	2.72E+01 ±1.68E-02	1.14E+01 ±8.81E-03	1.58E+01 ±1.90E-02	8.12E-01 ±1.68E-02	5.70E-01 ±6.60E-03 $p^{control\ well\text{-}fed}$ =1.29E-05

control 2d starved	2.77E+01 ±1.59E-02	1.16E+01 ±1.41E-02	1.61E+01 ±2.13E-02	1.13 ±1.60E-02	4.58E-01 ±5.04E-03 $p^{control\ well\text{-}fed}$ =4.48E-06
control 3d starved	2.85E+01 ±1.43E-01	1.21E+01 ±7.67E-02	1.64E+01 ±7.80E-02	1.38 ±1.43E-02	3.84E-01 ±3.80E-03 $p^{control\ well\text{-}fed}$ =2.46E-06
control 4d starved	2.86E+01 ±1.75E-02	1.19E+01 ±7.45E-02	1.67E+01 ±7.66E-02	1.68 ±1.75E-02	3.11E-01 ±3.81E-03 $p^{control\ well\text{-}fed}$ =1.58E-06
control well-fed[5-8d]	2.79E+01 ±3.37E-02	1.28E+01 ±4.74E-02	1.52E+01 ±5.82E-02	0.00 ±3.37E-02	1.00 ±2.36E-02
control 5d starved	2.95E+01 ±3.24E-02	1.24E+01 ±1.73E-02	1.71E+01 ±3.68E-02	1.93 ±3.24E-02	2.62E-01 ±5.92E-03 $p^{control\ well\text{-}fed}$ =6.98E-06
control 6d starved	2.96E+01 ±2.88E-02	1.22E+01 ±9.05E-03	1.74E+01 ±3.02E-02	2.23 ±2.88E-02	2.13E-01 ±4.22E-03 $p^{control\ well\text{-}fed}$ =5.09E-06
control 7d starved	2.96E+01 ±6.68E-02	1.21E+01 ±9.25E-02	1.75E+01 ±1.14E-01	2.38 ±6.68E-02	1.92E-01 ±8.76E-03 $p^{control\ well\text{-}fed}$ =5.59E-06
control 8d starved	3.06E+01 ±5.11E-03	1.24E+01 ±2.43E-02	1.82E+01 ±2.49E-02	3.04 ±5.11E-03	1.21E-01 ±4.30E-04 $p^{control\ well\text{-}fed}$ =3.08E-06

[a] The formula $2^{-\Delta\Delta CT}$ was used to calculate relative miRNA levels

[b] Average (AVE) and standard error of the mean (SEM) values were calculated using four biological replicates for each sample. For *mir-310s* samples (negative controls) AVE and SEM values show results from three technical replicates.

[c] Two-tailed, non-paired Student's t-test was used to determine p values and for significance testing.

[d] AVE and SEM values were calculated using three technical replicates for each sample.

Table 11. *Rab23* downregulation rescues the phenotypes caused by *mir-310s* loss

Genotype Phenotype	*control*		*mir-310s*		*mir-310s; bab1>Gal4, UAS-Rab23-RNAi*	
Perturbed differentiation: Frequency of FasIII^{+} late stalk cells n=number of stalks analyzed	5% n=20		65% n=20		15% n=20	
Perturbed cyst budding: Frequency of germaria with encapsulated cysts n=number of germaria analyzed	86% n=50		29.2% n=48		75% n=20	
Genotype Phenotype	*control*	*mir-310s*	*bab1>Gal4, UAS-Rab23*	*bab1>Gal4, UAS-hh*	*mir-310s; bab1>Gal4, UAS-Rab23-RNAi*	*mir-310s; bab1>Gal4, UAS-hh-RNAi*
Excessive division: Number of PH3^{+} follicle cells (AVE±SEM) n=number of stage 2 egg chambers analyzed	0.2±0.09 n=30	0.8±0.19 n=30 $p^{control}$=0.015	1.13±0.29 n=15 $p^{control}$=0.007	1.07±0.23 n=15 $p^{control}$=0.006	0.33±0.13 n=15 $p^{control}$=0.3	0.4±0.13 n=15 $p^{control}$=0.2

Significance was tested using Mann-Whitney U test and z statistics

(Çiçek et al., 2016)

Table 12. Rab23-YFP-4xmyc co-immunoprecipitated proteins

Gene names	CG Number
Rab23	CG2108
	CG7920
Pcmt	CG2152
me31B	CG4916
fln	CG7445
	CG30395
Lsp1gamma	CG6821
Mf	CG6803
Jon25Bi	CG8867
eIF3-S5-1	CG9769
desat1	CG5887
yps	CG5654
scu	CG7113
eIF-2beta	CG4153
Hsp27	CG4466
Mgstl	CG1742
ps	CG16765
wupA	CG7178
vig2;fdy	CG11844
Nap1	CG5330
Jon99Fii;Jon99Fi	CG2229
	CG4769
CG10306	CG10306
CG3800	CG3800
l(2)efl	CG4533
Hsp26	CG4183
Capr	CG18811
alphaTub67C	CG8308
Jafrac1	CG1633
	CG9641
fau	CG45077
mt:CoII	CG34069
Rox8	CG5422
Jon25Biii	CG8871
BEST:CK01296	CG5885

bl	CG13425
NHP2	CG5258
La	CG10922
DnaJ-1	CG10578
Sc2	CG10849
	CG6543
BEST:GH09393	CG4302
CG5641	CG5641
eIF-1A	CG8053
Ef1beta	CG6341
und	CG4008
vig	CG4170
CG4666	CG4666
Rm62	CG10279
Fer2LCH	CG1469
Nop56	CG13849
SF2	CG6987
ATPsyn-b	CG8189
dhd	CG4193
eEF1delta	CG4912
RfC38	CG6258
SmD3	CG8427
B52	CG10851
Cyp4g1	CG3972
RfC4	CG14999
	CG6617
pont	CG4003
Rbp1	CG17136
Jon99Cii	CG31362
deltaCOP	CG14813
nop5	CG10206
RfC3	CG5313
SmB	CG5352
l(1)G0320	CG32701
Tcp-1zeta	CG8231
Actn	CG4376
	CG8142

Mcm7	CG4978
	CG4611
l(2)35Di	CG13240
	CG11835
fau	CG45076
	CG7172
Nmt	CG7436
CG6693	CG6693
	CG9306
Nlp	CG7917
Jabba	CG15092
Cctgamma	CG8977
	CG13887
CG7637	CG7637
	CG18067
Pdsw	CG8844
DIP1	CG17686
Pros26.4	CG5289
mTerf3	CG5047
Pen	CG4799
	CG11107
T-cp1	CG5374
Gdi	CG4422
SmE	CG18591
lig	CG8715
Mcm5	CG4082
Fer1HCH	CG2216
	CG12203
CG10628	CG10628
or	CG3029
	CG5167
polo	CG12306
	CG4729
Cp15	CG6519
CG30185;Gr59f	CG30185
	CG7182
gammaTub37C	CG17566

	CG11999
Smn	CG16725
levy	CG17280
	CG3446
	CG12400
	CG4553
ATPCL	CG8322
ogre	CG3039
	CG6094
	CG10097
Pros45	CG1489
HspB8	CG14207
eIF6	CG17611
Nop60B	CG3333
	CG7409
ND23	CG3944
CG12138	CG30008
RnrL	CG5371
l(2)04524	CG3267
BicC	CG4824
	CG5903
Ski6	CG15481
BcDNA.GH04962	CG14476
	CG3436
CG7477	CG31249
	CG6746
Bub3	CG7581
CG7378-RA	CG7378
Sod2	CG8905
	CG6013
dpa	CG1616
Dlic	CG1938
Nurf-38	CG4634
	CG7911
Eaat1	CG3747
	CG4164
Surf4	CG6202

Appendix

	CG4619
	CG13126
	CG5703
CG9798	CG31523
Myo61F	CG9155
	CG8258
wibg	CG30176
26-29-p	CG8947
TfIIS	CG3710
caz	CG3606
SmD2	CG1249
	CG13163
	CG3683
	CG12984
	CG8547
Hsc70-5	CG8542
	CG7033
Mcm3	CG4206
CG12163	CG12163
CHOp24	CG3564
Cyp28d1	CG10833
Prx3	CG5826
eIF2B-gamma	CG8190
KdelR	CG5183
	CG7006
Cbp20	CG12357
fzy	CG4274
Ostgamma	CG7830
CG16912	CG16912
BcDNA.GH07066;CG5508-RC	CG5508
Mov34	CG3416
eIF4AIII	CG7483
wds	CG17437
	CG4020
CG9548	CG9548
alphaTry	CG18444
Ref1	CG1101
Acp65Aa	CG10297

msps	CG5000
	CG3420
	CG14309
CG9987	CG9987
LanB1	CG7123
Spase25	CG1751
	CG8680
aub	CG6137
Pros28.1	CG3422
	CG10469
Pros54	CG7619
dre4	CG1828
CG34026-RA	CG34026
mfas	CG3359
RFeSP	CG7361
Ddx1	CG9054
Tcp-1eta	CG8351
	CG16904
ced-6	CG11804
	CG9302
CstF-64	CG7697
	CG9172
asf1	CG9383
GstD1	CG10045
	CG7488
bol	CG4760
Klp10A	CG1453
sea	CG6782
Tudor-SN	CG7008
	CG11876
Hsp23	CG4463
LSm1	CG4279
vnc	CG11989
AP-1sigma	CG5864
CG13644	CG44255
SMC2	CG10212
	CG10470
nito	CG2910
CG15735	CG15735
lin19	CG1877

snRNP-U1-70K	CG8749
	CG5548
Cul-4	CG8711
skpA	CG16983
Cyp309a2	CG18559
	CG7946
NAT1	CG3845
CG13298	CG13298
eca;p24-2	CG33104
	CG2014
	CG5555
Dhod	CG9741
path	CG3424
Aats-asn	CG10687
sgg	CG2621
	CG13091
CG6183	CG42807
Grip84	CG3917
	CG3909
Rab5	CG3664
NTPase	CG3059
	CG15877
	CG32441
Zasp66	CG6416
cathD	CG1548
Su(var)205	CG8409
LSm7	CG13277
x16	CG10203
	CG4115
spag	CG13570
Ndg	CG12908
bai	CG11785
	CG15531
Csl4	CG6249
Ance	CG8827
Reg-2	CG3200
	CG1703
CG4447-RA	CG4447
CG11837	CG11837
Sec22	CG7359

Atpalpha	CG5670
ref(2)P	CG10360
	CG2604
Ranbp9	CG5252
rig	CG30149
tws	CG6235
CG17556-RA	CG3678
tst	CG10210
Kap-alpha1	CG8548
aur	CG3068
41974	CG2175
pit	CG6375
	CG3295
	CG9018
pelo	CG3959
	CG9799
Ubqn	CG14224
Nup93-1	CG11092
loqs	CG6866
Gnf1	CG1119
Iswi	CG8625
Sac1	CG9128
	CG3815
egl	CG4051
mt:CoIII	CG34074
	CG1091
Cpr62Bb	CG13935
Vinc	CG3299
	CG8397
Prat	CG2867
CoVb	CG11015
yellow-d	CG9889
Ser6	CG2071
U2af38	CG3582
Dbp21E2	CG3561
Fen1	CG8648
Orc5	CG7833
sns	CG33141
	CG7288
Hpr1	CG2031

Appendix

CG1307	CG1307
Abi	CG9749
gnu	CG5272
BEAF-32	CG10159
	CG31368
	CG11137
EG:25E8.3	CG3071
ns3	CG14788
lat	CG4088
mts	CG7109
ssx	CG3056
Kr-h2	CG9159
	CG31717
	CG18347
CG4038	CG4038
cdc2c	CG10498
	CG13472
	CG6841
	CG9350
	CG10472
Clc	CG6948
Prosbeta7	CG12000
LysB;LysD;LysA;LysE	CG1179
	CG11777
pen	CG1685
CG6089	CG33129
Cyp12d1-d	CG33503
Mcm6	CG4039
	CG9547
	CG10333
Pu	CG9441
gammaTub23C	CG3157
CG5001-RA	CG5001
TfIIB	CG5193
mTTF	CG18124
ocn	CG7929
	CG12128
Rab1	CG3320
Cul-5	CG1401

slmb	CG3412
Elp3	CG15433
l(2)35Df	CG4152
CG3501	CG3501
glu	CG11397
CG9253-RA	CG9253
	CG4365
	CG17454
	CG7970
U2A	CG1406
msi	CG5099
	CG3625
Art4	CG5358
smid	CG8571
CG11583	CG11583
CG10326	CG10326
CG17018-RC;CG17018-RD	CG17018
SelD	CG8553
CG9267-RA	CG9267
	CG3262
	CG5205
	CG12325
Klp61F	CG9191
fax	CG4609
CG7375	CG7375
	CG5726
Pros26	CG4097
	CG11984
HspB8	CG14207
TBPH	CG10327
poly	CG9829
CG11007	CG11007
Rab6;Rab39	CG6601
fu12	CG17608
	CG12170
lva	CG6450
Fbp1	CG17285
	CG3509
Rsf1	CG5655

anon-i1	CG2034
CG9246	CG9246
	CG12333
	CG3605
Su(P)	CG4086
Pcd	CG1963
san	CG12352
	CG10673
twin	CG31137
CG14100	CG14100
CG3224	CG3224
CG11077	CG11077
Syf2	CG12343
Cap	CG9802
CG2875-RB	CG2875
Adgf-D	CG9621
	CG8323
Glg1	CG33214
	CG5913
att-ORFA	CG4241
Txl	CG5495
CG6907	CG6907
	CG6796
DNApol-alpha60	CG5553
	CG2076
uri	CG11416
Nup37	CG11875
	CG11241
tyf	CG4857
	CG7910
SC35	CG5442
Orc4	CG2917
Pros25	CG5266
DNApol-alpha73	CG5923
Arf79F	CG8385
Bap60	CG4303
Rheb	CG1081
Cyp6g1	CG8453
	CG7382

Spase22-23	CG5677
Ote	CG5581
Cul-2	CG1512
ida	CG10850
Eb1	CG3265
vps2	CG14542
Spt5	CG7626
Elp1	CG10535
mTerf5	CG7175
Nup205	CG11943
Vps16A	CG8454
MED18	CG14802
Edc3	CG6311
rad50	CG6339
Taf5	CG7704
DNApol-delta	CG5949
dia	CG1768
	CG8360
Send2	CG18125
	CG10254
mtrm	CG18543
	CG9143
	CG33523
CG12702-RA	CG12702
CG8306	CG8306
Uch-L5	CG3431
	CG9446
	CG9890
R	CG1956
CG34325-RA	CG34325
	CG14995
l(2)k01209	CG4798
CG32638-RB	CG32638
l(1)dd4	CG10988
	CG3808
Nrg	CG1634
Rga	CG2161
Mtch	CG6851
Rcd-1	CG14213

Appendix

noi	CG2925
	CG2789
Prosbeta5	CG12323
	CG2051
brm	CG5942
	CG4901
nocte	CG17255
	CG9300
	CG9399
twr	CG2358
stnB	CG12473
poe	CG14472
	CG12320
CG18259-RA	CG18259
Lip4	CG6113
CG18190-RB	CG18190
DNApol-epsilon	CG6768
ctp;Cdlc2	CG6998
	CG4461
Rnp4F	CG3312
Aac11	CG6582
pnut	CG8705
Snp	CG44248
	CG45076
TfIIEalpha	CG10415
MED31	CG1057
Dlc90F	CG12363
tsr	CG4254
CG5198	CG5198
Spn28B	CG6717
mei-9	CG3697
IntS9	CG5222
SmG	CG9742
ck	CG7595
Dhpr	CG4665
Nup133	CG6958
nxf2	CG4118
	CG5989
spel1	CG4215

tho2	CG31671
Elp2	CG11887
Patr-1	CG5208
pcm	CG3291
sip1	CG7238
Rbp9	CG3151
CG6197-RA	CG6197
Sucb	CG10622
mib2	CG17492
btz	CG12878
psd	CG9050
CG12050-RB	CG12050
Aats-met	CG31322
CG10189	CG10189
	CG17337
Arf51F	CG8156
CG32549-RE;CG32549-RF;CG32549-RA;CG6247	CG32549
CG4091	CG4091
shot	CG18076
Mpp6	CG9250
futsch	CG34387
lds	CG2684
Nxt1	CG12752
MED14	CG12031
sub	CG12298
	CG6967
Usp7	CG1490
Pitslre	CG4268
	CG14257
PpV	CG12217
CG12542	CG32732
Rb97D	CG6354
	CG10153
Rtnl1	CG33113
	CG1750
	CG18273
mri	CG1216

Prosbeta3	CG11981
Saf-B	CG6995
PCID2	CG7351
CG8545-RA	CG8545
	CG6805
	CG9323
	CG17259
CG6316	CG32075
Taf6	CG32211
CaMKII	CG18069
rok	CG9774
CG9791	CG9791
alpha-Cat	CG17947
	CG8778
CG12272;CG12272-RA	CG12272
	CG8602
	CG7433
DNApol-alpha180	CG6349
ecd	CG5714
metro	CG30021
	CG34033
	CG5819
membrin	CG4780
IntS4	CG12113
Hexo1	CG1318
Ufd1-like	CG6233
yl	CG1372
Acph-1	CG7899
	CG10418
	CG33217
MRG15	CG6363
Not1	CG34407
	CG6418
CG11414-RA	CG11414
defl	CG18176
NELF-B	CG32721
CSN4	CG8725
Ercc1	CG10215
WRNexo	CG7670

Pdcd4	CG10990
Nmd3	CG3460
tobi	CG11909
kappaB-Ras	CG1669
Gbeta13F	CG10545
	CG4165
Klp3A	CG8590
U3-55K	CG33505
psidin	CG4845
blanks	CG10630
Clp	CG3642
	CG18600
TfIIEbeta	CG1276
	CG12391
Cdk8	CG10572
Sfp24F	CG42468
Prosalpha5	CG10938
dor	CG3093
CG4572-RC	CG4572
Pi3K21B	CG2699
par-6	CG5884
	CG1597
ncd	CG7831
DNApol-alpha50	CG7108
Tap42	CG31852
mrj	CG8448
IntS1	CG3173
MED16	CG5465
CG16892-RA	CG16892
	CG7718
APC7	CG14444
rnh1	CG8729
AGO3	CG40300
Pka-C1	CG4379
SA	CG3423
MED7	CG31390
	CG34034
CG1440-RC	CG1440
	CG9104

Appendix

	CG4764
	CG6769
spt4	CG12372
CG7338	CG7338
CSN3	CG18332
IntS2	CG8211
Smc5	CG32438
DMAP1	CG11132
	CG5168
aPKC	CG10261
didum	CG2146
CG12018	CG12018
	CG2941
Msh6	CG7003
EG:BAC R7A4.14	CG3699
	CG34424
zwilch	CG18729
wdb	CG5643
CG9630	CG9630
if	CG9623
Cnot4	CG31716
Hsc70Cb	CG6603
Prosbeta1	CG8392
Psa	CG1009
	CG30488
Ars2	CG7843
CG11334	CG11334
Mad1	CG2072
dnc	CG32498
CAP-D2	CG1911
	CG7839
spg	CG31048
CG14286	CG14286
	CG15701
Grip75	CG6176
Lis-1	CG8440
Cyp1	CG9916
Vha100-1	CG1709
	CG4749
MED20	CG18780

Hel89B	CG4261
Nup50	CG2158
asp	CG6875
EfSec	CG9841
cutlet	CG33122
omd	CG9591
GNBP3	CG5008
CG7741	CG7741
CG4364	CG4364
Hlc	CG1666
mrn	CG7764
CG4291-RA	CG4291
	CG9248
Mat89Ba	CG12785
faf	CG1945
IntS3	CG17665
pum	CG9755
l(1)G0193	CG2206
	CG5800
hyx	CG11990
CG13957	CG13957
MED24	CG7999
hay	CG8019
	CG9925
	CG11710
	CG2124
CG16865	CG16865
	CG17912
sle;CG12592	CG12819
	CG9953
	CG9067
CG9297-RA	CG9297
	CG16812
	CG9997
Aats-ala-m	CG4633
	CG17242
MTA1-like	CG2244
Myd88	CG2078
	CG13492

dlg1	CG1725
CG14215	CG14215
CG11722	CG11722
CG9601-RA	CG9601
	CG12267
	CG31418
mask	CG33106
	CG7261
	CG10347
Cyp12a5	CG11821
Klp67A	CG10923
CG6364	CG6364
CG5116-RA	CG5116
GstO2	CG6673
	CG10092
Prx2540-2;CG12896-RA;Prx2540-1	CG12896
cerv	CG15645
Ranbp16	CG33180
GM130	CG11061
CG14299	CG14299
l(2)NC136	CG8426
	CG31278
hd	CG2669
Sin	CG10582
Cdc27	CG8610
	CG7180
Sin3A	CG8815
CG10517	CG33056
Rad17	CG7825
Sema-2a	CG4700
clos	CG42600
cg	CG8367
cort	CG11330
Aats-tyr	CG4561
Asun	CG6814
pgant9	CG30463
pav	CG1258
ctrip	CG42574

Pol32	CG3975
	CG8771
Inos	CG11143
fd68A	CG11799
Pex1	CG6760
sbr	CG1664
CG34408-RA	CG34408
shtd	CG9198
wcd	CG7989
Ranbp11	CG33139
CG32473-RB;CG32473-RC	CG32473
lid	CG9088
barr	CG10726
CG8915-RA	CG8915
Nf1	CG8318
Bre1	CG10542
CG11486-RB;CG11486-RK	CG11486
zormin	CG33484
ash2	CG6677
Rop	CG15811
Letm1	CG4589
HDAC6	CG6170
crm	CG2701
Mhcl	CG31045
	CG13142
Cht3	CG18140
	CG3999
Prosbeta2	CG3329
fs(1)M3	CG4790
rod	CG1569
Nipped-B	CG17704
CG6379	CG6379
Pkn	CG2049
	CG6415
	CG9911
Gfat2	CG1345
	CG4069
kz	CG3228

Appendix

Chd3	CG9594
Parg	CG2864
	CG11120
Hsp60C	CG7235
MED1	CG7162
Dcr-1	CG4792
lola	CG12052
	CG6511
Rip11	CG6606
	CG17209
Atg5	CG1643
CycB	CG3510
wisp	CG15737
CG17338	CG31793
MBD-R2	CG10042
Pxt	CG7660
alpha-Est1	CG1031

SIDL	CG6623
eIF-4B	CG10837
Uba1	CG1782
xmas-2	CG32562
	CG12010
fs(1)N	CG11411
Atu	CG1433
Nup153	CG4453
lqfR	CG42250
Orc2	CG3041
CG43078-RA;CG32352	CG43078
	CG4554
RecQ4	CG7487
Hira	CG12153
l(1)G0007	CG32604
	CG12090

	CG12499
fs(1)Ya	CG2707
mus210	CG8153
sls	CG1915
IntS8	CG5859
egg	CG12196
ESTS:172 F5T	CG13397
LM408	CG6206
	CG3520
Mms19	CG12005
Nipped-A	CG33554
tefu	CG6535
CG11955	CG31445
Nelf-A	CG5874
Gem3	CG6539
CG7337-RB;CG7337-RA	CG7337

Strn-Mlck	CG44162
lap	CG2520
Mur2B	CG14796
	CG2747

For full list of identified proteins see supplementary spreadsheets in the digital appendix (Çiçek et al., 2016).

List of Abbreviations

Technical abbreviations

A	ampere
AVE	average
BCA	bicinchoninic acid
bp	base pair
BSA	bovine serum albumin
CAFE	capillary feeder (assay)
CCA	coupled colorimetric assay
cDNA	complementary DNA
C_T	threshold cycle
DAPI	4’,6-diamidino-2-phenylindole
DGRC	Drosophila Genomics Resource Center
DNA	deoxyribonucleic acid
DNAse	deoxyribonuclease
DSHB	Developmental Studies Hybridoma Bank
DTT	dithiothreitol
E.Coli	*Escherichia coli*
ECL	enhanced chemiluminescence
EDTA	ethylenediaminetetraacetic acid
ESI	electrospray ionization
Flp	flippase
FRT	flippase recognition target
HCD	higher collision-induced dissociation
HRP	horseradish peroxidase
LDS	lithium dodecyl sulfate
Lys-0	Lysine-12C614N2
Lys-8	Lysine-13C615N2
MS	mass spectrometry
NGS	normal goat serum
OD	optical density
PAGE	Polyacrylamide gel electrophoresis
PBS	phosphate buffered saline
PBT	PBS-Tween (buffer)
PBTB	PBT-blocking (buffer)
PCR	polymerase chain reaction
PFA	paraformaldehyde
PVDF	polyvinylidene difluoride
qPCR	quantitative PCR
qRT-PCR	quantitative reverse transcription PCR

RIPA	radioimmunoprecipitation assay
RNA	ribonucleic acid
Rpm	revolutions per minute
RT	reverse transcriptase
RT	room temperature
S. cerevisiae	*Saccharomyces cerevisiae*
S2 cells	Schneider 2 cells
SDS	sodium dodecyl sulfate
SEM	standard error of the mean
TAG	triglyceride
TOF	time of flight
Tris	tris-hydroxymethyl-aminomethane
V	volt
w/v	weight to volume
YPD	yeast extract-peptone-dextrose

Biological abbreviations

AMPK	AMP-activated protein kinase
A-P axis	anterior-posterior axis
CB	cystoblast
CpC	cap cell
C-terminus	carboxyl-terminus
Dme	*Drosophila melanogaster*
Dre	*Danio rerio*
Drosophila	*Drosophila melanogaster*
dsRBD	double stranded RNA binding domain protein
EC	escort cell
ER	endoplasmic reticulum
FC	follicle cell
FSC	follicle stem cell
GFP	green fluorescent protein
GO	Gene Ontology
GSC	germline stem cell
hsa	*homo sapiens*
IGF	insulin-like growth factor
mCD8-GFP	membrane CD8-GFP
mGFP	membrane GFP
miRNA	microRNA
mmu	*mus musculus*
mRNA	messenger RNA
nLacZ	nuclear LacZ
N-terminus	amino-terminus
PI4P	phosphatidylinositol-4-phosphate
PKA	cAMP-dependent protein kinase
Pol	polymerase
Pre-miRNA	precursor microRNA
Pri-miRNA	primary microRNA
RISC	RNA-induced silencing complex
RNAi	RNA interference
RNase	ribonuclease
rRNA	ribosomal RNA
SILAC	stable isotope labeling by amino acids in cell culture
siRNA	Small interfering RNA
TF	terminal filament
TOR	target of rapamycin
UAS	upstream activation sequence
UTR	untranslated region
YFP	yellow fluorescent protein

Gene and protein names

act	*actin*
Actin 88F	
Add	Adducin
bab1	*bric à brac 1*
Boi	Brother of IHog
Ci	Cubitus Interruptus
CKI	Casein kinase Iα
COP	coat protein complex
Cos2	Costal 2
Cpr100A	*Cuticular protein 100A*
Cpr62Bc	*Cuticular protein 62Bc*
Cpr72Ec	*Cuticular protein 72Ec*
DE-Cad	DE-Cadherin
DHR96	*Hormone receptor-like in 96*
Dpp	*Decapentaplegic*
FasIII	Fasciclin III
GSK3	Shaggy
hh	*hedgehog*
IHog	Interference Hedgehog
LamC	Lamin C
Lsp1beta	*Larval serum protein 1 β*
Lsp2	*Larval serum protein 2*
mir-310s	refers to *mir-310, mir-311, mir-312,* and *mir-313* together
Obp56a	*Odorant-binding protein 56a*
Obp56e	*Odorant-binding protein 56e*
Obp99b	*Odorant-binding protein 99b*
PH3	Phospho-Histone H3
pro-PO-A1	*Prophenoloxidase 1*
ptc	*patched*
Rab23	
smo	*smoothened*
ttk	*tramtrack*
tub	*tubulin*
wg	*wingless*

Digital Appendix

Supplementary spreadsheets for the SILAC and Co-IP experiments

Affidavit

I, Ibrahim Ömer Çiçek born 28.07.1986 in Istanbul, Turkey, herewith declare that I prepared this Doctoral Thesis titled “The role of the *mir-310s* in Hedgehog signaling regulation under dietary stress in *Drosophila* ovary” on my own and with no other sources other than cited.

Göttingen, 02.02.2016

Ibrahim Ömer Çiçek

Curriculum Vitae

Ibrahim Ömer Çiçek
E-Mail: icicek@gwdg.de
Mobile: 017670321778
Address: Kurze Geismar Strasse 36
37073 Göttingen

Research Experience

Max Planck Institute for Biophysical Chemistry, Göttingen

2011-2015 Identification of novel miRNA functions by proteomics and transcriptomics. Further studies with qRT-PCR and immunohistochemistry (*Drosophila melanogaster)*

2011 Functional analysis of a novel gene by genetics, RNAi and immunohistochemistry (*D. melanogaster)*; orthologue search in *Mus musculus* by sequence analysis and western blotting

2011 Establishment and characterization of pluripotent stem cell lines from embryonic fibroblasts using FuGENE and retroviral transfection techniques, culture conditions, and isolated embryonic epiblasts (*M. musculus*)

Göttingen Zentrum für Molekulare Biowissenschaften

2011 Investigation of the role of endocytosis in cell signaling by gene expression analyses, *in situ* hybridization and luciferase based reporter assays (*Xenopus laevis*)

Boğaziçi University, Istanbul

2009-2010 Analysis of adult neurogenesis dynamics in olfactory epithelium using transgenesis and BrdU labeling (*Danio rerio*)

Westfälische Wilhelms University, Münster

2009 Study of olfactory receptor gene choice by *in vivo* RNAi screen via immunohistochemistry and confocal imaging (*D. melanogaster*)

Istanbul University, Istanbul Medical Faculty

2008 Biomarker identification in Behçet's disease patients by qRT-PCR and ELISA (in blood and cerebrospinal fluid)

2007 HLA genotyping of pre- and posttransplantation patients by PCR and DNA hybridization

Professional Experience

2013	Organizing PhD Student Symposium "10th Horizons in Molecular Biology" being responsible for financing and fundraising by contacting company representatives for sponsorship, Göttingen
2005-2009	Organizing an annual national Molecular Biology and Genetics Congress at Boğaziçi University as head supervisor also being responsible for financing and fundraising, Istanbul
2011	Establishment of a graduate program in Turkish-German University by participation in discussions on finances and academic schedule in the Turkish-German Life Sciences Workshop, Istanbul
2012	Supervision, experimental and schedule planning of research projects for long-term internship students at Max Planck Institute for biophysical Chemistry, Göttingen
2012-2015	Tutoring MSc/PhD students for molecular biology courses (RNA interference, Cell Adhesion) at Georg-August University, Göttingen
2013-2014	Co-revision of scientific papers for publication in peer-reviewed journals
2010	Student assistant of an introductory science course for non-science students at Boğaziçi University, Istanbul

Scholarships and Awards

2011-2015	Doctoral Stipend awarded by the Max Planck Institute for biophysical Chemistry
2012	Travel Grant awarded by the Göttingen Graduate School for Neurosciences, Biophysics, and Molecular Biosciences
2012	DAAD-RISE fellowship for supervision of a 12 weeks student internship
2010-2011	Stipend of the Excellence Foundation for the Promotion of Max Planck Society
2009-2010	Excellence scholarship awarded by Boğaziçi University for science students with volunteer experience in social projects

2005-2010 Scholarship awarded by the Turkish Scientific and Technological Research Foundation due to success in the national examination for university entrance

2003-2005 Scholarship by private institutions for the university entrance preparation

Education

2011-2015 **Graduate Student,** Max Planck Institute for Biophysical Chemistry, Research Group for Gene Expression and Signaling, Göttingen

2010-2011 **MSc/PhD Molecular Biology Program**, International Max Planck Research School, Direct admission to PhD without having to complete Master's thesis, Göttingen

2005-2010 **Bachelor of Science,** Boğaziçi University, Major Molecular Biology and Genetics, English proficiency, Istanbul

1997-2005 **German Abitur Diploma in English, Science, and Mathematics**, Istanbul Erkek Lisesi

Publications

I. Ö. Çiçek, S. Karaca, M. Brankatschk, S. Eaton, H. Urlaub, and H. R. Shcherbata (2016) *"Hedgehog Signaling strength is Orchestrated by the mir-310 Cluster of microRNAs in Response to Diet."* - Genetics.

Presentations

2013-2015 GSA 54th, 55th, and 56th Annual Drosophila Research Conference, Washington, DC; San Diego, CA; Chicago, IL

2013 23rd European Drosophila Research Conference, Barcelona

2013 CSHL meeting "Stem Cells", Cold Spring Harbor, NY

2012-2013 EMBO|EMBL Symposia the Complex Life of mRNA; the Non-Coding Genome, Heidelberg

2014 Turkish-German Workshop for Molecular Neurosciences, Istanbul

2014 GfE School for "Stem Cells in Development and Cell Diversity", Ulm

Memberships

Genetics Society of America (GSA) 2013-

Gesellschaft für Entwicklungsbiologie (GfE) 2014-

Languages

Turkish (native)

German (Full professional proficiency, Abitur)

English (Full professional proficiency)

Computer Skills

DNA STAR Laser Gene
Vector NTI
Zeiss-Zen
Python
Adobe Photoshop
Adobe Illustrator
MS Office

Skills and Expertise

qRT-PCR
Fluorescent Immunohistochemistry
Confocal imaging
Cell culture
Transfection
D. melanogaster genetics
in vivo, in vitro RNAi
Luciferase expression assays
Enzyme based colorimetric assays
Stable Isotope Labeling in *D.melanogaster*
Co-immunoprecipitation
Western Blot
Histology
Transgenesis
Molecular Cloning
Primer design